SAND2008-1509C

MEMS-Based Techniques for Nanomechanical Characterization

Brad L. Boyce
Sandia National Laboratories
blboyce@sandia.gov

Sandia National Laboratories

TMS

HYSITRON

TMS 2008 Tutorial
New Orleans, LA, January 29th, 2008

Sandia is a multiprogram laboratory operated by Sandia Corporation, a Lockheed Martin Company, for the United States Department of Energy's National Nuclear Security Administration under contract DE-AC04-94AL85000.

Outline

1. Introduction
2. MEMS fabrication technologies
3. Examples of passive devices
4. Passive device technology
5. Examples of active devices
6. Active device technology

Outline

1. Introduction
    1. Characteristic scales in nanomechanics
    2. The need for high-precision structural sensors and actuators
    3. Dimensional limits of traditional fabrication and assembly
    4. History of micromachining.
2. MEMS fabrication technologies
3. Examples of passive devices
4. Passive device technology
5. Examples of active devices
6. Active device technology

1.1 Characteristic Scales in Nanomechanics

In biology…

1. A red blood cell is 6000-8000 nm in size.
2. The diameter of a single-walled carbon nanotube is ~1 nm.
3. The diameter of a DNA double helix is ~2 nm.
4. Weight of a single bacterium ~1 pN.
5. The step size of a conventional kinesin molecule is 8 nm. The required force to cause kinesin to walk backward ~10 pN (Q. Shao and Y.Q. Gao, PNAS, 2006).

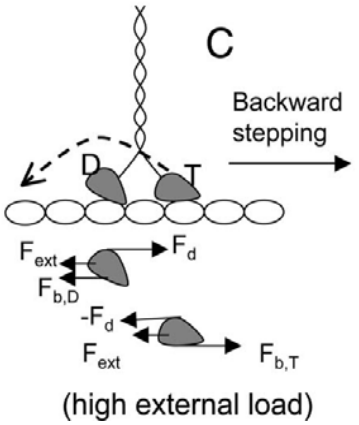

Q. Shao and Y.Q. Gao, PNAS, 2006

The national nanotechnology initiative (www.nano.gov) defines nanotechnology as technology governed by phenomena that occur at a length scale of <100 nm.

1.1 Characteristic Scales in Nanomechanics

In solid state materials…

1. Intel's new Penryn family of processors use 45 nm CPU technology (due out this year). 45nm defines the gate size, and typically the first metal layer feature size. Pentium II was a 250 nm technology.

2. Energy required to break a single C-C bond: 5.76×10^{-10} nJ! Bond length of a single C-C bond: 0.154 nm. Force to break a single C-C bond: order~ 10nN.

3. The force required for the onset of dislocation activity during nanoindentation of aluminum is <2 μN [Minor et al., Nature Materials, 2006].

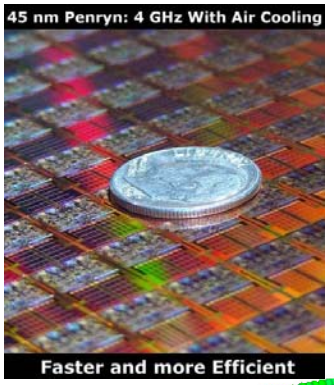

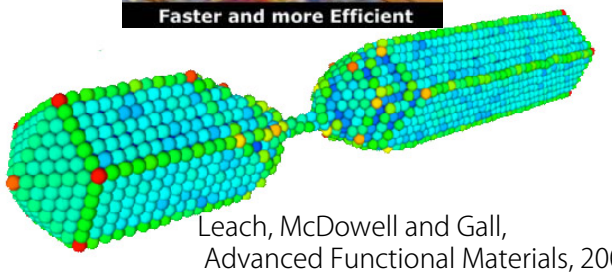

Leach, McDowell and Gall,
Advanced Functional Materials, 2007

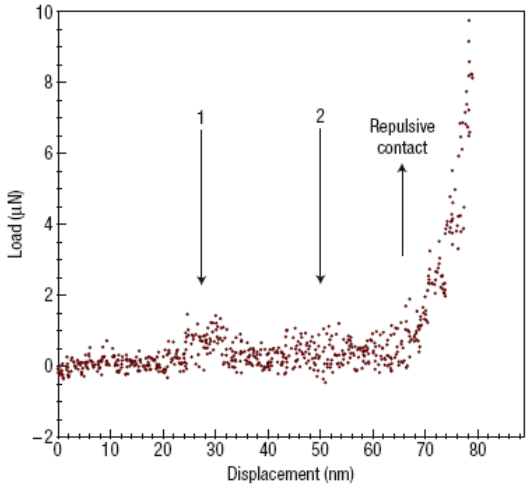

AM Minor et al, Nature Materials, 2006

The national nanotechnology initiative (www.nano.gov) defines nanotechnology as technology governed by phenomena that occur at a length scale of <100 nm.

1.2 The need for high-precision structural sensors and actuators

Sensitivity of a cantilever beam flexure…

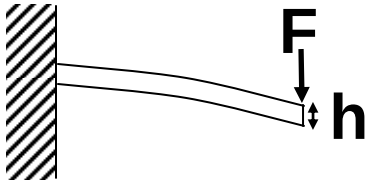

Fixed-free:

$$\max deflection,\ y = \frac{Fl^3}{3EI}$$

Fixed-Fixed:

$$\frac{Fl^3}{192EI}$$

$$I_{rect} = \frac{bh^3}{12}$$

Sensitivity of an electrostatic actuator…

Vertical:

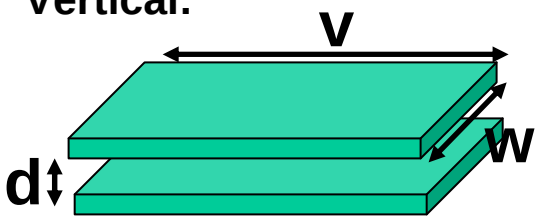

$$F_z = -\frac{\varepsilon_r \varepsilon_0 wvV^2}{2d^2}$$

Lateral:

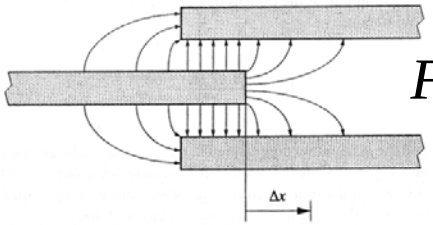

$$F_x = \frac{\varepsilon_r \varepsilon_0 wV^2}{2d}$$

1.4 History of Micromachining

1400's: Armor decorations were applied by acid-based etching through a wax mask. This is the earliest known application of patterned wet etching. This process continued to be practiced for 100's of years.

1822 Niépce invented photo-sensitive masks

1940's Lithography-based chemical milling used to produced printed circuit boards.

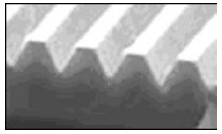

1950's Introduction of isotropic etching in silicon semiconductor processing, using mixtures of HF and HNO_3.

1960's Bell labs began working on anisotropic Si etch mixtures, beginning with KOH

1962 Honeywell (Tufte et al) made the first thin Si piezoresistive diaphrams, intended for measuring stress, strain, or pressure.

1972 Sensym/National Semiconductor introduced stand-alone Si sensor products.

1974 National Semiconductor released a catalog of available Si pressure sensor products.

1982 Petersen's paper on the "excellent mechanical properties" of Si led to a renewed interest in micromechanical Si components.

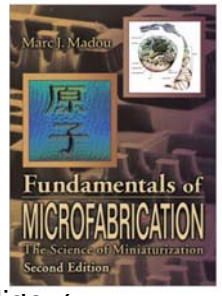

1994 An estimated 10,000 scientists and engineers are involved in Si sensor R&D worldwide.

1997 Madou's book on "Fundamentals of Microfabrication" (1st ed.) is released.

1.3 Dimensional Limits of Traditional Machining and Assembly

1. Conventional machining using an end mill and lathe produces tolerances as good as 25 µm. Minimum feature sizes (accounting for warpage induced by residual stress) are typically >250 µm.

2. Small scale machining can be accomplished by microEDM or diamond turning. The damaged recast layer in microEDM is typically ~5 µm or worse, leading to minimum feature sizes of ~100 µm.

3. Precision microassembly is an area of ongoing research. Positioning 100 µm parts with tolerances better than 3 µm is not trivial. See: www.sandia.gov/isrc/precmicroassy.html

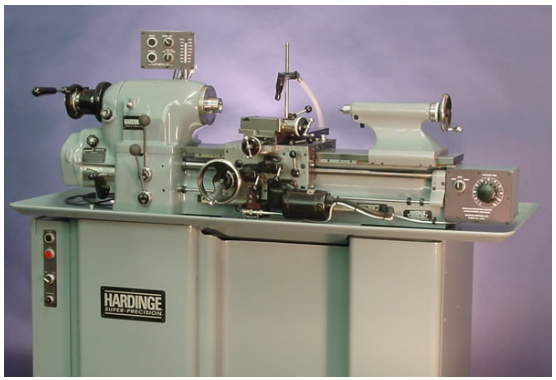

Outline

1. Introduction
2. MEMS fabrication technologies
   1. Background in Lithography
   2. Wet bulk micromachining
   3. Surface micromachining
   4. Micromolding
   5. Alternative fabrication methods
3. Examples of passive devices
4. Passive device technology
5. Examples of active devices
6. Active device technology

A Fast, Brief Primer On Microfabrication…
20 slides in ~30 minutes…

2.1 Background in Lithography

- **Photolithography:** Optical pattern transfer technique in which micro-pattern is transferred from a **photomask** to a **UV**-sensitive polymer layer (**photoresist**) coated on a substrate.

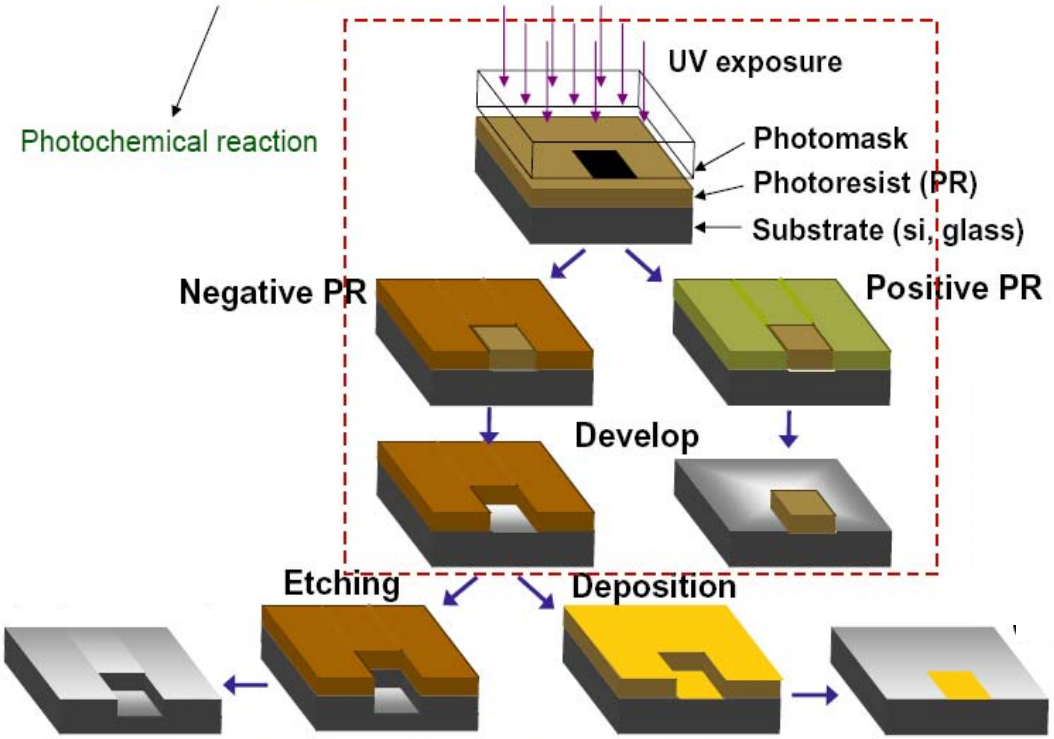

Photolithography Process

- Surface Preparation (Wafer Cleaning)
- Coating (Spin Coating)
- Pre-Bake (Soft Bake)
- **Alignment**
- **Exposure**
- (Post Exposure Bake)
- **Development**
- Post-Bake (Hard Bake)

Surface Prep -> Alignment

Wafer Cleaning

- **Typical contaminants**:
  - Atmospheric dust, bacteria, finger prints
  - Photoresist residue, solvent residue, H_2O residue
- **Standard degrease (organic cleaning)**:
  Soaking in (TCE →) acetone → methanol → DI water → Dry with N_2
- **Piranha cleaning**
  70% H_2SO_4 + 30% H_2O_2
- **RCA clean**: standard cleaning process for new silicon wafers out of the box
  - NH_4OH (1) + H_2O_2 (3) + H_2O (15) @ 70°C for 15 min. (organic)
  - HCl (1) + H_2O_2 (3) + H_2O (15) @ 70°C for 15 min. (metal ion)
  - 10:1 BOE for 1 min. (thin oxide)
- **Dehydration bake**

Pre-Bake (Soft Bake)

- After spin coating, the resist still contains up to 15% solvent and may contain built-in stresses.
- The wafers are baked to remove solvent and stress and to promote adhesion of the resist layer to the wafer.
- Hot plate or oven is used. Hot plating is faster and more controllable. Typical thermal cycles are:
  – 90-100°C for 20 min. in a convection oven
  – 80-90°C for 1 min. on a hot plate
- Convection ovens: solvent at surface of resist is evaporated first, which can cause resist to develop impermeable skin, trapping the remaining solvent inside
- Hot plate: temperature rise starts at bottom of wafer and works upward, more thoroughly evaporating the coating solvent

Spin Coating

- PR deposition methods: Spin, Spray, Lamination
- Spin coating is the most common method.

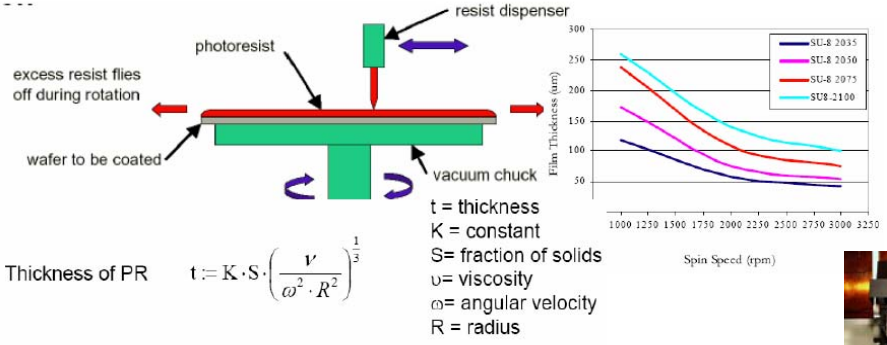

Thickness of PR $t := K \cdot S \cdot \left(\frac{\nu}{\omega^2 \cdot R^2} \right)^{\frac{1}{3}}$

t = thickness
K = constant
S= fraction of solids
υ= viscosity
ω= angular velocity
R = radius

- Primers are often used to enhance the adhesion between PR and substrate. e.g., 1,1,1,3,3,3-hexamethyldisilazane (HMDS)

PR SiO_2


Karlsuss MA6 Mask Aligner

Alignment

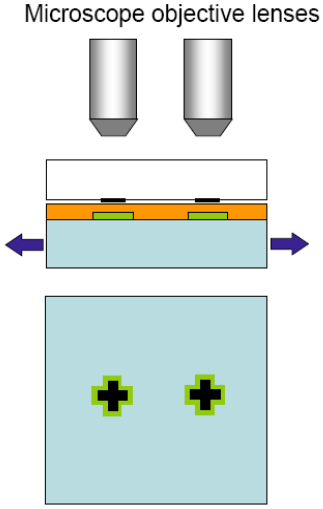

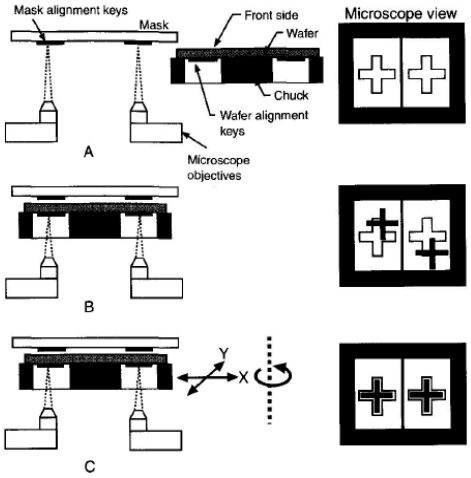

Microfabrication Slides Courtesy of Moses Noh, Drexel University

Sandia National Laboratories

Post-Exposure -> Stripping

Post-Exposure Bake (PEB) and Develop

- Post-exposure bake is required for some negative photoresist (SU-8).
- Wait until the substrate is completely cooled down before develop.
- Develop (automatic spray, manual agitation)
- Use proper developer and rinsing material.
- Parameters: concentration, time, agitation
- Dry with N_2

Post-Bake (Hard Bake)

- Used to stabilize and harden the developed photoresist prior to processing steps where the resist will be used as masking material.
- Postbake removes any remaining traces of the coating solvent or developer.
- Slow cooling is important for thick PR to avoid thermal stress
- Firm postbake is needed for acid etching, e.g. BOE.
- Postbake should NOT be done prior to a process in which a soft resist is desired, e.g. metal liftoff patterning.
- Photoresist will undergo plastic flow with sufficient time and/or temperature: Resist reflow can be used for tailoring sidewall angles.

PR Removal (Stripping)

- Remove the photoresist and any of its residues.
- Organic solvents (acetone) are generally sufficient for non-postbaked PRs:
- Commercial strippers are available depending on PR.
- Plasma etching with O_2 (ashing) is also effective for removing organic polymer debris.
- Piranha cleaning is often used for PR removal

Resolution in Photolithography

- Minimal feature size is a measure of the resolution of a lithographic process.
- The resolution is limited by a variety of factors.
  - Light diffraction
  - Alignment
  - Non-uniformities in wafer flatness
- The theoretical resolution for contact/proximity printing

$$R = b_{\min} = \frac{3}{2}\sqrt{\lambda\left(s + \frac{z}{2}\right)}$$

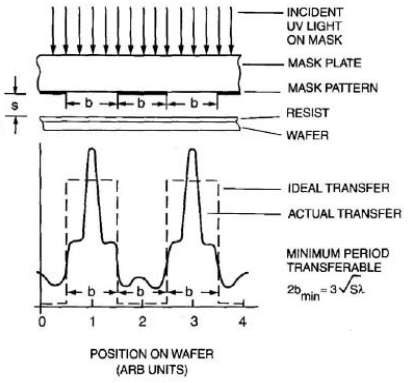

Figure 1.12 Light distribution profiles on a photoresist surface after light passes through a mask containing an equal line and space grating.

- High contrast PR produces vertical profile and better resolution.

About Photomasks

Photomasks

- The stencil used to repeatedly generate a desired pattern on PR-coated substrate
  - Flat glass plate with Cr patterns made by e-beam lithography or pattern generator (variable shape aperture)
- **Types:**
  - Cr on soda lime glass (most common)
  - Cr on quartz glass (transparent to deep UV, expensive)
  - Photographic emulsion on soda lime glass (less expensive)
  - Fe_2O_3 on soda lime glass (semi-transparent to visible light)
  - High resolution laser printing on transparency
- Dimensions: 4" x 4" for 3 inch wafers, 5" x 5" for 4 inch wafers

Photomasks

- Design with drawing software (AutoCad)
- Mask, wafer, and device sizes
- Multiple layers, alignment marks, labels
- **Example: Piezoresistive Si cantilevers**

How many masks do we need?

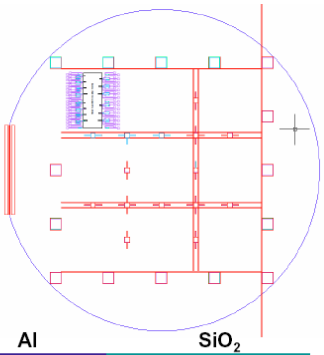

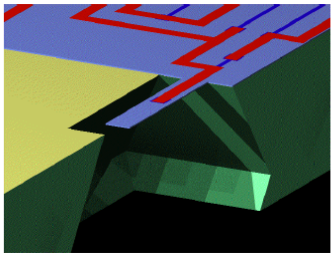

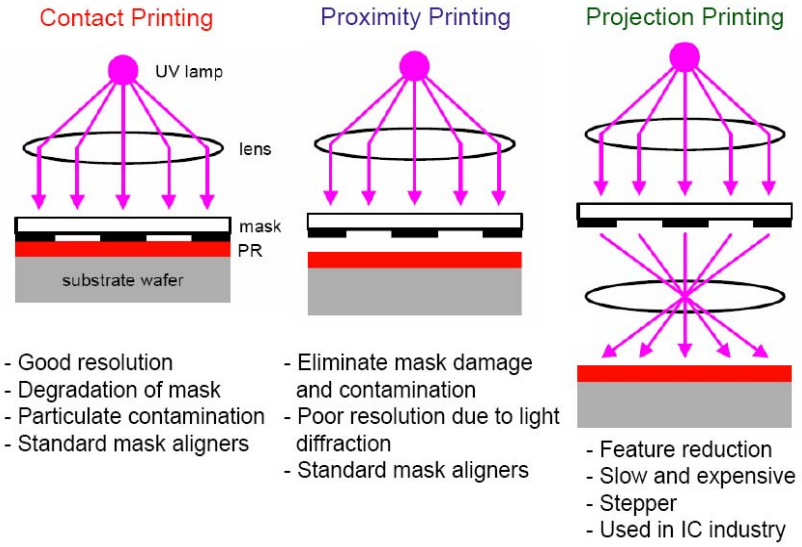

- Good resolution
- Degradation of mask
- Particulate contamination
- Standard mask aligners

- Eliminate mask damage and contamination
- Poor resolution due to light diffraction
- Standard mask aligners

- Feature reduction
- Slow and expensive
- Stepper
- Used in IC industry

About Photoresists

Positive Photoresist - PMMA

- **PMMA (Ploymethylmethacrylate)**
  - Chain scission type
  - Resin itself is photosensitive

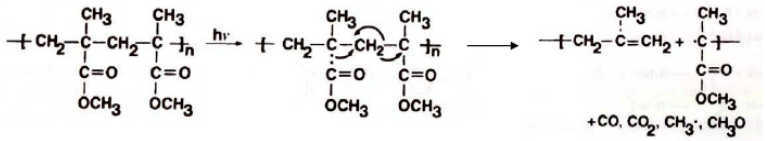

- Used for short-wavelength lithography: deep UV, extreme UV, X-ray lithography, electron-beam lithography
- **Disadvantages**
  - Plasma etch tolerance of the resist is very low (low selectivity).
  - Dissociation of PMMA changes the chemistry of the plasma etch and leads to polymeric deposits on the surface of the substrate.

Positive Photoresist - DQN

- **Novolac (N): polymer resin**
  - Dissolves in an aqueous solution easily.
  - Solvent added but most solvent is evaporated before exposure.
- **Diazoquinone (DQ): photoactive compound**
  - 20~50 % in weight
  - Insoluble in base solution.
  - Changes to carboxylic acid (dissolution enhancer) under UV light

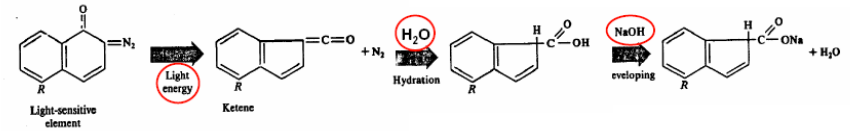

- **Advantages of DQN photoresists:**
  - Good resolution with near UV
  - Novolac is chemically resistant (good mask for plasma etching)
  - Environment-friendly (water-based developer)

Negative Photoresists

- **Advantages**
  - Good adhesion to substrate
  - Good resistance to chemicals and plasma etching
  - Good mechanical properties
- **Disadvantages**
  - Swelling of photoresists during the development. (The minimum feature size is limited to 2 μm)
  - Developer is usually organic solvent (less ecological)
  - Difficult to remove
- **SU-8** : Thick, high-aspect ratio structure, good mechanical properties
  - SU8 2005-2100
  - Xylene-based developer (PGMEA)
- **Futurrex**: Removable, good vertical profile control
  - Good for lift-off process
  - Water-based developer (RD6)
- **Dry film photoresists** are also available.

UV Light

- Near ultra-violet portion (λ = 350~500 nm) of electromagnetic spectrum is used in photolithography → DUV (λ = 150~300 nm)

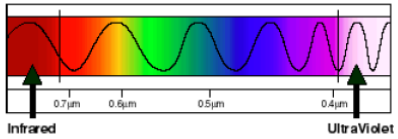

- Photon properties of UV light produce interaction with chemical bonds in the photoresist – i.e. produce bond breaking (positive resist) or induce a cross-linking reaction (negative resist).

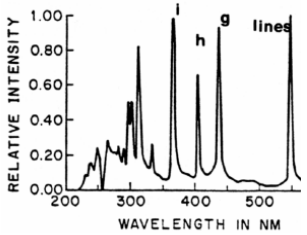

Arc lamp filled with Mercury

G-line:	436 nm
H-Line:	405 nm
I-Line:	365 nm
Mid-UV:	313 nm
DeepUV:	254 nm

Xenon is used for deep UV

2.2 Bulk Micromachining (Subtractive)

Silicon Atomic Structure

- Silicon has a **diamond-cubic** structure
  → Covalent bonding, lattice parameter, a = 5.43Å

- Atomic packing factor (APF): percent of volume occupied by atoms.
  Si = 34% (FCC = 74%)

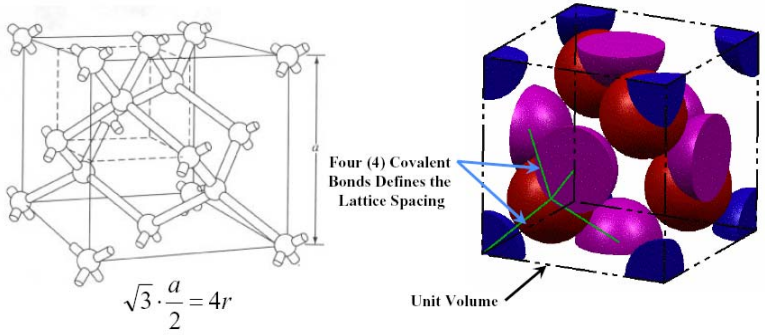

$$\sqrt{3}\cdot\frac{a}{2}=4r$$

Silicon Properties

- Density: ρ = 2.33 g/cm^3, atomic density = 5x10^{22} atoms/cm^3
- Band Gap: E_G = 1.12 eV, Intrinsic resistivity = 2.3x10^5 Ω-cm
  - Thermal excitation: electron-hole pair @RT ~ 10^{10} /cm^3.
    (For insulators, E_G > 10 eV)
  - Doping effect (n-type: P or As; p-type: B or Ga): a few atomic %
    EHP increases greatly, resistivity = 1-10 Ω-cm

- Young's Modulus (anisotropic)
  E_{100} = 131 GPa, E_{110} = 169 GPa, **E_{111} = 187 GPa**
- Poisson's Ratio (γ) = 0.29, Maximum Stress = 3x10^{10} Pa (Brittle)
- Coefficient of thermal expansion (CTE) = 2.6x10^{-6} (low)
- Melting Point 1421°C, heat capacity = 20 J/mole K at 25°C
- Piezoresistive (anisotropic)
- Dielectric Constant (ε) = 11.8, refractive index (n) = 3.42

Terminology in Etching

- **Etch rate**: rate of removal of material [Å/sec, μm/min]
- (Etch rate %) **Uniformity** = $\frac{(Etch_{Hi}-Etch_{Lo})}{(Etch_{Hi}+Etch_{Lo})}\times 100$
- **Anisotropy**: etch rate as a function of direction
  Lateral etch rate ratio = horizontal / vertical
  (Isotropic etch equal to 1)
  e.g. 85°C, 50wt% KOH etching (110):(100):(111)=400:200:1
- **Over etching**: produces undercut profile
- **Selectivity** = $\frac{Etch\ rate\ of\ target\ film}{Etch\ rate\ of\ mask}:1$
- **Loading effect**: effect of total area to be etched
- Feature size effect and aspect ratio effect

Wet and Dry Etching

Classification			Example
Wet Etching (Chemical)		Isotropic	HNA for Si BOE for SiO_2
		Anisotropic	KOH, TMAH for Si
Dry Etching	Plasma-based	Physical (Anisotropic)	Ion beam milling
		Physical+chemical (Anisotropic)	RIE, ICP
	w/o Plasma	Chemical (Isotropic)	XeF_2 for Si

(TMAH: Trimethyl-2-hydroxyethyl ammonium hydroxide)

Isotropic Etching

Isotropic Etching of Silicon

- **Hydrofluoric/Nitric/Acetic acids (HNA)**
  - **Oxidation by charge transfer and dissolution reaction**
    $HNO_3 + H_2O + HNO_2 \rightarrow 2HNO_2 + 2OH^- + 2h^+$
    $Si^{4+} + 4OH^- \rightarrow SiO_2 + H_2$ (Hole injection followed by oxidation)
    $SiO_2 + 6HF \rightarrow H_2SiF_6 + 2H_2O$ (dissolution of hydrated silicon)
    $Si + HNO_3 + 6HF \rightarrow H_2SiF_6$ (water soluble) $+ HNO_2 + H_2$ (g) $+ H_2O$
  - **Concentration determines etch rate**
    High HF/Low HNO_3: Etch rate controlled by HNO_3 concentration and oxidation step, Si → SiO_2 (see the next page)
    Low HF/High HNO_3: Etch rate controlled by HF concentration and removal of SiO_2 layer
  - **Agitation** is important
  - **Masking material**: SiO_2 (300-800 Å/min) for shallow etching
    Au or Si_3N_4 (no etching) for deep etching

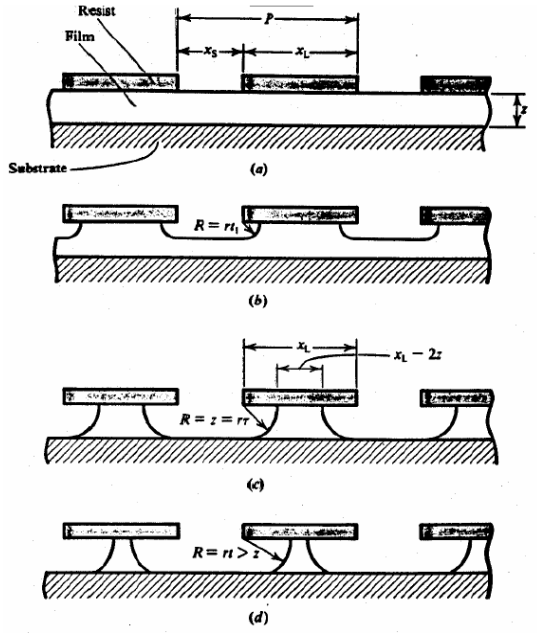

Isotropic Etching of Silicon

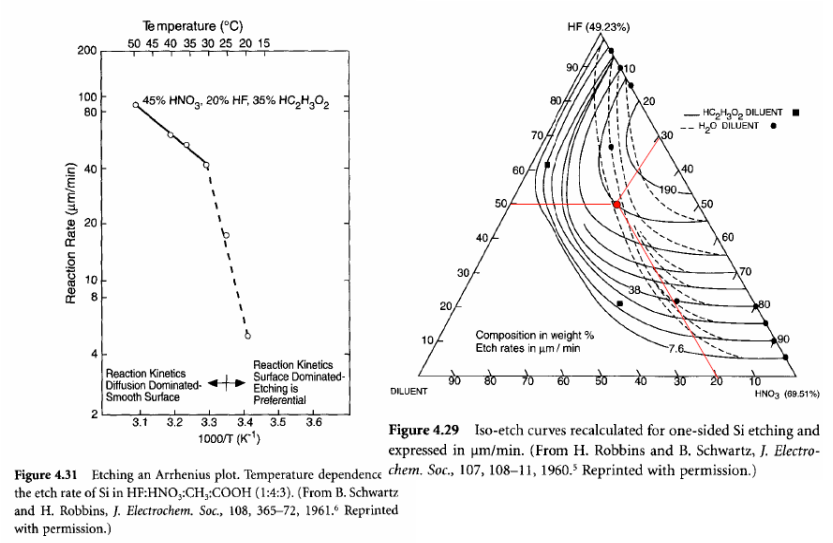

Figure 4.31 Etching an Arrhenius plot. Temperature dependence the etch rate of Si in HF:HNO_3:CH_3COOH (1:4:3). (From B. Schwartz and H. Robbins, *J. Electrochem. Soc.*, 108, 365–72, 1961.[6] Reprinted with permission.)

Figure 4.29 Iso-etch curves recalculated for one-sided Si etching and expressed in μm/min. (From H. Robbins and B. Schwartz, *J. Electrochem. Soc.*, 107, 108–11, 1960.[5] Reprinted with permission.)

Isotropic Etching of SiO_2 and Si_3N_4 Films

- Diluted HF (6:1, 10:1, and 20:1).
  HF (6:1) etches thermally grown SiO_2 at about 1200 Å/min.
- Chemical reaction
  $SiO_2 + 6HF \rightarrow H_2SiF_6 + 2H_2O$
- To avoid etch rate decrease with time (due to the consumption of HF), a buffering agent (NH_4F) is added → "BOE"
  $NH_4F \rightarrow NH_3 + HF$
- Si_3N_4 is also etched by HF but much slower than SiO_2
  SiO_2 300 Å/min, Si_3N_4 10 Å/min in HF (20:1) @ room temp.
- H_3PO_4 (140-200°C) is a common etchant for Si_3N_4. Typical selectivities are 10:1 for nitride over oxide and 30:1 for nitride over silicon (polysilicon is a good mask material).

Anisotropic Etching

Anisotropic Etching of Silicon

- Etch-rate limited process → Temperature dependent
- Slower than isotropic etching but solved the lateral dimension control lacking in isotropic etchant
- Etchant
  - Alkaline aqueous solutions (KOH, NaOH, CsOH, NH_4OH,…)
  - Alkaline organics (Ethylenediamine/Pyrazine-EDP, Trimethyl-2-hydroxyethyl ammonium hydroxide-TMAH,…)
- Orientation dependence: Etch rate (110) > (100) > (111) ~ 400:200:1
- Reaction rate is plane dependent because of availability of back-bonds to chemical attack.

Wafer Orientation

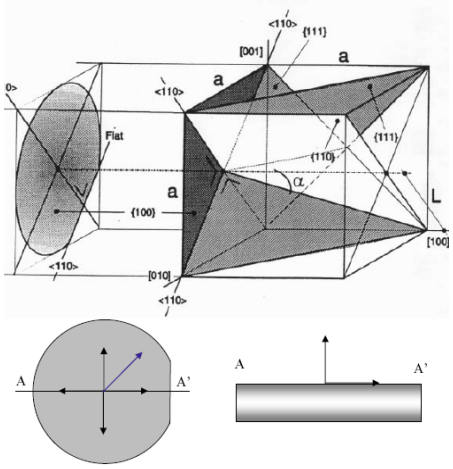

Etch Rate

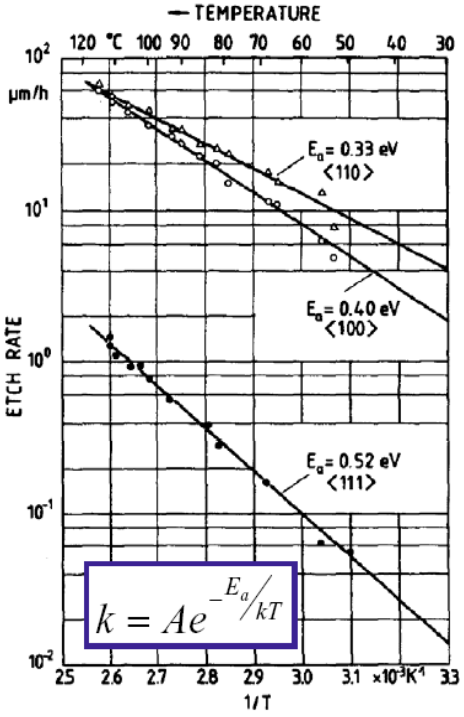

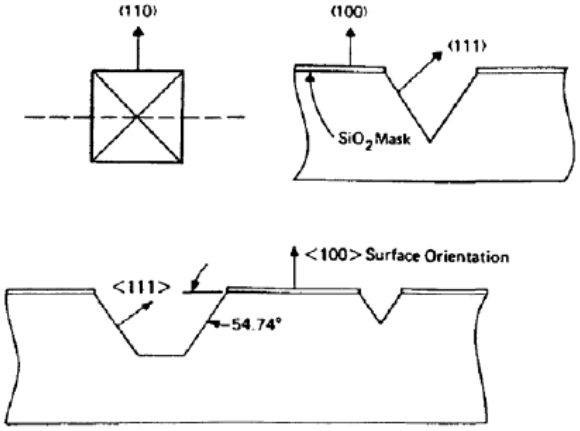

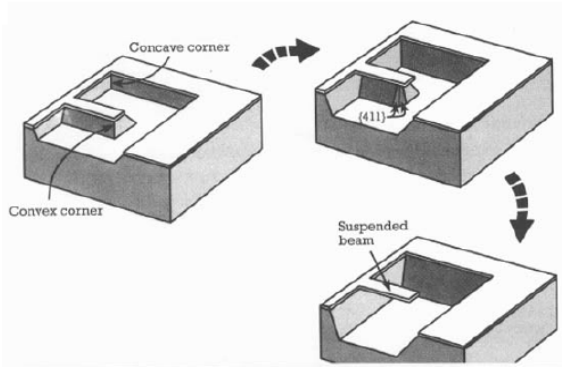

Figure 4.34 Vertical etch rates as a function of temperature for different crystal orientations: (100), (110), and (111). Etch solution is EDP (133 mL H_2O, 160 g pyrocatechol, 6 g pyrazine, and 1 L ED). (From H. Seidel, et al., *J. Electrochem. Soc.*, 137, 3612–26, 1990.[106] Reprinted with permission.)

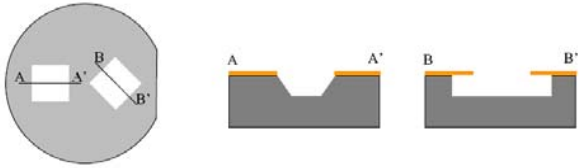

2.3 Surface Micromachining (Additive)

Additive Processes

- Two major categories
  - **PVD**: Direct line-of-sight impingement deposition techniques
    - **Thermal evaporation**
    - **Sputtering**
  - **CVD**: A diffusive-convective mass transfer technique.
    - **LPCVD**
    - **PECVD**
- Other deposition techniques commonly used in MEMS
  - Spin coating, dip coating (polymers)
  - Electrochemical deposition (metals)

Thermal Evaporation

- The boiling off (or sublimating) of a heated material onto a substrate in a vacuum.
- **Common evaporation methods for metal deposition**
  - Resistive heating (filament) or electron beam (E-beam) heating
  - Deposition rate (50-500 nm/min)

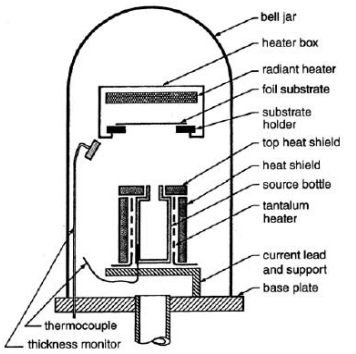

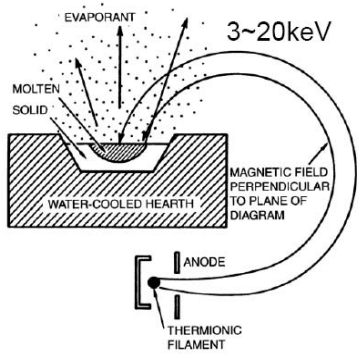

Sputtering

- The target at the high negative potential is bombarded with positive argon ions created in a plasma. The target material is sputtered away mainly as neutral atoms and the ejected atoms are deposited onto the substrate placed on the anode.
- Metals (DC sputtering), insulators (RF sputtering)

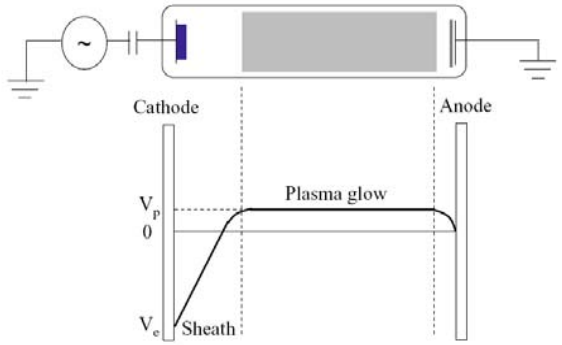

Sputtering vs. Evaporation

- **Wider choice of materials**
  - Metals (Al, Cr, Au, Ni, Pt, Ti, etc.)
  - Insulators (SiO_2, Si_3N_4, Ta_2O_5, etc.) – RF sputtering
  - Compound semiconductors such as Indium tin oxide (ITO)
- **Better step coverage:** Because of the multiple collisions of the metal atoms in the path between the cathode and the anode, the metal atoms arrive at the anode at random incident angles.
- **Better adhesion to the substrate** at low pressure (Sputtered atoms have higher energy).
- Widely used in CD, DVD industry

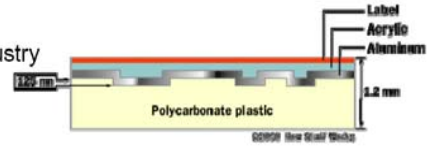

- **Disadvantages**

  Slower deposition rate, heating due to secondary electron bombardment

Chemical Vapor Deposition

Chemical Vapor Deposition (CVD)

- A diffusive-convective mass transfer technique

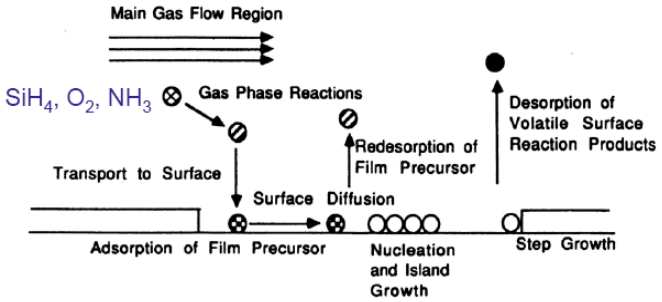

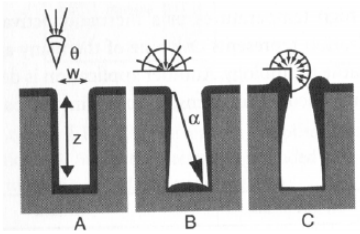

LPCVD

- Horizontal tube, hot wall reactor

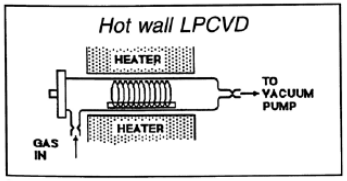

- **Low pressure (< 10 Pa)**
  → Large diffusion coefficient
- **Excellent purity, uniformity, conformal step coverage, and large wafer capacity.**
- LPCVD polysilicon is used as structural layers in surface micromachining, and LPCVD SiO_2 and phosphosilicate glass (PSG) are used as sacrificial layers.
- **Disadvantages**
  High operating temperature (500-900°C).

PECVD

- **Lower substrate temperatures (250-350°C), fast, good adhesion, good step coverage**

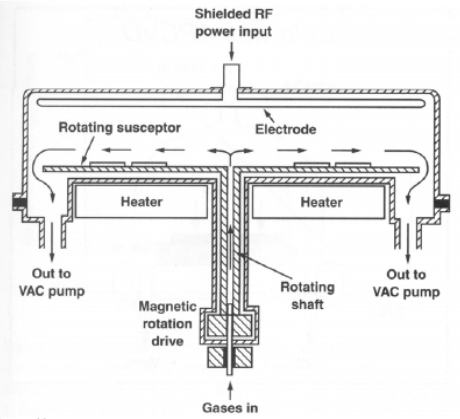

- Disadvantage: contamination
- Just as RIE etching occurs mainly through neutral species, deposition almost exclusively involves neutrals.

Surface Micromachining Process Steps

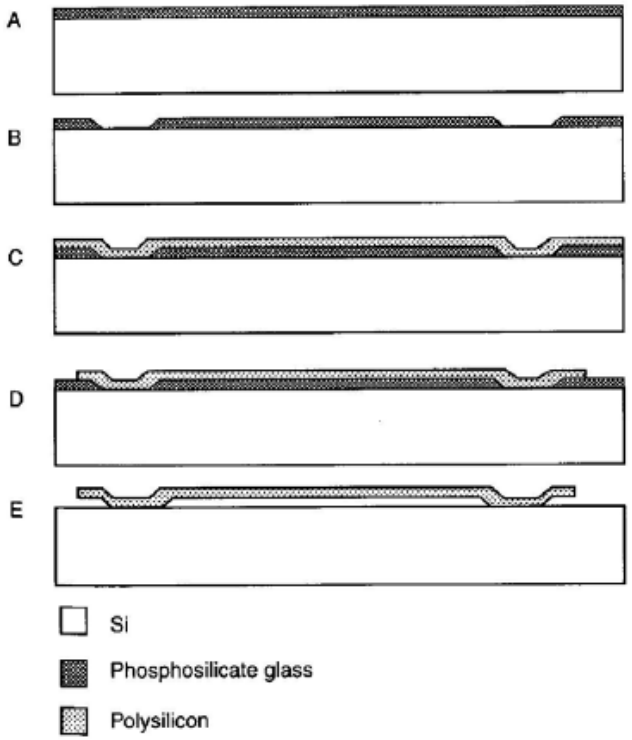

Figure 5.13 Basic surface micromachining process sequence. (A) Spacer layer deposition (the thin dielectric insulator layer is not shown). (B) Base patterning with mask 1. (C) Microstructure layer deposition. (D) Pattern microstructure with mask 2. (E) Selective etching of spacer layer.

From Madou, *Fundamentals of Microfabrication*

MEMSCAP's POLYMUMPS

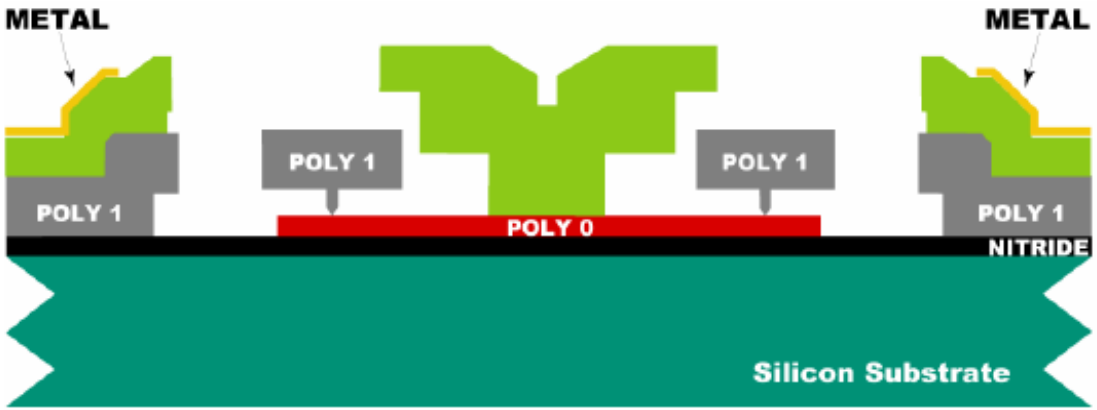

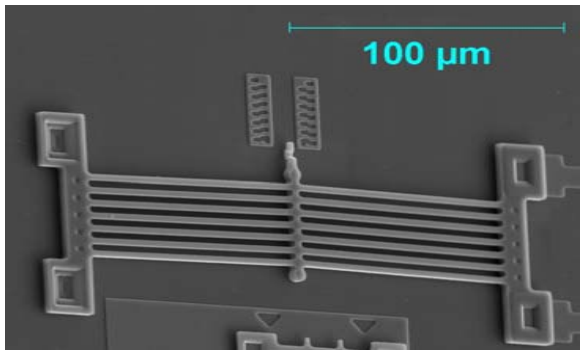

Sandia's SUMMiT V Process

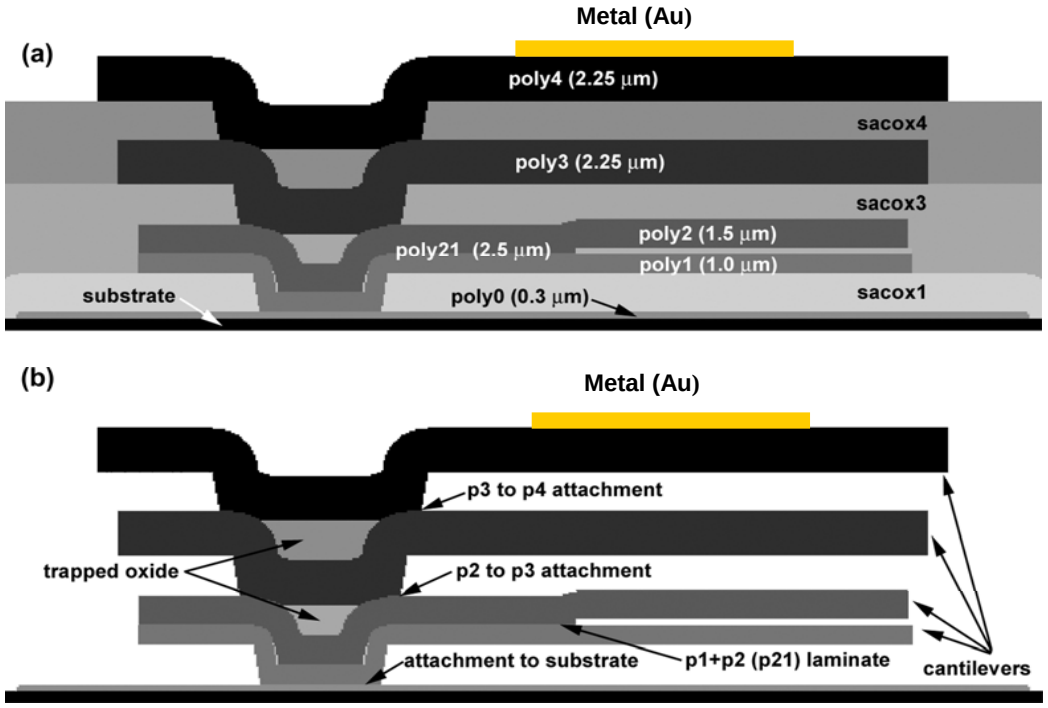

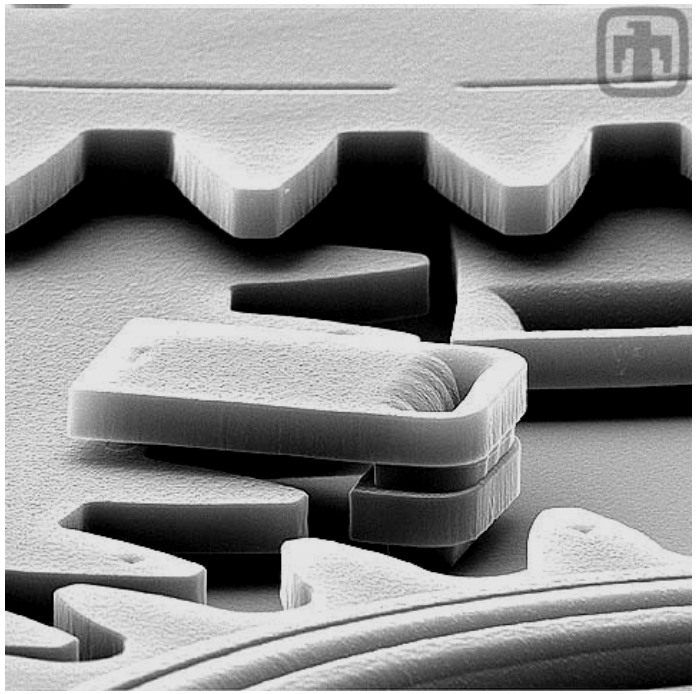

MEMSCAP's SOIMUMPS

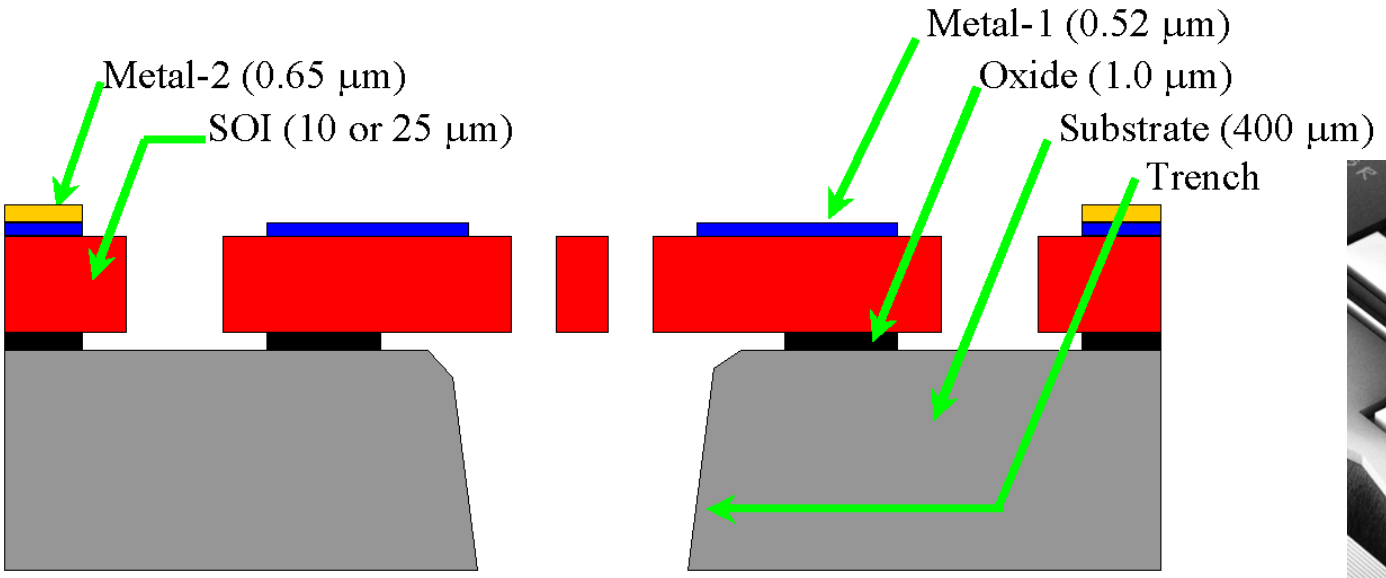

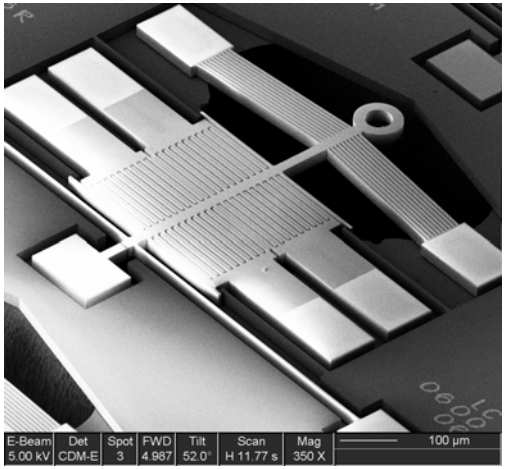

The Brittle Nature of Silicon Makes Its Structural Reliability Challenging

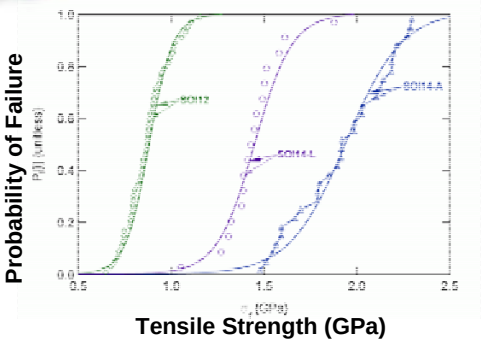

1. ***Statistically Unreliable.*** **While Silicon has a "typical" or characteristic strength of >>1 GPa, there is a lot of scatter in the distribution of strengths.**

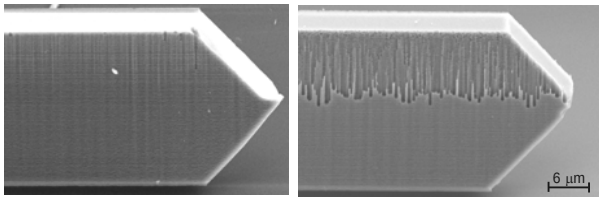

2. ***Process Sensitive.*** ***Strength is strongly dependent on process conditions.***

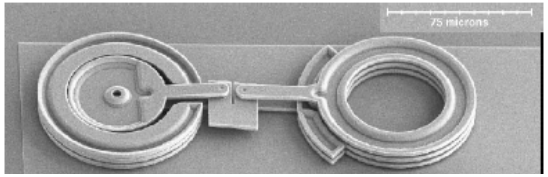

3. ***Low Toughness.*** ***Fracture toughness ~1.0 MPa$\sqrt{m}$ is like window-pane glass! Very small flaws cause fracture.***

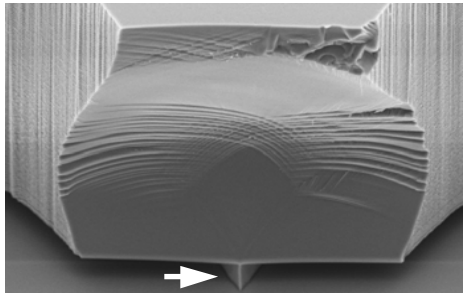

4. ***Sensitive to Flaws and Stress-Concentrations.*** ***No ability to accommodate unexpected flaws or stress-concentrations.***

2.4 Micromolding

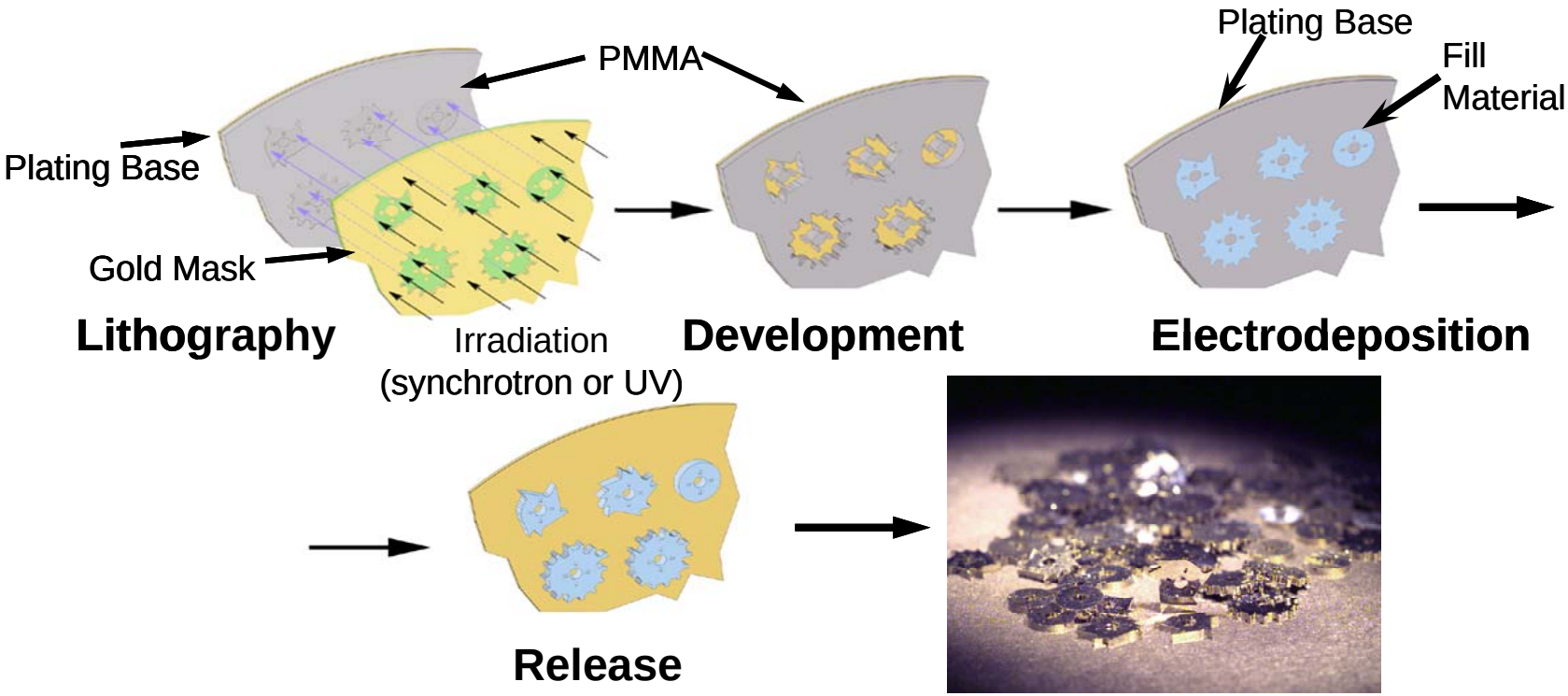

Microfabrica

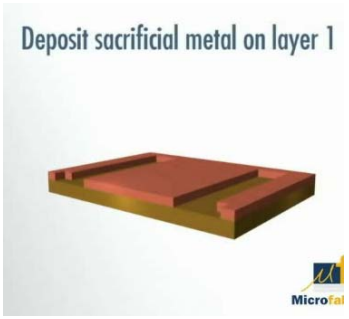

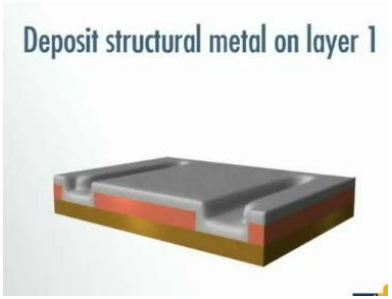

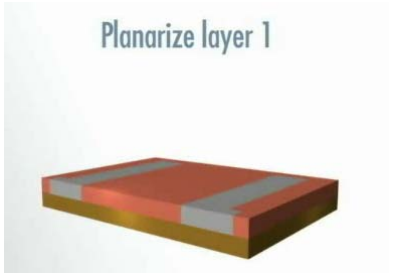

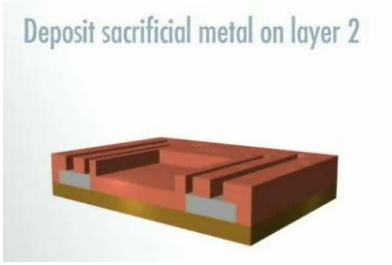

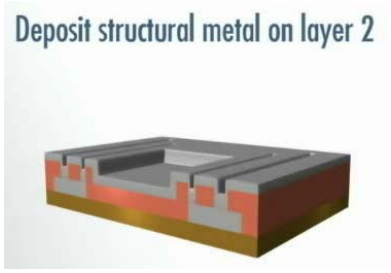

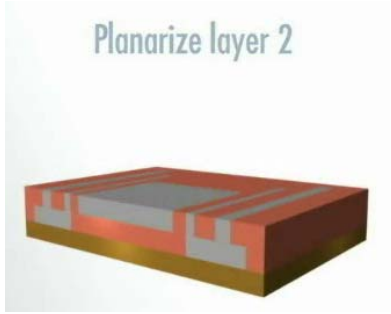

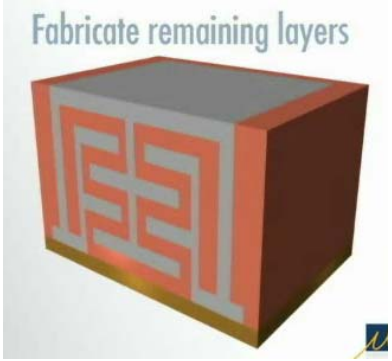

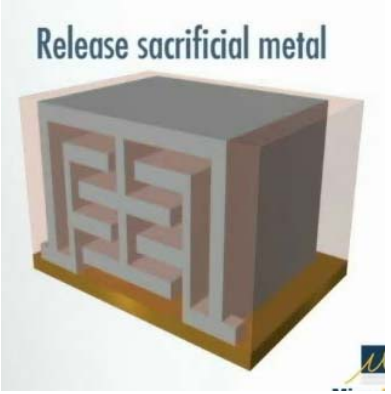

Microfabrica patterns Cu as the sacrificial layer interspersed with electrodeposited Ni-based or Rh-based alloy layers at the structural layer. Sulfuric acid etches Cu preferentially over Ni.

Microfabrica

Advantages of Microfabrica Process (from website):

» Mechanisms with multiple moving parts made without assembly
» Intricate free-form shapes, including internal features
» Features smaller than 5 µm [0.0002 inch]
» 2 µm [0.00008 inch] accuracy and repeatability
» All designs made by a single, well-characterized process
» Net shape fabrication, without burrs or artifacts and thus ready-to-use
» Multiple design variations produced in parallel
» Complex geometries for the price of simple ones
» Low-cost volume production in a matter of weeks

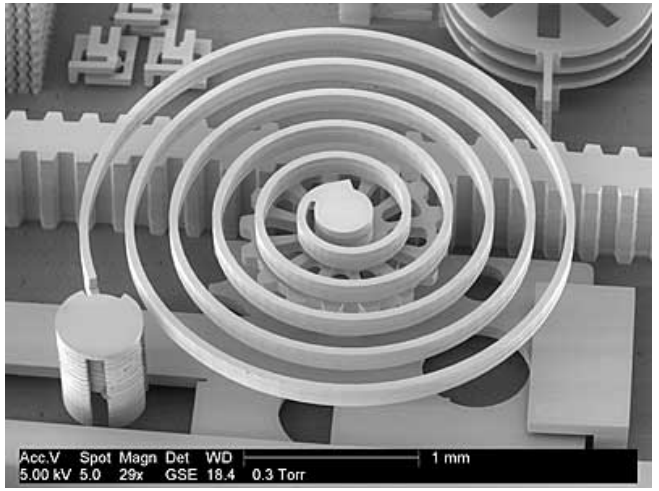

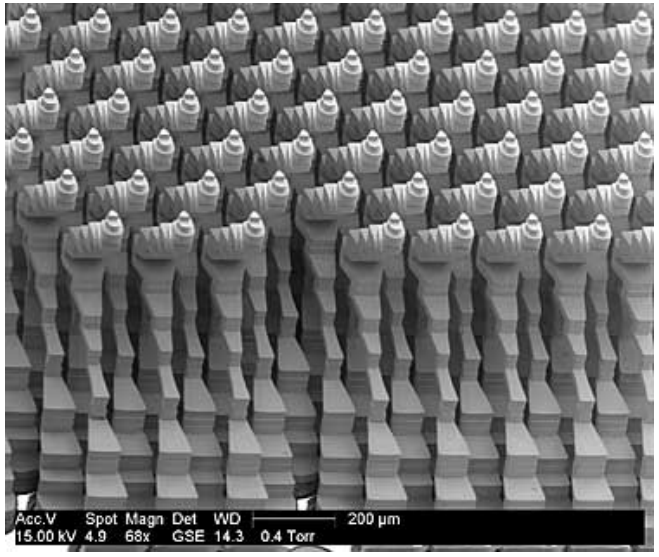

Valloy-120 Material Properties (Ni-Co alloy)

Ultimate tensile strength, MPa [ksi]	1,100 [160]
Yield strength, MPa [ksi]	900 [131]
Hardness, HV [Rc]	>400 [~40 Rc]
Modulus of elasticity, GPa [ksi]	180 [26,107]
Density, g/cm3	8.9
Interlayer adhesion, MPa [ksi]	~600 [87]
Fatigue life, MPa [ksi]	Infinite @ <400 [58] stress

Edura-180 Material Properties (Rhodium)

Hardness, HV [Rc]	>940 [>68 Rc]
Density, g/cm3	12.4

2.5 Alternative fabrication methods

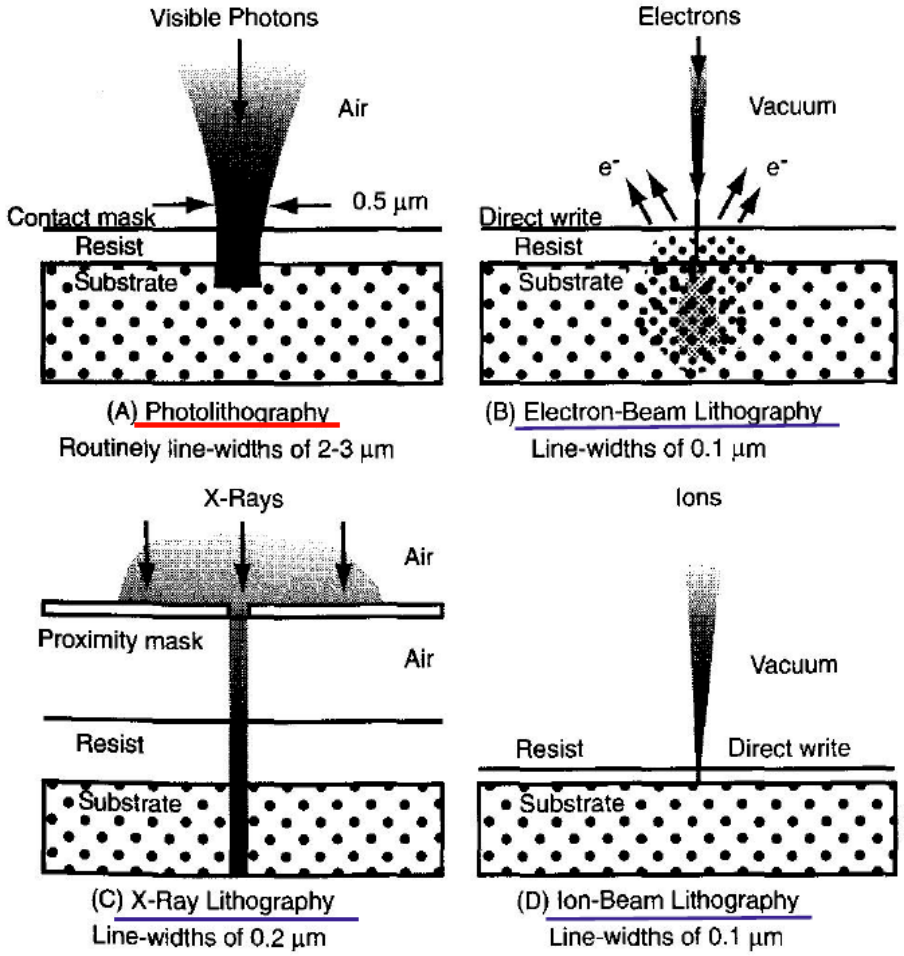

MicroEDM, MicroGrinding

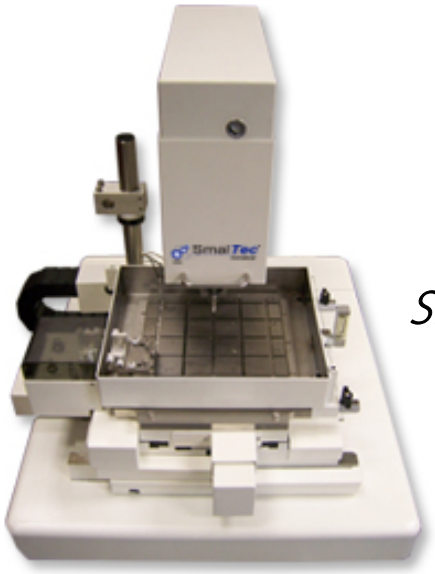

Smaltec EM203

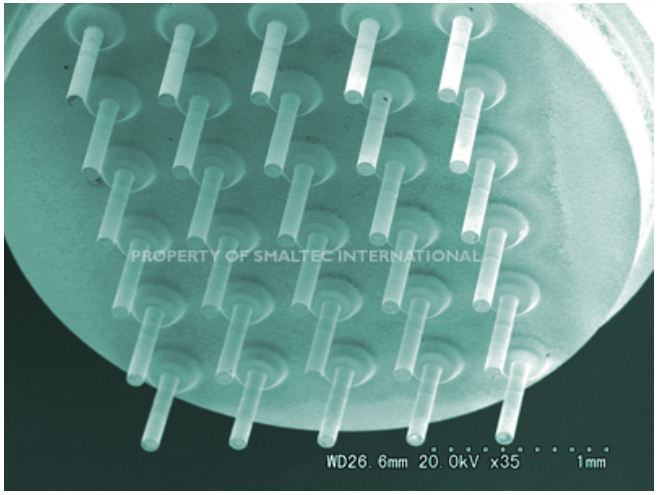

- micrometer (micron or µm) dimensions to within +/- 100 nanometers (nm) tolerances.
- True CNC movement in all 3 axes
- Any electrically conductive material can be machined
- Perfect round holes as small as 4 µm diameter (0.00015").
- Complex micro patterns to true 3-D contoured shapes.
- Ultra-high precision machining can be done on curved surfaces, inclined surfaces and thin materials, which are very difficult to produce with other available technologies.
- A mirror finish surface roughness of 10 nm Rmax, or 2.8 nm RMS, can be achieved.
- 8" x 8" work area
- Automatic part detection and location
- Auto tool wear compensation

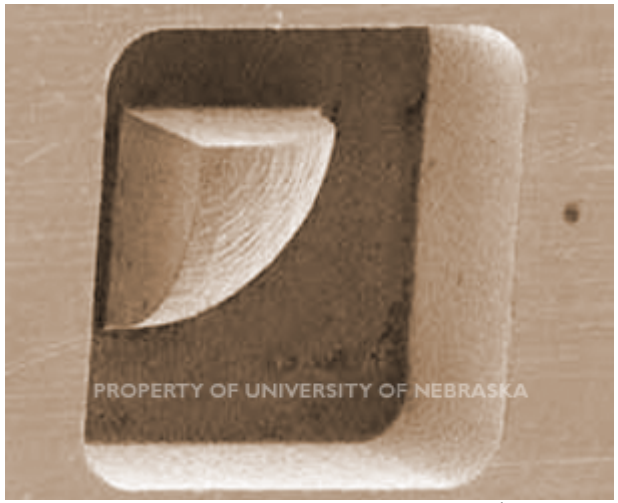

www.smaltec.com

A Fast, Brief Primer On Microfabrication…

IS COMPLETE…

Outline

1. Introduction
2. MEMS fabrication technologies
3. Examples of passive devices for nanomechanics
   1. Cantilevers
   2. Residual stress indicators
   3. Tensile testers
4. Passive device technology
5. Active device technology
6. Examples of active devices for nanomechanics

3.1 Cantilevers

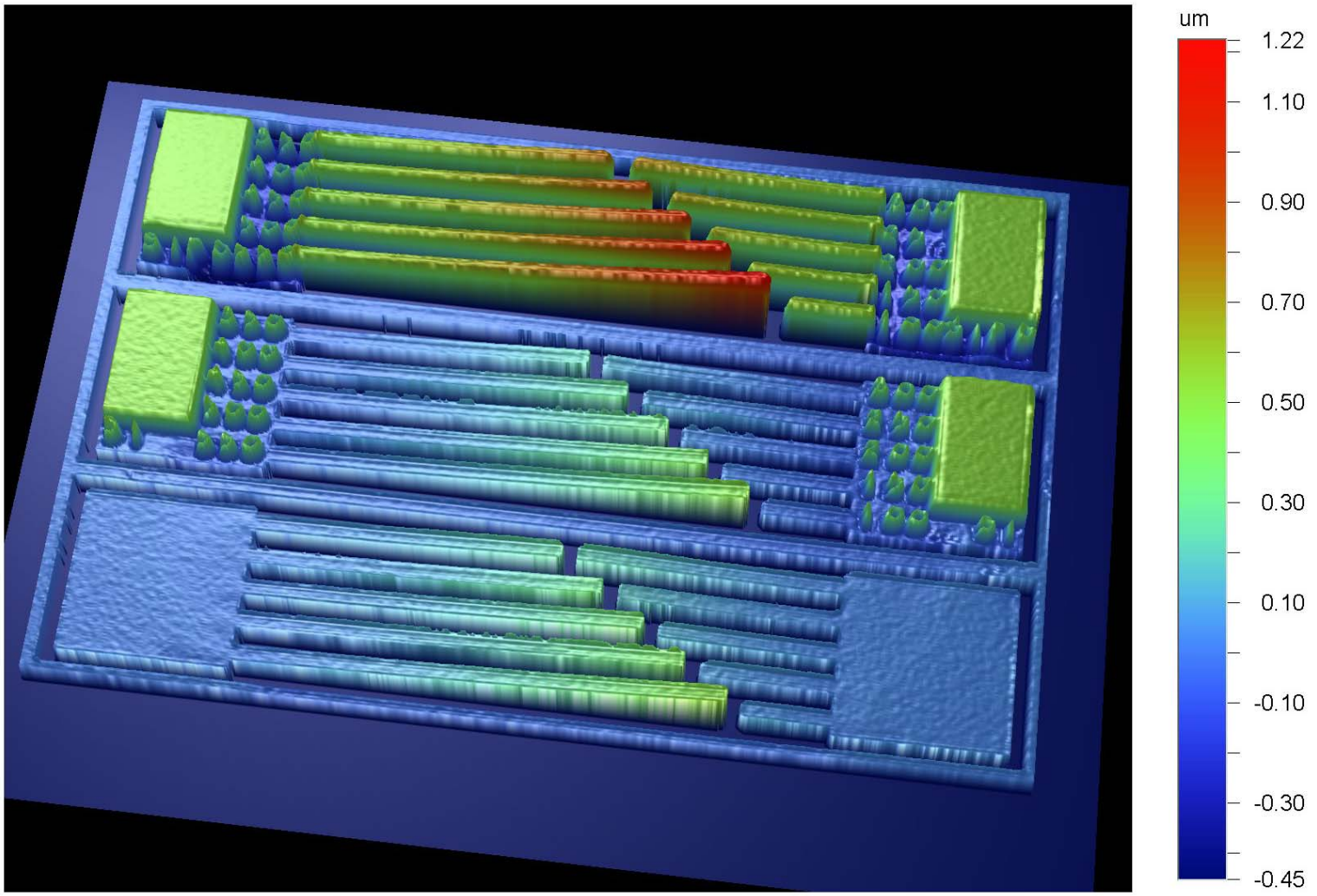

The Most Common MEMS Cantilever For Nanomechanics: AFM Cantilevers

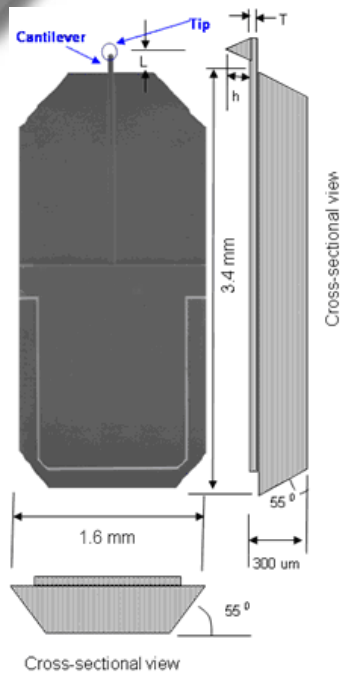

Standard cantilever types for common applications:

Dynamic mode / tapping mode AFM Available as a long (225 µm) or short (125 µm) cantilever	Length: Typically 125 - 225 µm Width: Typically 40 µm Thickness: 4 - 8 µm Resonant Freq: 190 - 300 KHz Spring Constant: 40 - 48 N/m
Force Modulation mode AFM	Length: Typically 225 µm Width: Typically 45µm Thickness: 2.5 µm Resonant Freq: 60 KHz Spring Constant: 3 N/m
Contact mode AFM Available as a long (450 µm) or short (225 µm) cantilever	Length: Typically 225 - 450µm Width: Typically 28-40 µm Thickness: 1- 2 µm Resonant Freq: 12 - 28 KHz Spring Constant: 0.1 - 0.2 N/m

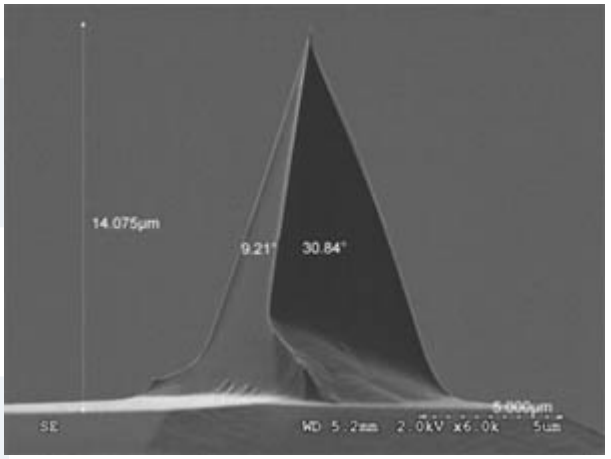

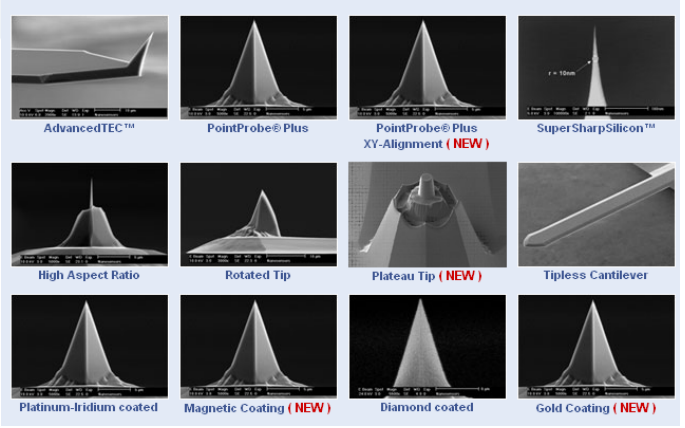

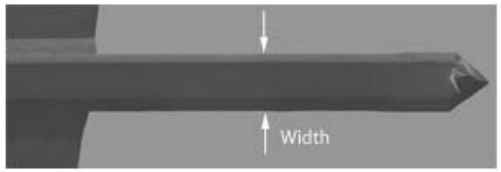

AFM Cantilevers are specified by their width, length, and thickness.

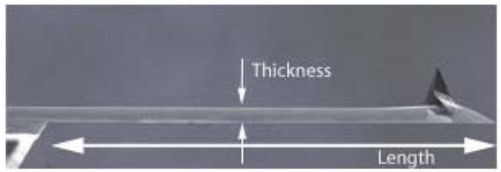

These parameters determine important factors like resonance frequency and spring constant.

AFM Tips are Typically Bulk Micromachined Monolithic Silicon or Si_3N_4. Their compliant response and integrated laser-interference sensing deflection make them nearly ideal high-resolution load cells.

Standard cantilever types for common applications:

The Most Common MEMS Cantilever For Nanomechanics: AFM Cantilevers

An Individual MWCNT

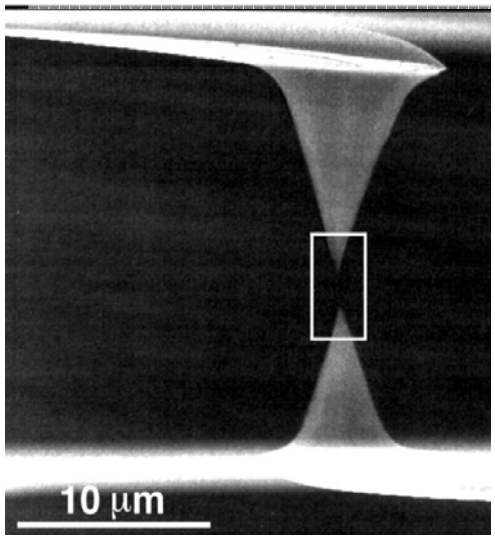

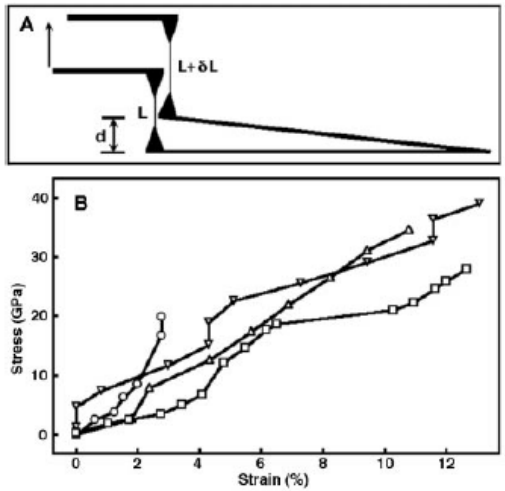

Operation
- displacement range ~ 15 μm
- applied force range ~ 1.5 μN
- K_{LC} = 0.1 N/m

Yu, Lourie, Dyer, Moloni, Kelly, and Ruoff, *Science*, 2000

This highly cited work on the mechanical deformation of mutliwalled carbon nanotubes from 2000 shows one of the first applications of AFM cantilevers/tips to nanomechanics. One challenge that remains is how to attach the nanowire or nanotube to the AFM tips. In this case, it was accomplished by electron beam-induced deposition of carbonaceous material from vacuum impurities.

MEMS Cantilevers As A Test Platform

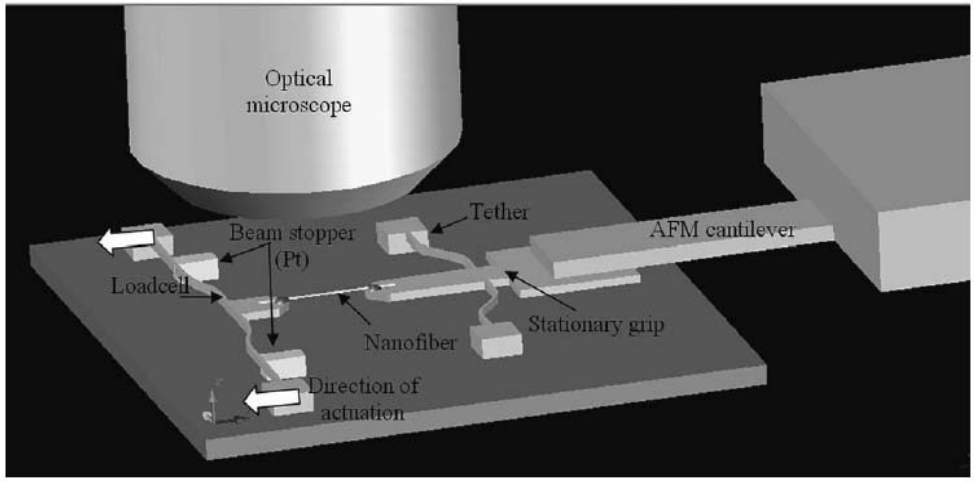

FIG. 1. Application of the test platform for nanofiber testing. The fiber length in this figure is 50 μm.

Electrospn polyacrylonitrile nanofibers were tested on a MEMS test bed with external AFM piezoelectric actuation and optical digital image correlation of crosshead displacements. The AFM cantilever was epoxied to hold the stationary grip rigid during the piezotranslation of the stage. The "tether" maintained planarity of motion. The device loadcell was calibrated against an AFM cantilever of known stiffness.

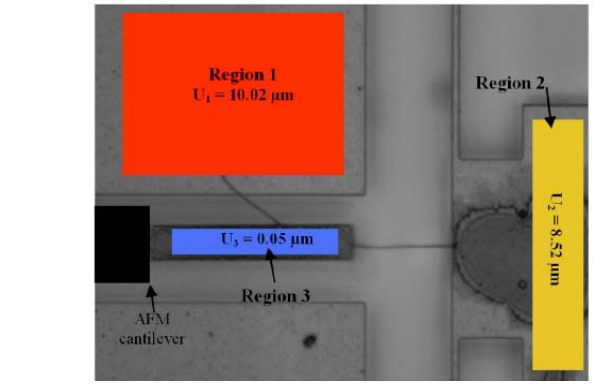

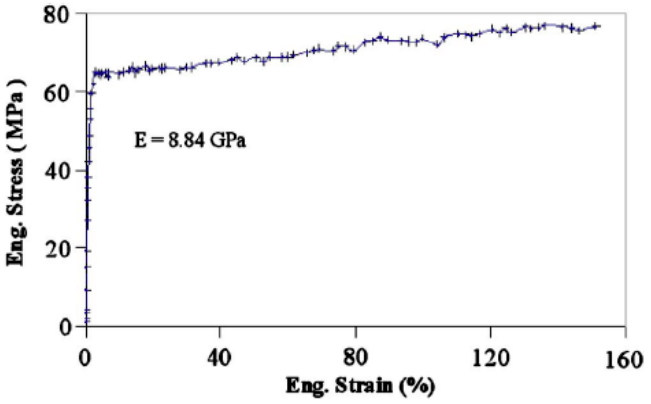

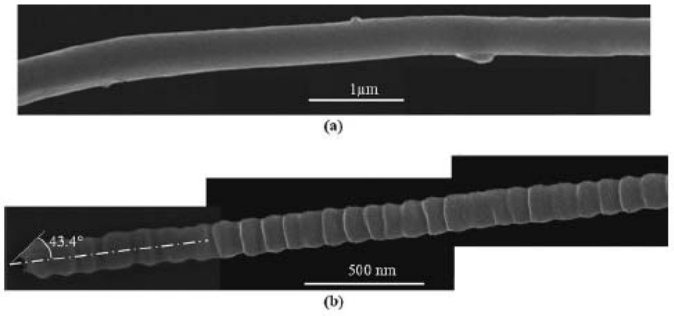

FIG. 6. SEM images of (a) undeformed PAN nanofiber and (b) deformed PAN nanofiber, with multiple surface ripples formed during drawing. The fracture surface is typical for ductile fracture.

Naraghi, Chasiotis, Kahn, Wen, and Dzenis, *Rev Sci Inst*, 2007

Cantilever Arrays as Force Probes

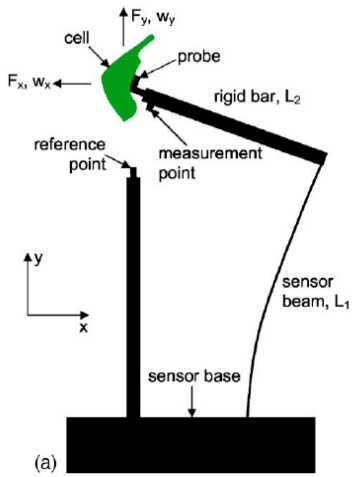

$$\begin{bmatrix} F_x \\ F_y \end{bmatrix} = \frac{2EI}{L_1^3} \begin{bmatrix} 6 & 3\frac{L_1}{L_2} \\ 3\frac{L_1}{L_2} & 2\left(\frac{L_1}{L_2}\right)^2 \end{bmatrix} \begin{bmatrix} w_x \\ w_y \end{bmatrix}$$

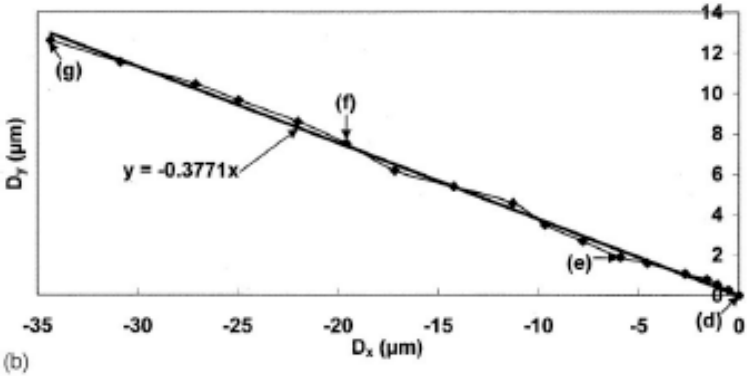

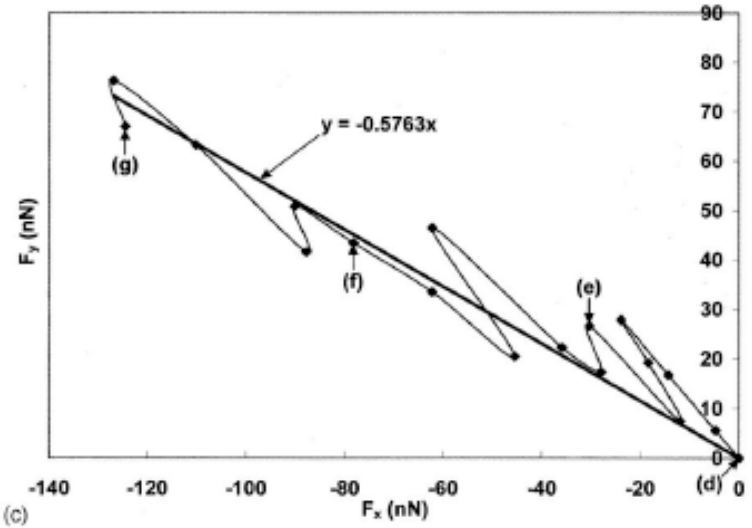

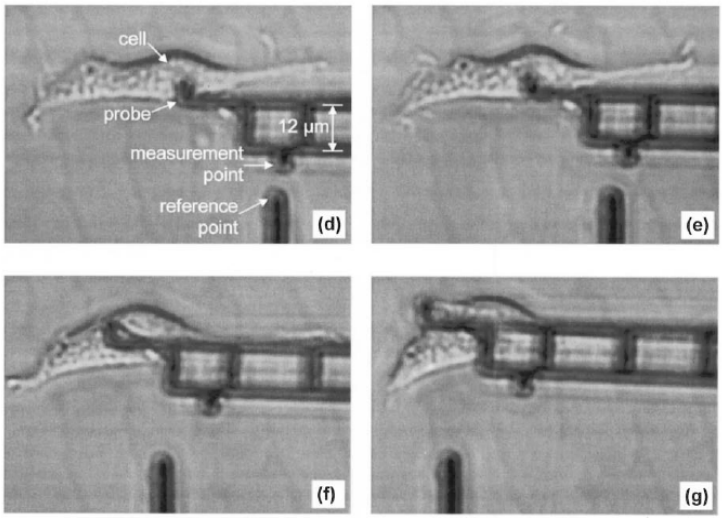

Yang and Saif, *Rev Sci Inst,* 2005

Center For Integrated Nanotechnology (CINT) Nanomechanics "Discovery Platform"

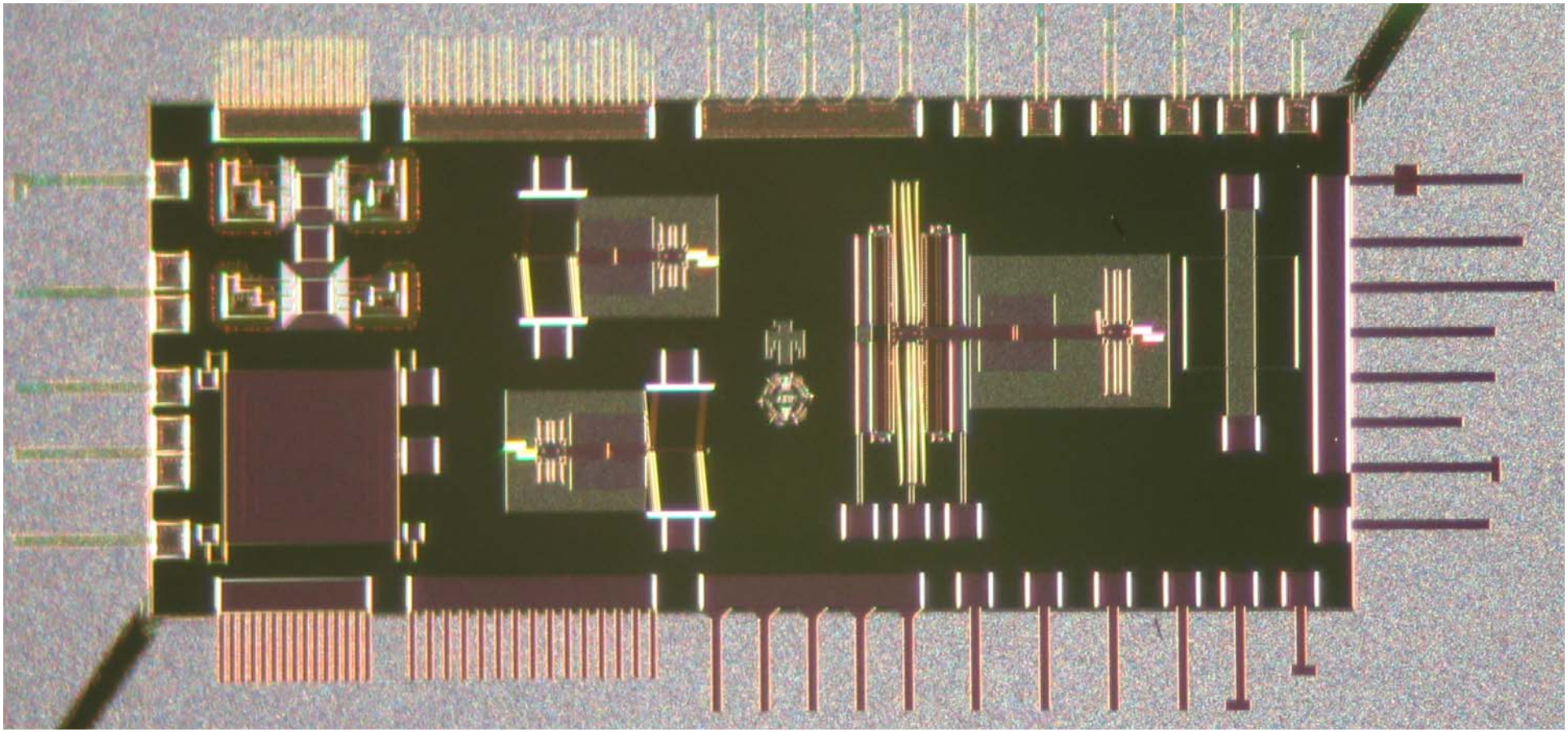

Center For Integrated Nanotechnology (CINT) Nanomechanics "Discovery Platform"

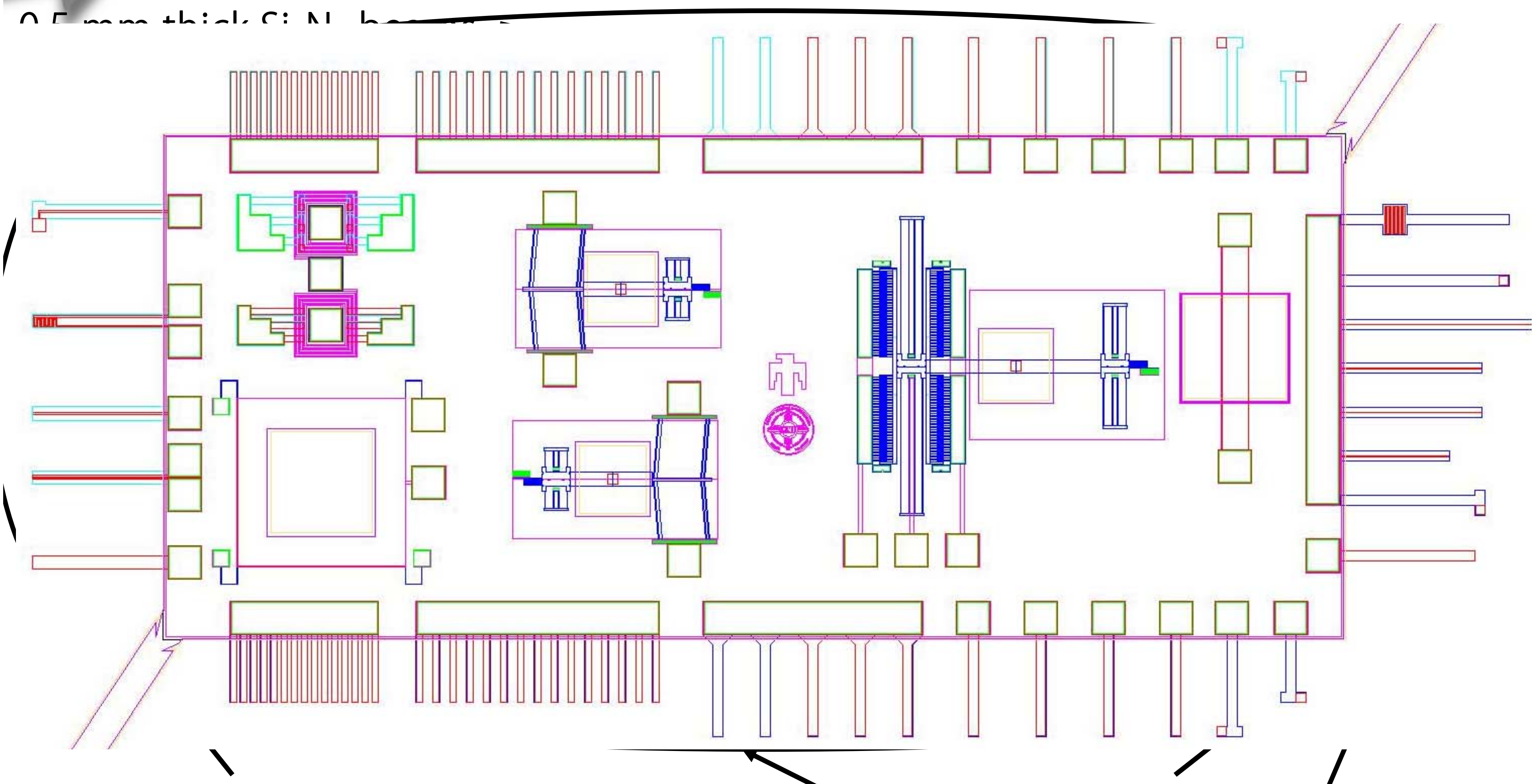

2.25 mm thick doped polycrystalline Si beams

... defined material

... beams, MEMS structures, contact pads, etc.

Other features of the CINT Nanomechanics Discovery Platform

Shadow mask allows deposition of user-defined materials In certain regions of the test structures.

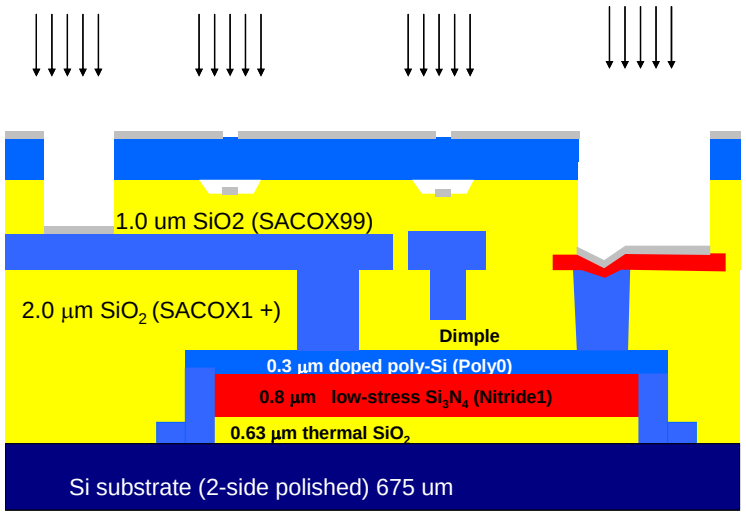

Chip size is designed to match AFM chips so that cantilevers can be used as functionalized AFM tips.

CINT Nanomechanics Chip

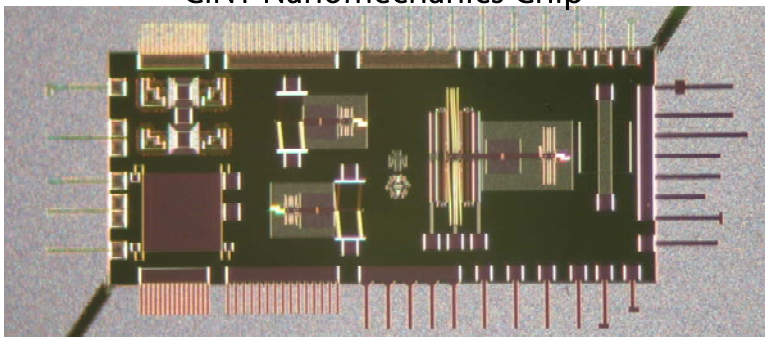

Standard AFM Chip

Discovery Platform Information Courtesy of John P. Sullivan, CINT/Sandia

Example Studies Using CINT Cantilevers

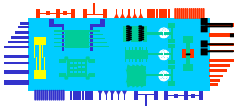

I. Internal dissipation

- *defect relaxation in materials*

$$Q_{defect} = A\left[\frac{\omega\tau^*}{1+(\omega\tau^*)^2}\right]^{-1}, \qquad \frac{1}{\tau^*} = \frac{1}{\tau_0}\exp\left(\frac{-E_A}{k_B T}\right),$$

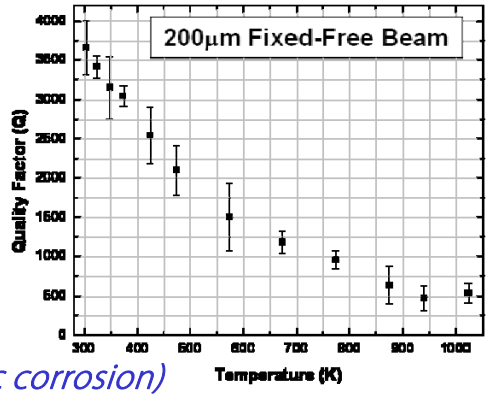

II. Cantilevers as sensors

- *atmospheric corrosion sensing*

Cu-coated cantilever (atmpospheric corrosion)

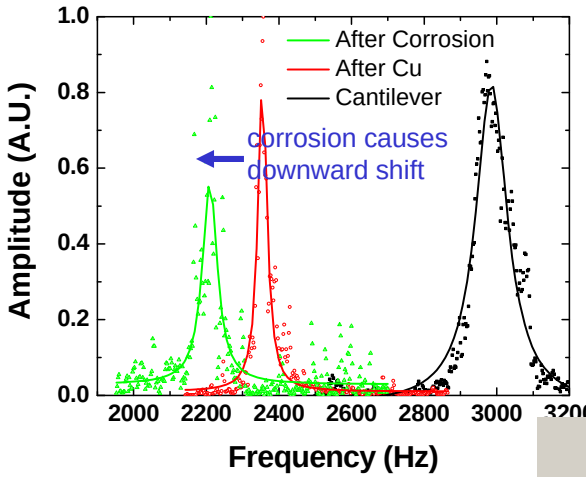

Local corrosion of Al coating

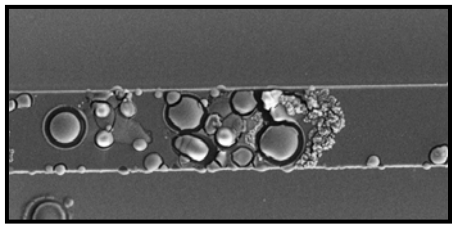

III. Coupled oscillator arrays

- *arrays with low to high degrees of coupling*

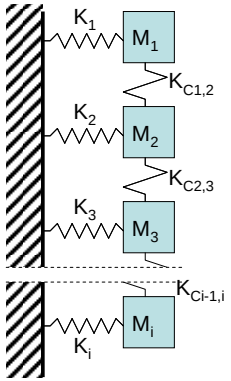

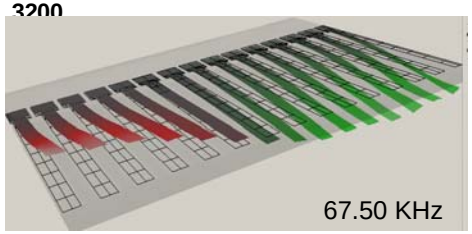

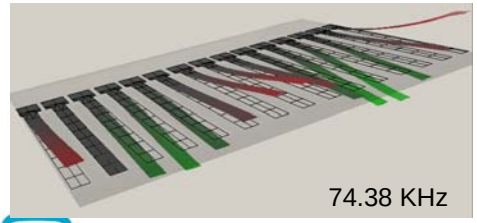

Sandia National Laboratories

CINT Nanomechanics "Chip 2" Contains Additional Structures

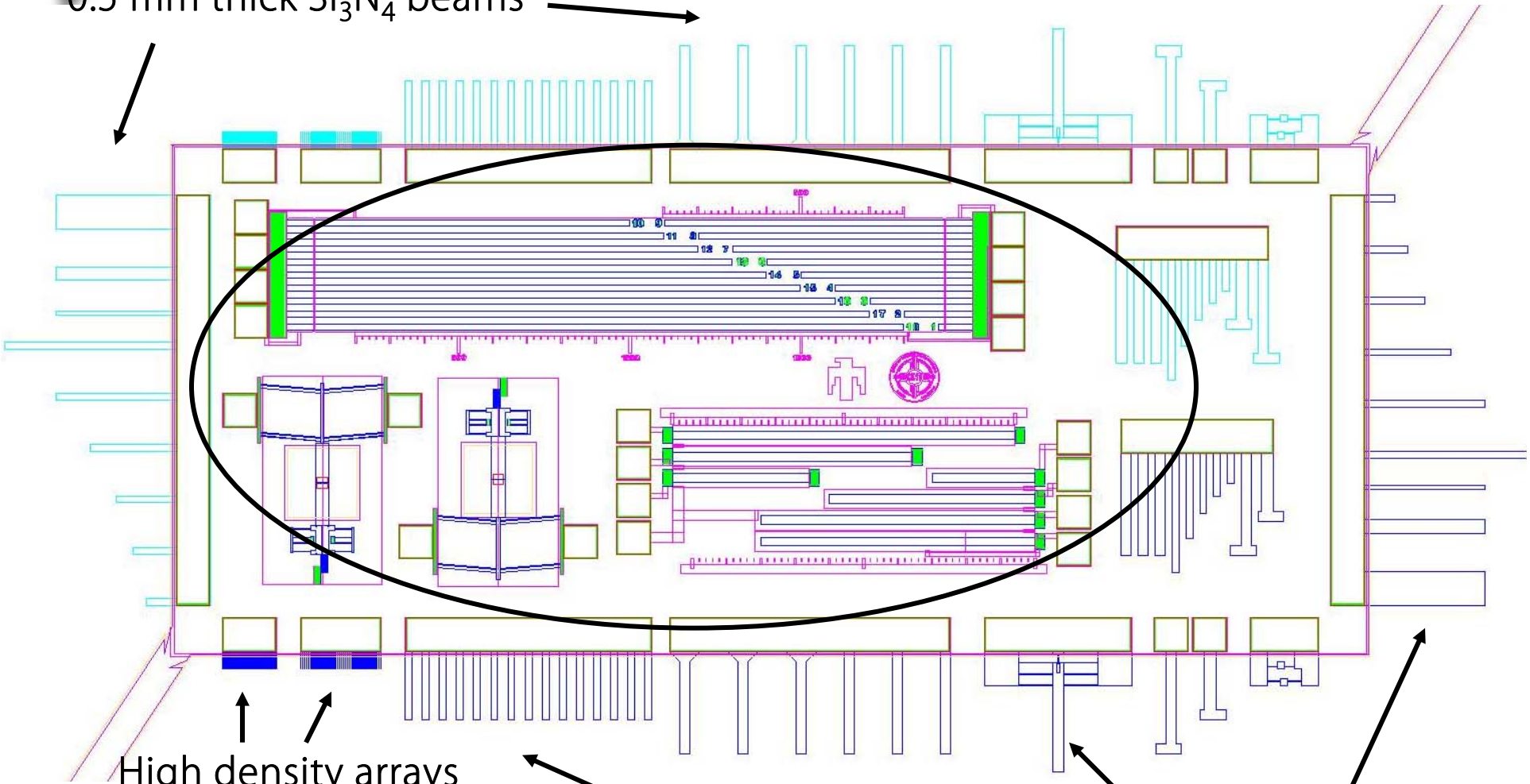

Cantilever Adhesion Structures

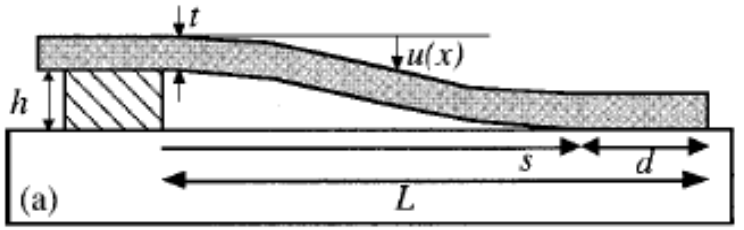

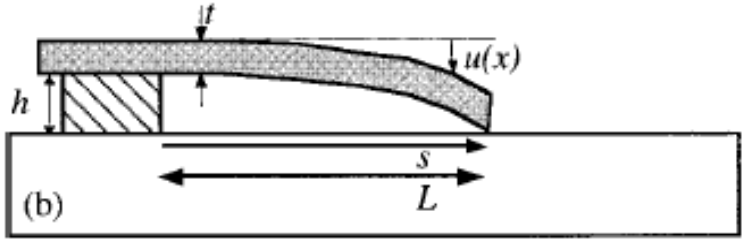

FIG. 1. (a) S-shaped beams ($m=0$) are attached over a long length d. (b) Arc-shaped beams ($m=3/2$) are attached only very near their tips.

Interferometry of Partially-Adhered Cantilevers:

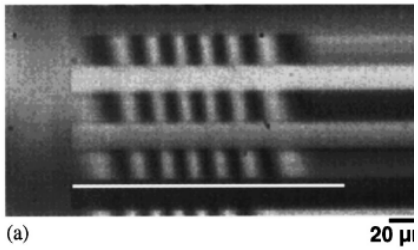

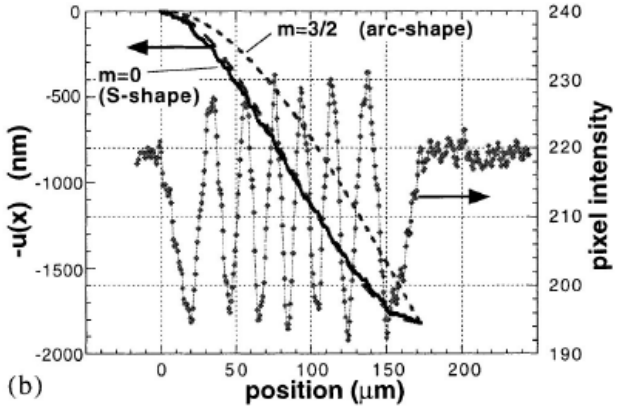

De Boer and Michalske, *J Appl Phys,* 1999

m = "slope" parameter:

$$m(s)=\frac{\frac{16}{5}\left(\frac{t}{d}\right)^3\left(\frac{t}{s}\right)\left[1+\frac{15}{32}\left(\frac{d}{t}\right)^2\left(\frac{E}{G_2}\right)\right]}{1+\frac{32}{15}\left(\frac{t}{d}\right)^3\left(\frac{t}{s}\right)\left[1+\frac{15}{32}\left(\frac{d}{t}\right)^2\left(\frac{E}{G_s}\right)\right]},$$

G = Work of Adhesion, or Strain Energy Release Rate:

$$G=\frac{Et^3h^2}{2}\left\{(3s^{-4})\left[\frac{m^2(s)}{3}-m(s)+1\right]+(s^{-3})\frac{dm(s)}{ds}\left[\frac{2m(s)}{3}-1\right]\right\}.$$

G for specific cases of m:

$$G=\frac{3}{2}\left(\frac{Et^3h^2}{s^4}\right), \quad \text{for } m=0,$$

$$G=\frac{3}{8}\left(\frac{Et^3h^2}{s^4}\right), \quad \text{for } m=3/2.$$

Cantilever Through-Thickness Strain-Gradient Structures

- Out of plane curvature related to through-thickness stress gradient (TTSG)
- Stiffness can be measured by point-deflection (such as via a nanoindenter) or through resonant excitation.

PROCESS	LAYER	CURVATURE {m^{-1}}	MAXIMUM STRESS {MPa}
SOI, 10-μm	SOI	16.7 ± 0.4	14.0 ± 0.3
SOI, 10-μm	SOI+ Metal-1	39.1 ± 2.2	N/A
SOI, 25-μm	SOI	2.5 ±0.9	5.3 ± 1.9
SOI, 25-μm	SOI+ Metal-1	4.3 ± 0.9	N/A
PolyMUMPs	Poly-1	2.5 ± 4.2	0.4 ± 0.7
PolyMUMPs	Poly-2	-27.7± 3.4	3.4 ± 0.4
PolyMUMPs	Poly-2+ Metal	253.5 ± 6.6	N/A
PolyMUMPs	Poly-1+ Poly-2	0.8 ± 2.3	0.2 ± 0.7
PolyMUMPs	Poly-1+ Poly-2+ Metal	69.5 ± 2.9	N/A
PolyMUMPs	Poly-1+ Oxide-2+ Poly-2	-42.6 ± 2.9	N/A
PolyMUMPs	Poly-1+ Oxide-2+ Poly-2+ Metal	27.3± 0.9	N/A

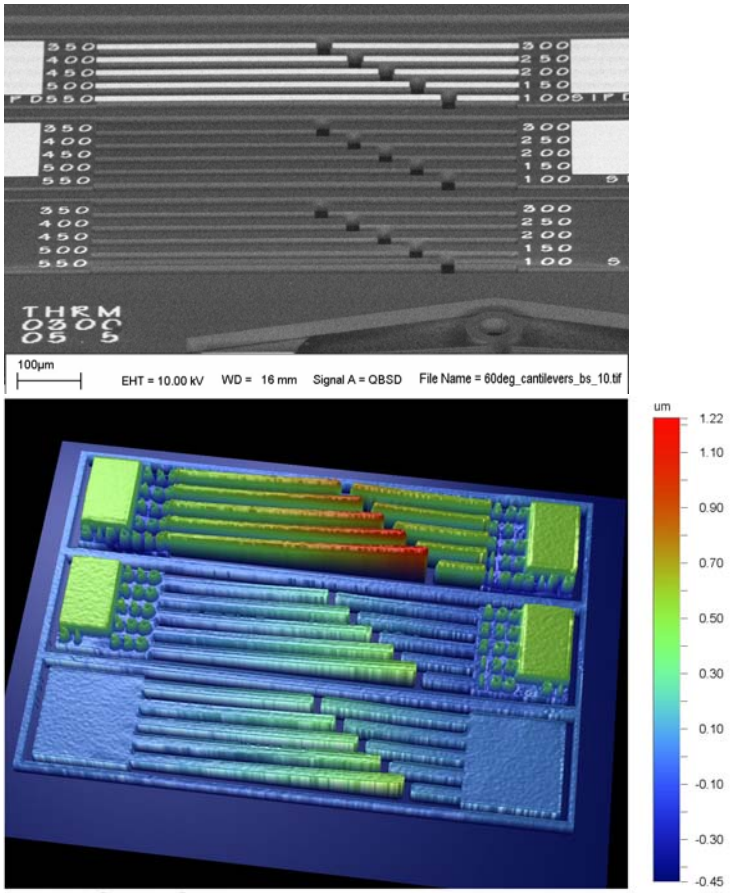

WYKO interferograph (Oblique view)

$$\delta_{fixed-free} = \frac{PL^3}{3EI} \qquad \delta_{fixed-guided} = \frac{PL^3}{12EI}$$

Curvature, from polynomial fit (WYKO):

$$\kappa = \frac{\partial^2}{\partial x^2} F(x)$$

Curvature vs. mechanics vs. shape:

$$\kappa = \frac{1}{\rho} = \frac{M}{EI} = \frac{2\delta}{\delta^2 + L^2}$$

Cantilever Through-Thickness Strain-Gradient Structures

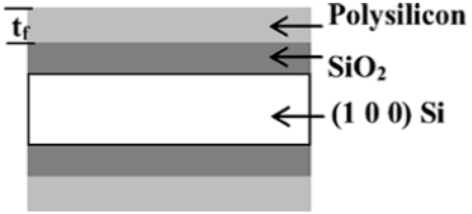

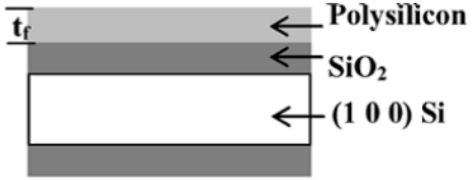

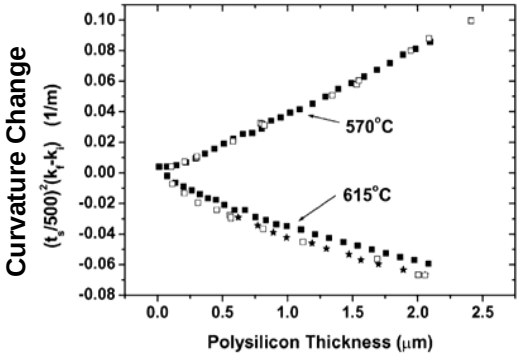

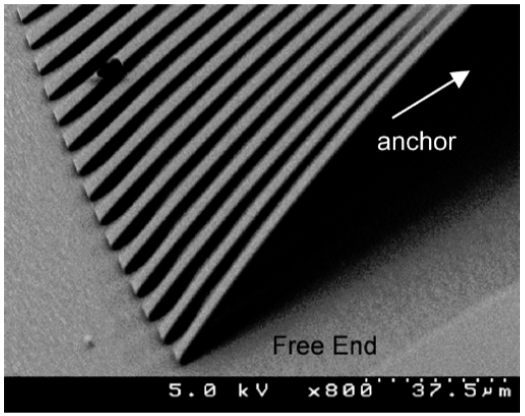

Film Thickness (μm)	Deposition Temperature (^oC)	Released Radius of Curvature (m)	
		Predicted	Measured
0.82	570	-0.17e-2	>-0.15e-3
1.34	570	-0.80e-2	[-0.2e-2, -0.18e-2]
0.56	615	0.45e-3	0.36e-3
1.12	615	0.70e-3	0.75e-3

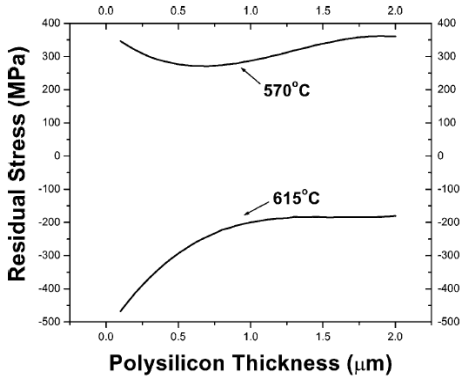

In this work, researchers deposited and released LPCVD polysilicon. To determine the through-thickness stress gradient, they etched the topside Si away in 100 nm increments using a chlorine plasma, measuring the cantilever curvature at each increment.

Wang, Ballarini, Kahn, and Heuer, *J MEMS,* 2005

Cantilevers for Fatigue: Fatigue of Micromolded Alloys

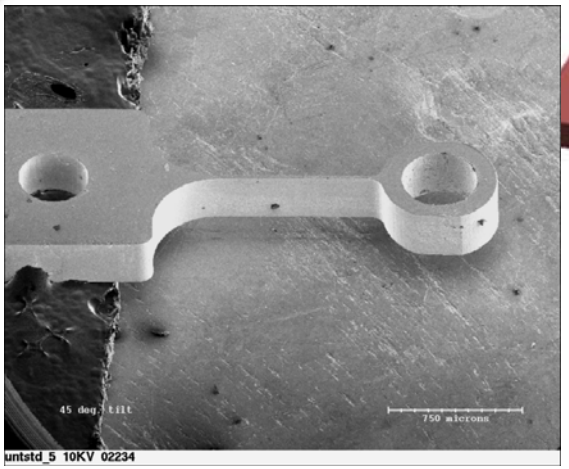

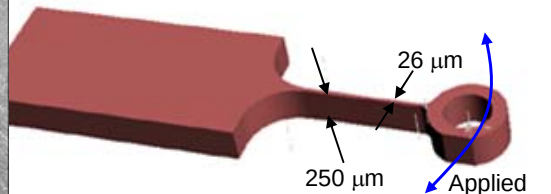

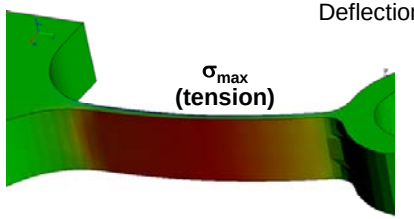

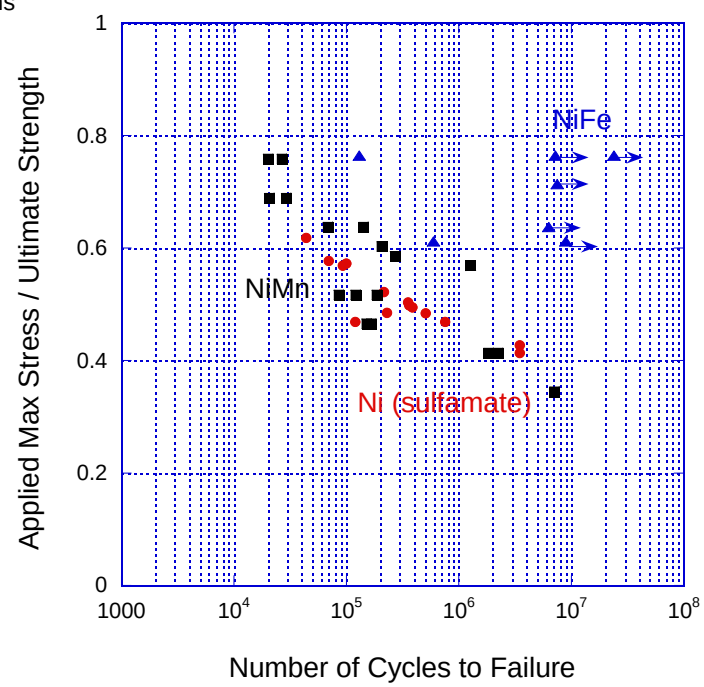

***Ni** (sulfamate bath)*

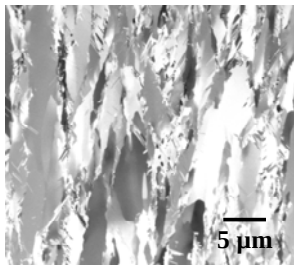

Grain Size ~ 3000 nm
Ultimate Strength ~ 500 MPa

Ni-Mn

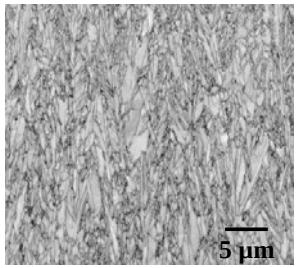

Grain Size ~ 100 nm
Ultimate Strength ~ 1500 MPa

Ni-Fe

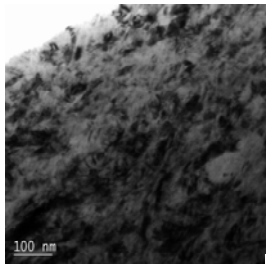

Grain Size < 50 nm
Ultimate Strength ~ 2000 MPa

3.2 Residual stress indicators

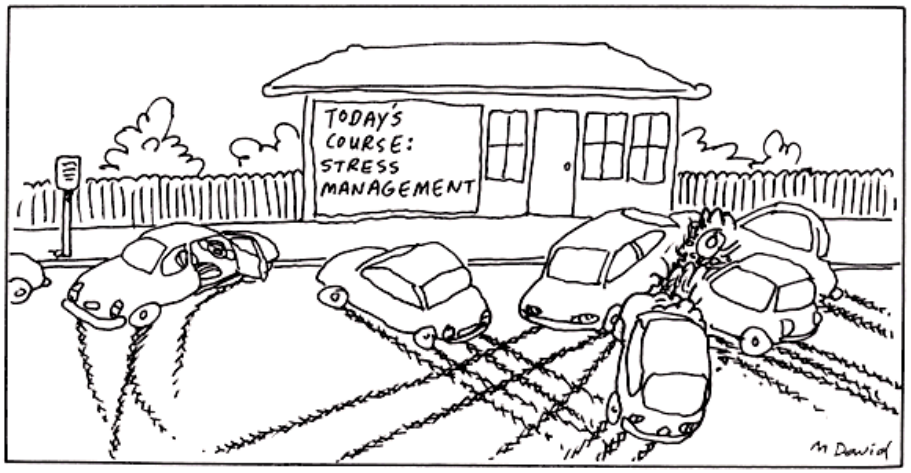

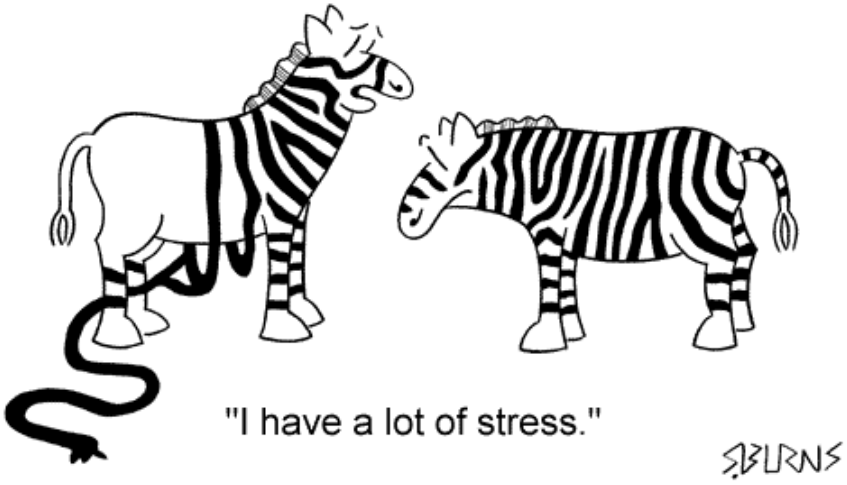

A Non-Symmetric Single-Arm Indicator

First(?) Work Using Pointer Structure:
Drieenhuizen et. al.,Sens. Act. A, ***37-38****, 1993, pp. 756-765.*

- A non-symmetric design is robust against buckling, hence a "better" design for thin films than double arm pointer.
- As with the previous design, strain is independent of film thickness
- Limitations include longer area/footprint for same resolution, multiple buckling criteria
- 0.25 μm pitch mismatch between teeth ⇒ 0.125 μm resolution

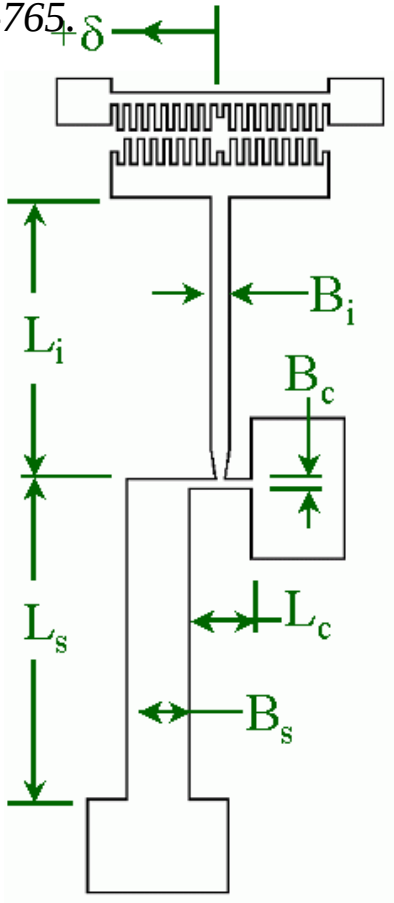

$$e = \frac{2L_c\delta}{3L_iL_s}\frac{1}{C_1}$$

$$C_1 = \frac{1-(\frac{B_i}{L_c})^2}{1-(\frac{B_i}{L_c})^3}$$

Variables
δ= *Deflection*
B = Width
L = Length
O = Offset
t = Thickness
Subscripts
c = Coupling beam
i = Indicator beam
s = Specimen beam

$$e_{crit} = \frac{\pi^2 B_s L_c^3 t^2}{3B_c^3 L_s^3} \ldots for \ldots all$$

$$e_{crit} = \frac{4\pi^2 B_c L_s^2 t^2}{3B_s^3 L_c^2} \ldots for \ldots B_c > t$$

$$e_{crit} = \frac{4\pi^2 B_c^3 L_s^2}{3B_s^3 L_c^2} \ldots for \ldots B_c < t$$

Lin et. al., J MEMS, 6, 1997, pp. 313-321.

Residual Stress of MUMPs Silicon (poly and mono)

- Pointer resolution: 12.1 με ~ 1.6 MPa (old, SOI 12)
- Pointer resolution: 3.0 με ~ 0.39 MPa (new, SOI 14)
- Vernier: 4.00 vs. 4.25 μm pitch with mask resolution of 0.25 μm

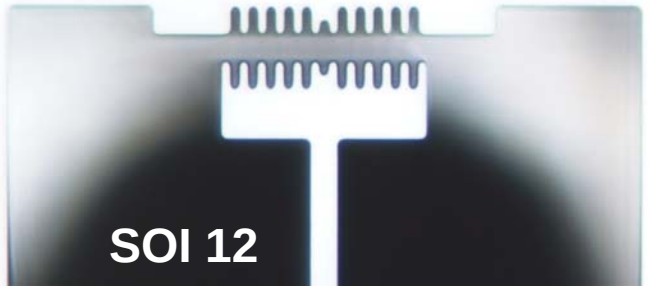

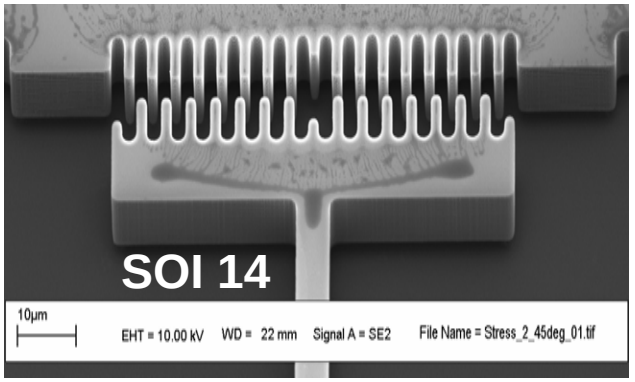

PROCESS	LAYER	μSTRAIN	STRESS, MEASURED	STRESS, VENDOR
		{μm/m }	{MPa}	{MPa}
SOI, 10-μm	SOI	-30.5 ± 11.9	-3.9 ± 1.5	N/A
SOI, 25-μm	SOI	-8.8 ± 6.3	-1.9 ± 2.4	N/A
PolyMUMPs	Poly-1	-53.2 ± 7.4	-8.6 ± 1.2	-4.4
PolyMUMPs	Poly-2	-94.6 ± 9.3	-15.3 ± 1.5	-12.7
PolyMUMPs	Poly-1+ Poly-2	-21.6 ± 11.6	-3.5 ± 1.9	N/A
SOI, 10-μm	Metal-1 on SOI	4018.8 ± 17.0	312.3 ± 1.3	N/A
SOI, 25-μm	Metal-1 on SOI	2671.9 ± 1.8	207.6 ± 0.1	N/A
PolyMUMPs	Metal-1 on Poly-2	479.8 ± 110.2	37.3 ± 8.6	19.1
PolyMUMPs	Metal-1 on Poly-1 + Poly-2	811.3 ± 30.2	63.0 ± 2.4	19.1
PolyMUMPs	Oxide-2 in Poly-1 + Poly-2	5703.2 ± 19.5	410.6 ±- 1.4	N/A

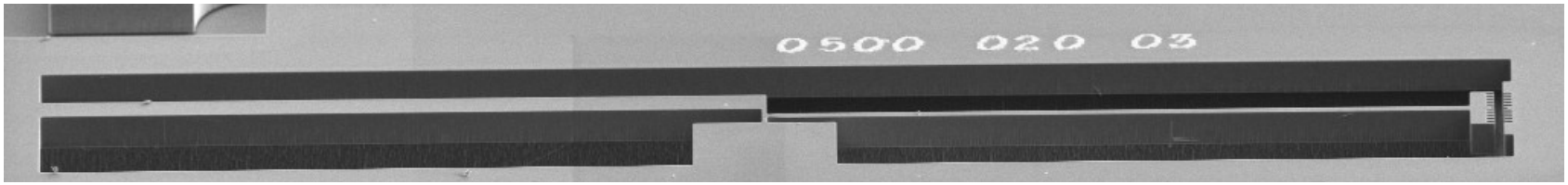

Miller, Boyce, Dugger, Buchheit, and Gall, *Sens Act A,* 2007

Residual Stress in SiC using A Double Double-Arm Indicator

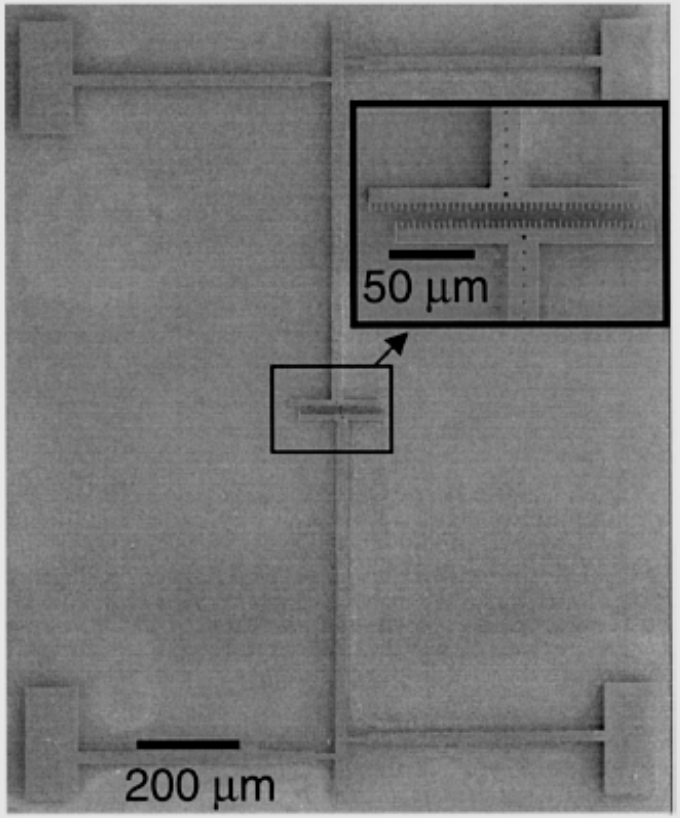

FIG. 2. Scanning electronl micrograph of a poly-SiC microstrain gauge used to measure residual stress and strain. The inset shows a higher magnification micrograph of the verniers after release, indicating a residual tensile strain of 0.038% (residual tensile stress of 150 MPa).

Bellante, Kahn, Ballarini, Zorman, Mehregany, and Heuer, *Appl Phys Lett,* 2005

The residual stress in SiC deposited in an atmospheric pressure chemical vapor deposition chamber (APCVD) ranged from 149-214 MPa, "due to the vagaries of our CVD reactor".

3.3 Tensile testers

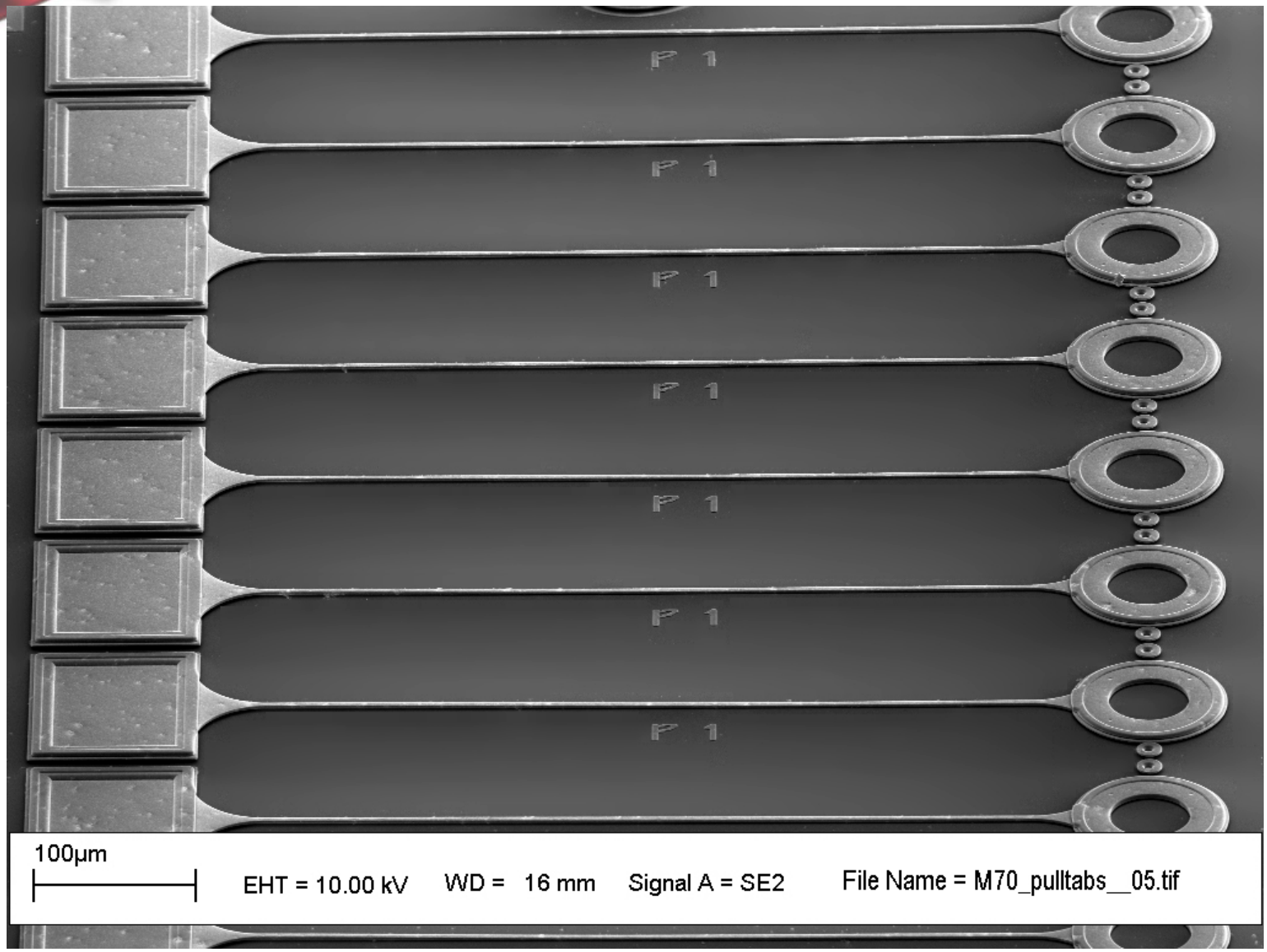

Tensile Strength of Microfabricated Si

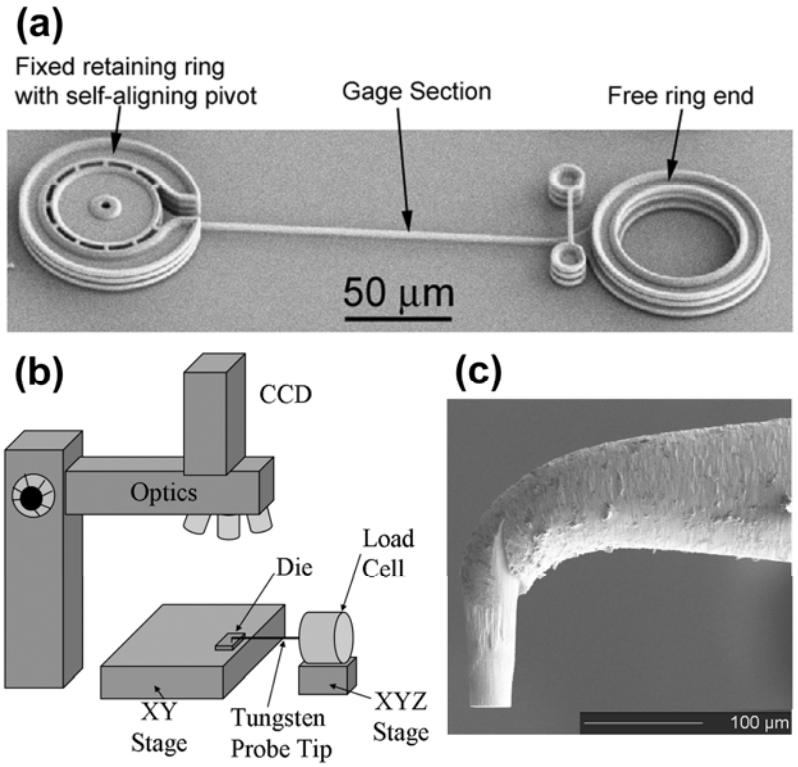

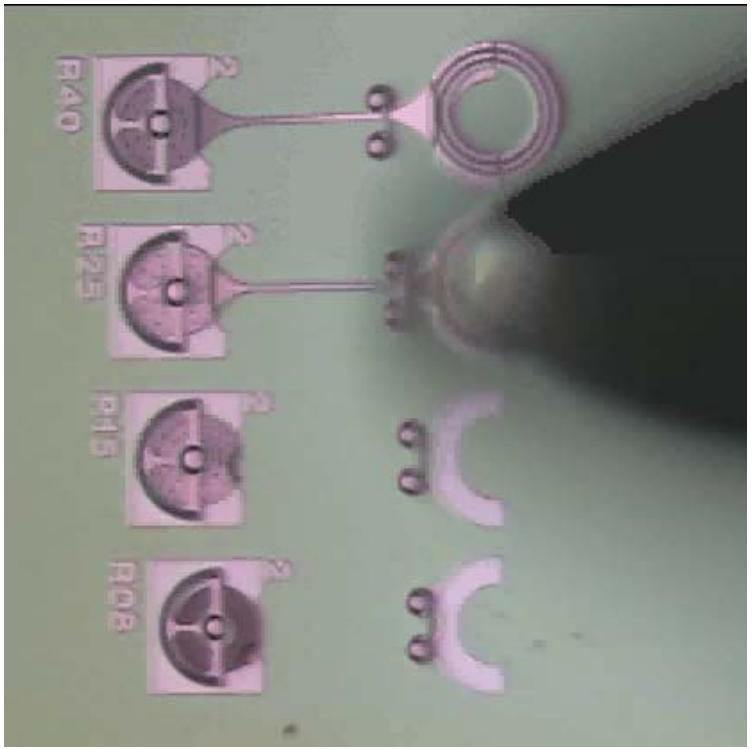

Tensile Strength of Microfabricated Si

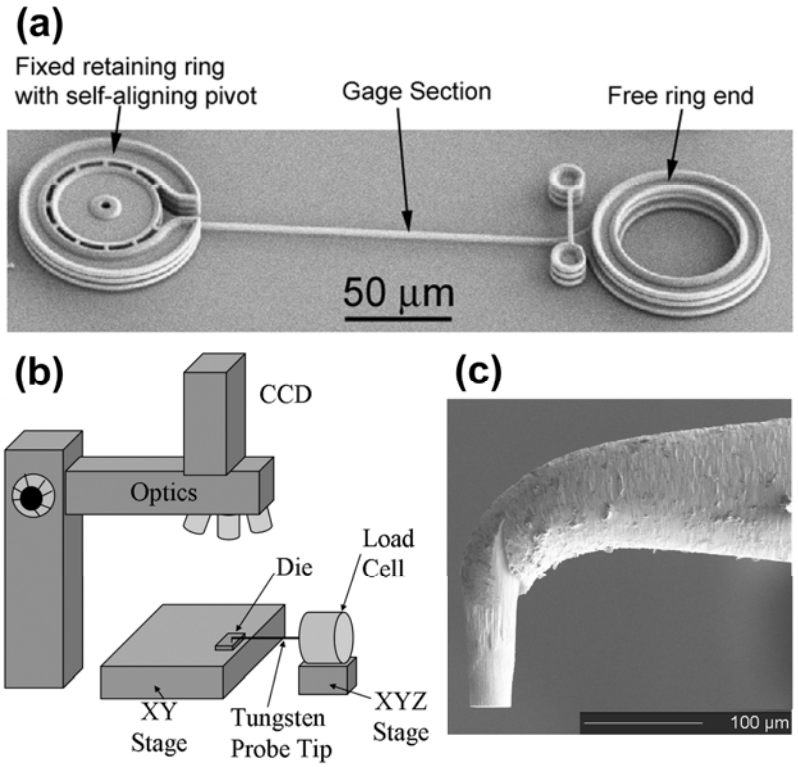

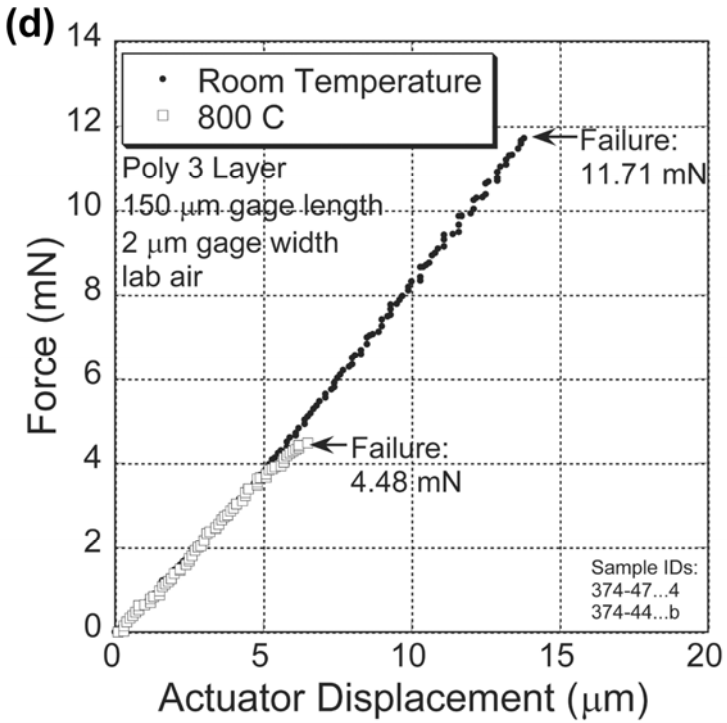

Boyce, Grazier, Buchheit, and Shaw, *J MEMS,* 2007

B.L. Boyce et al., J. MEMS ***16****:179-90, 2007*

Tensile Strength of Microfabricated Si

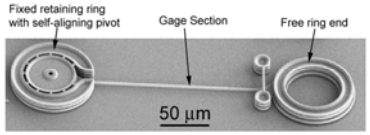

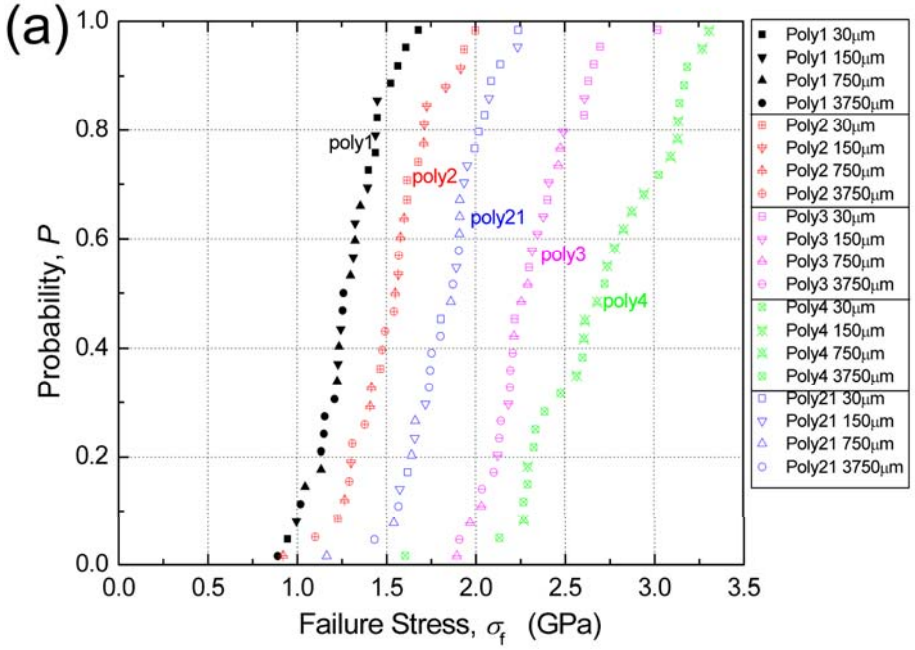

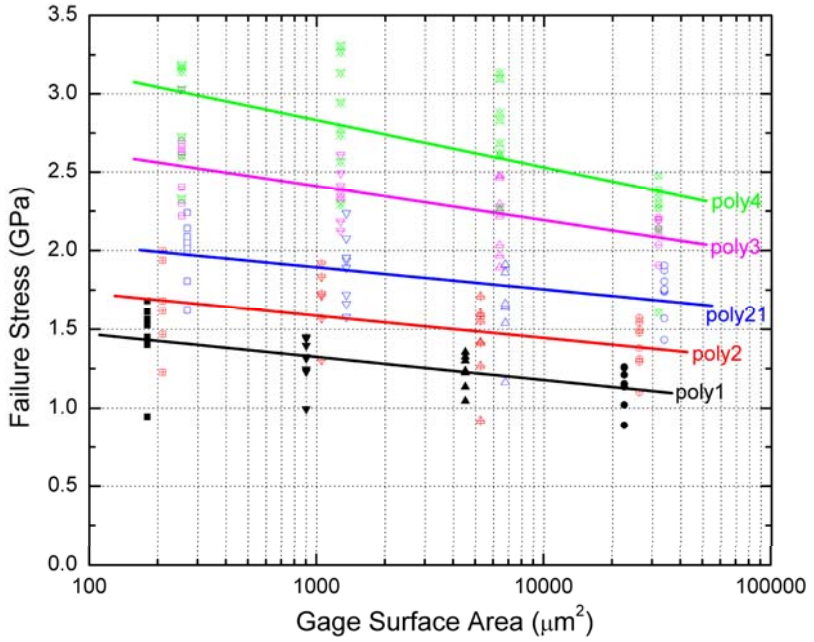

Each of SUMMiT's 5 layers has a different strength.

The strength of silicon depends on the size of the MEMS component (so-called "Weibull Size Effect")

$$P = 1 - \exp\left[-\left(\frac{\sigma}{\sigma_\theta}\right)^m\right]$$

$$\left(\frac{\sigma_1}{\sigma_2}\right) = \left(\frac{A_2}{A_1}\right)^{1/m}$$

Boyce, Grazier, Buchheit, and Shaw, *J MEMS,* 2007

Perforated Tensile Bar (Chasiotis and Co-workers)

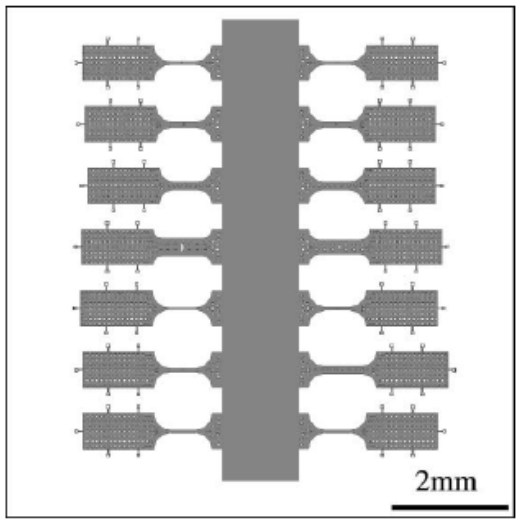

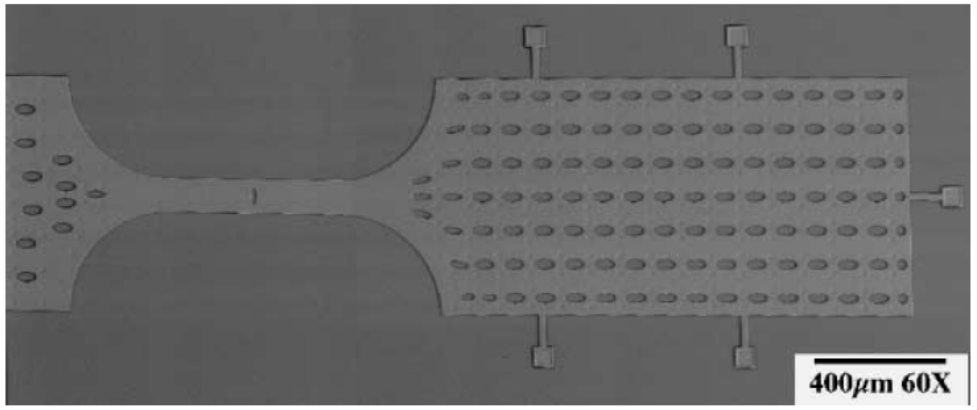

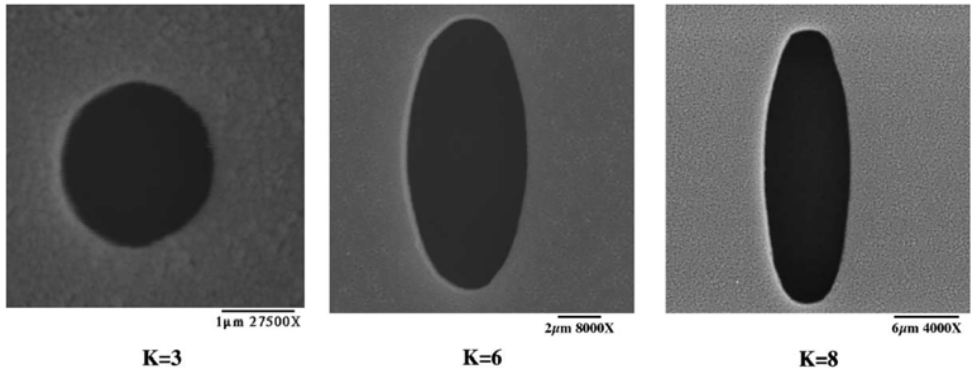

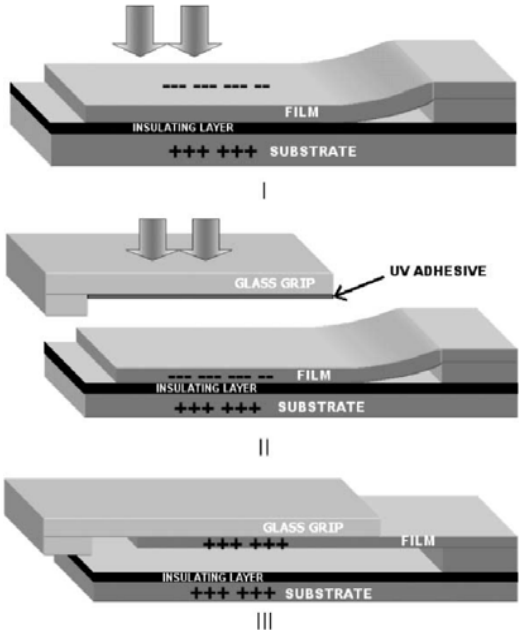

A glass grip with UV adhesive is used to affix to these relatively large tensile bars with various perforations in the middle of the gage section.

Knauss, Chasiotis, and Huang, *Mechanics of Materials,*2003

Perforated Tensile Bar (Chasiotis and Co-workers)

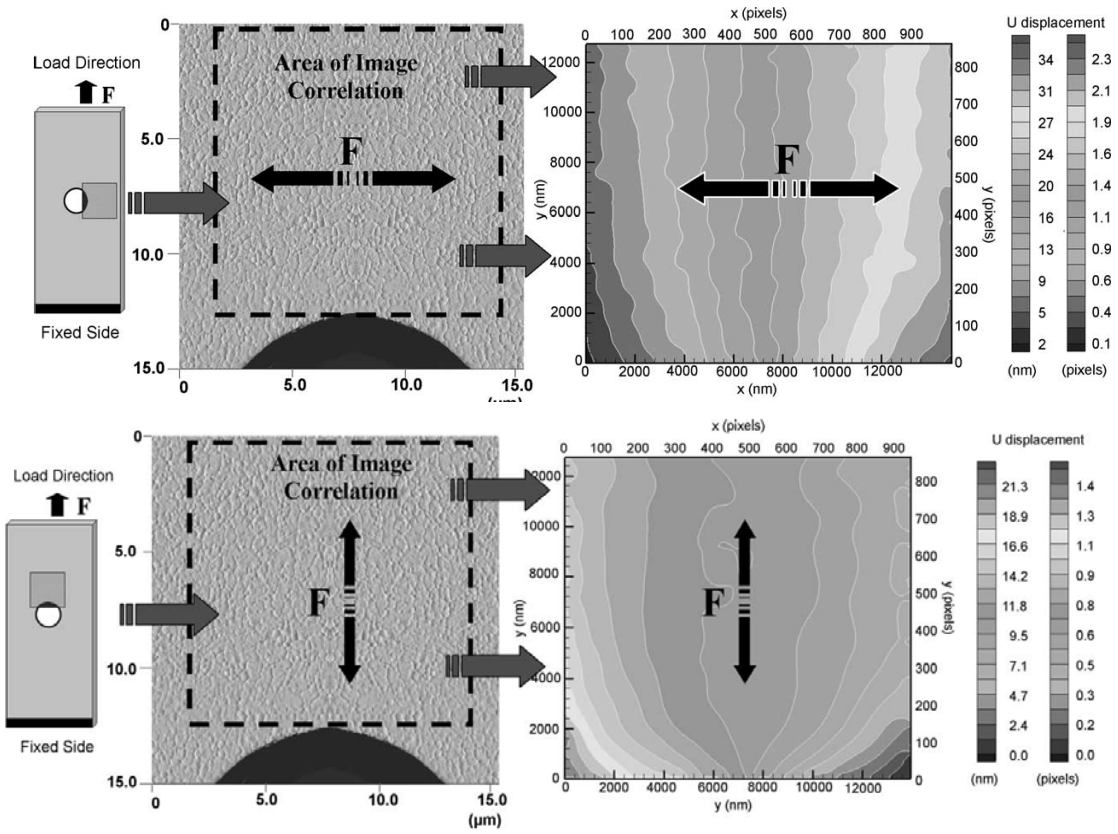

Test	Elastic modulus, E (GPa)	Poisson's ratio, ν
Hole radius = 6.3 μm (measured)		
1	162.5	0.22
2	158.7	0.25
3	150.8	0.18
4	146.8	0.16
5	159.5	0.15
Average	155.6 ± 6.6	0.20 ± 0.04
Hole radius = 6 μm (nominal)		
1	138.9	0.18
2	136.6	0.21
3	128.0	0.12
4	125.0	0.13
5	135.4	0.13
Average	133.4 ± 5.9	0.15 ± 0.04

Through the use of AFM-based microDIC, the inverse hole problem was used to accurately determine the elastic modulus and Poisson's ratio for polyMUMPs Si.

Cho, Cardenas-Garcia, and Chasiotis, *Sens Act A,* 2007

Digital Image Correlation

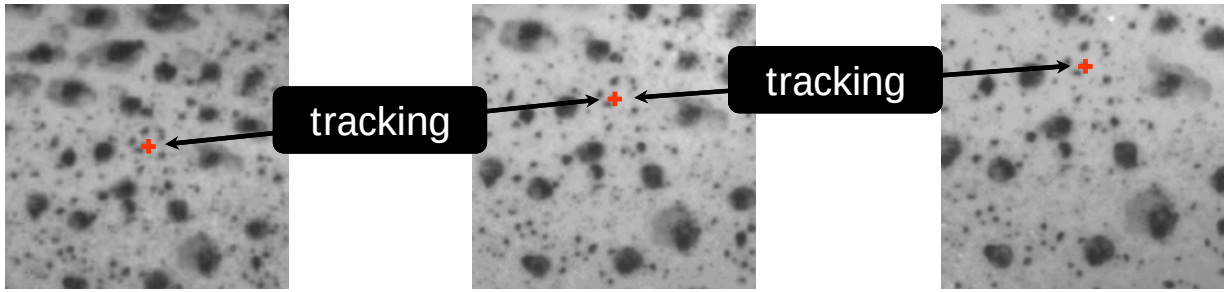

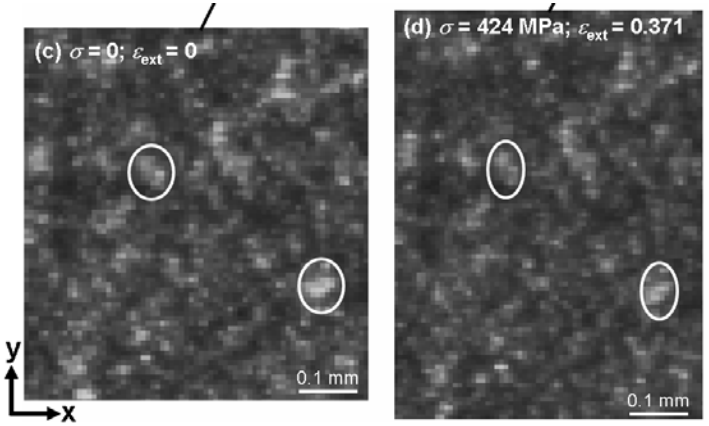

Pixel coord., reference image | Pixel value at $(x+i; y+j)$ | Pixel value at $(x+u+i; y+v+j)$

$$C(\underline{x,y},\underline{u,v}) = \sum_{i,j=-n/2}^{n/2} (I(x+i, y+j) - I^*(x+u+i, y+v+j))^2$$

Image before motion | Image after motion

n: subset size (9 in our example)

Displacement (disparity)

Correlation function

From Correlated Solutions – SEM short course

Numerically, this is an inverse problem to solve for the rigid body motion and deformation field that minimizes the correlation function: a scalar pixel intensity difference for a matrix of pixels.

See: Cheng, Sutton, and Schreier, *Exp. Mech.*, 2002.; McGinnis, Pessiki, and Turker, *Exp. Mech.*, 2005; Kang et al. *Acta Mater.* 2006

Fracture Strength and Failure Origins of SiC

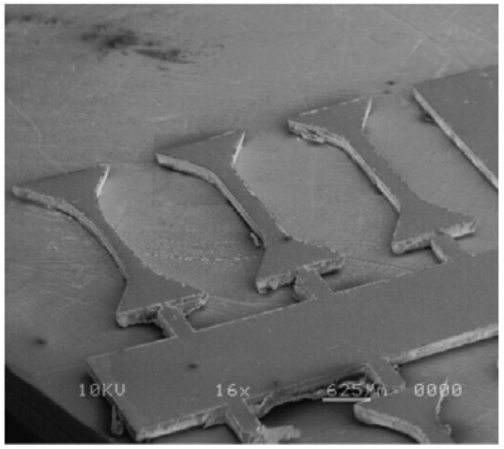

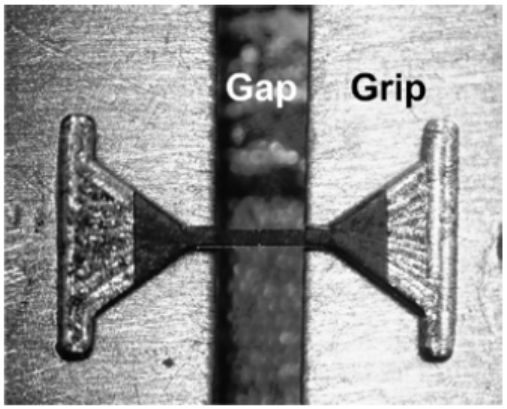

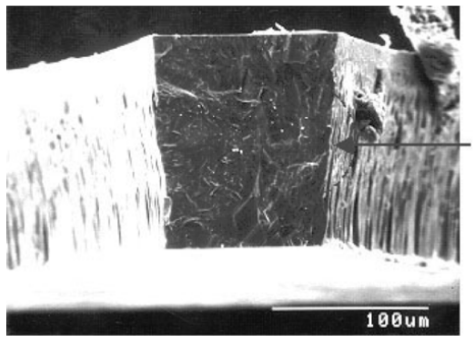

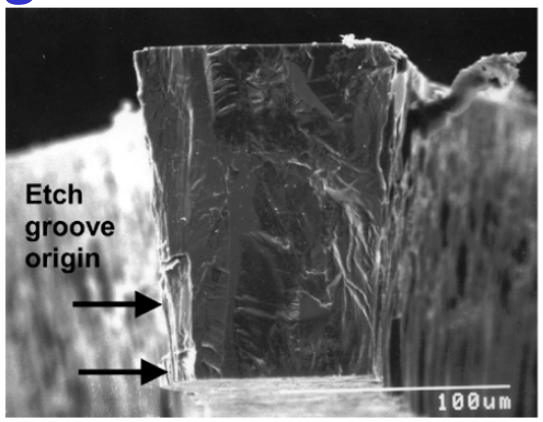

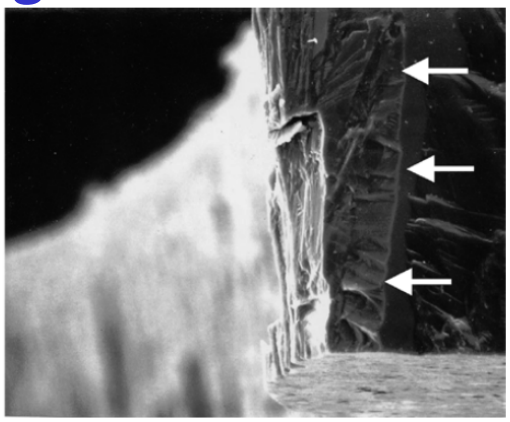

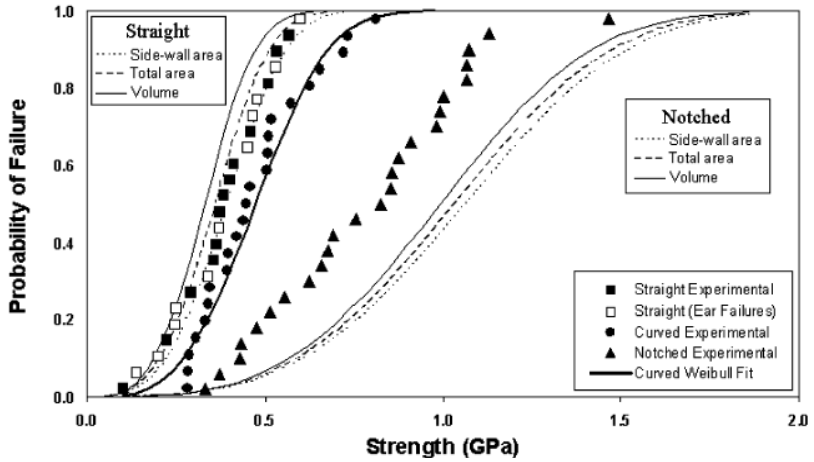

These 3.1 mm long mini-tensile samples are quite large compared to many other MEMS designs. They were gripped with conventionally-machined Al grips and actuated with a motorized stage. Failure initiation was often at the fillet corner, at sidewall etch grooves (i.e. so-called "curtain" defects).

Sharpe, Jadaan, Beheim, Quinn, and Nemeth, *J MEMS,* 2005

Wire Bending or Membrane Tension (Using MEMS Holes + Nanoindenter)

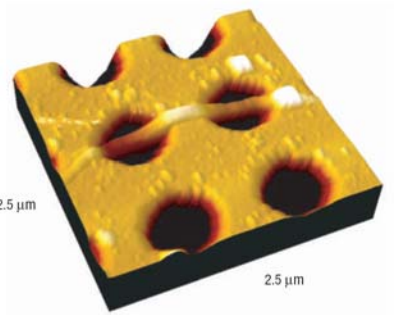

Kis et. al., *Nat Mat*, 2004

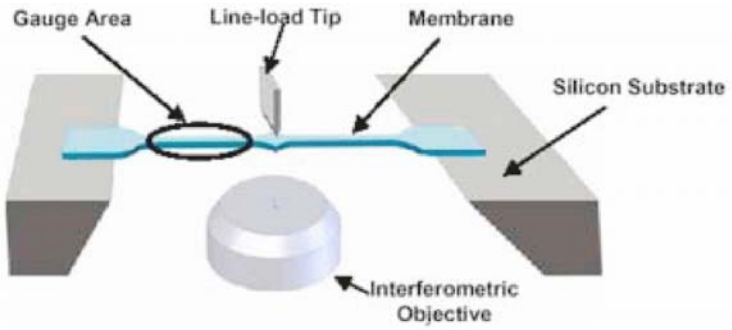

Espinosa et. al., J. Mech. Phys. Solids, 2003

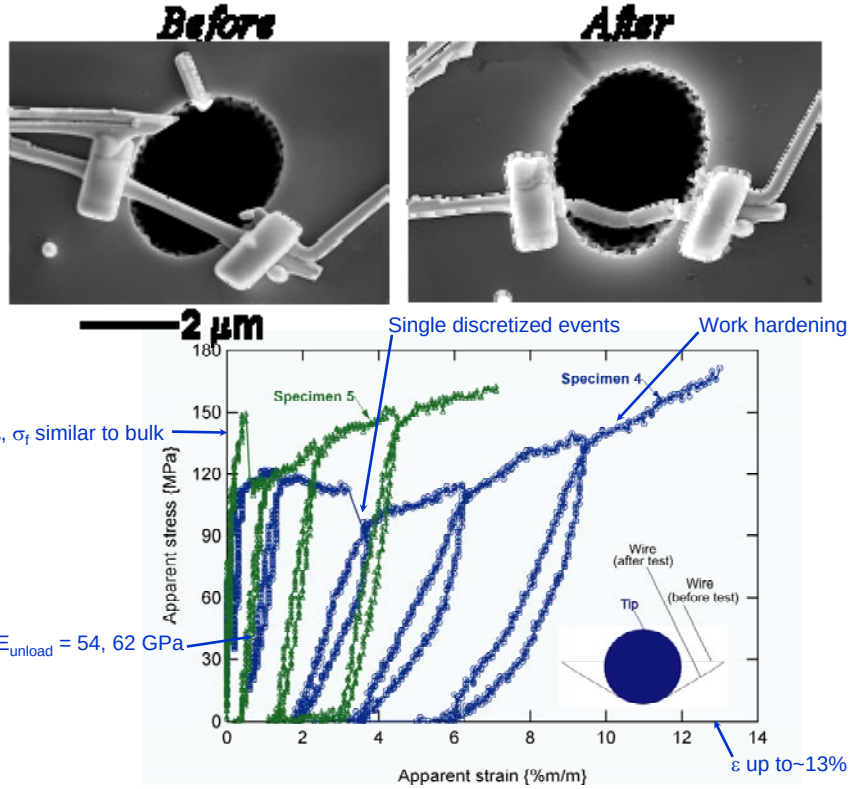

$$\sigma = \frac{F_R}{A} \qquad \varepsilon = \frac{\Delta L}{L} = \frac{\sqrt{h^2 + \left(\frac{L_h}{2}\right)^2} - L_h}{L_h}$$

$$F_R = \frac{P}{2\sin[\tan^{-1}[\frac{h}{L_h}]]}$$

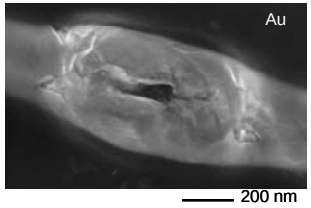

Limitations

- Accurate determination of tip geometry
- Placement accuracy of tip
- Assumptions:
  - No deformation at contact region
  - No σ concentration at attachment
  - Symmetry, uniformity

Other Passive micro-Tensile Methods

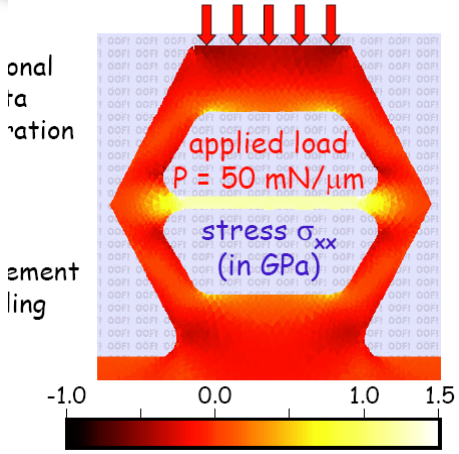

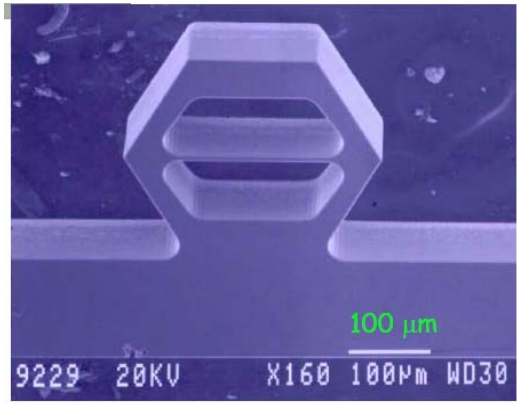

GD Quinn, ER Fuller Jr,

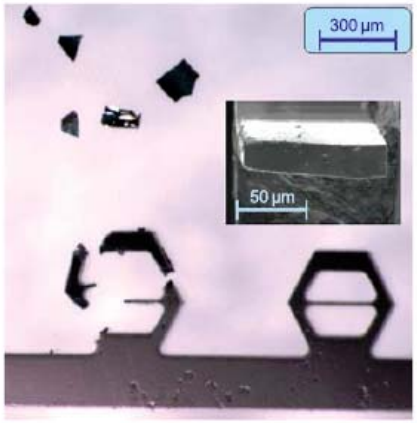

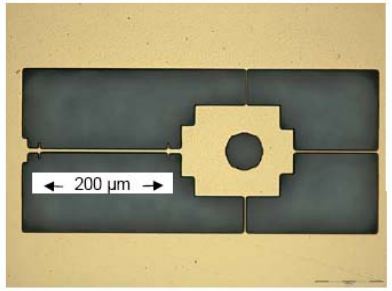

D. Read JD McColskey, Y-W Cheng

Autonomous Fracture Toughness Test Using a Residual Stress Actuator and an Indent Precrack

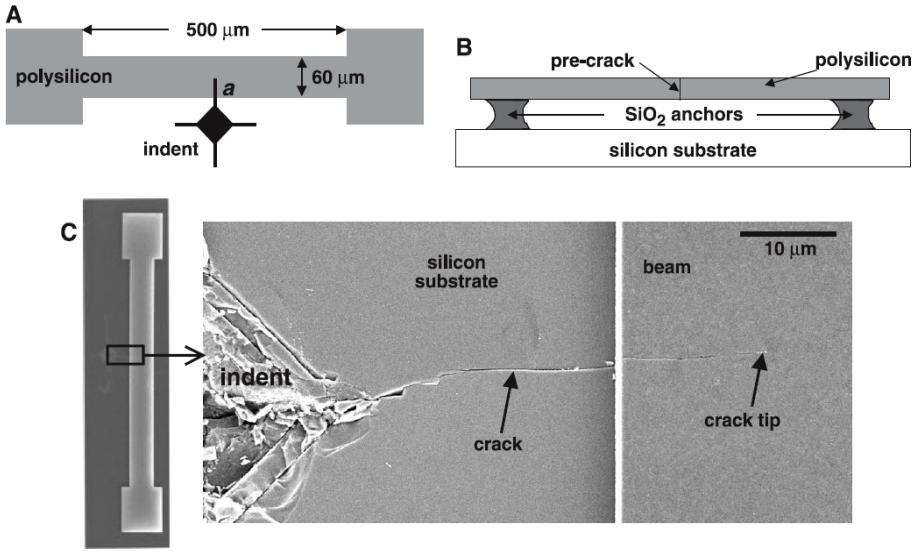

Kahn, Ballarini, Bellante, and Heuer, *Science*, 2002

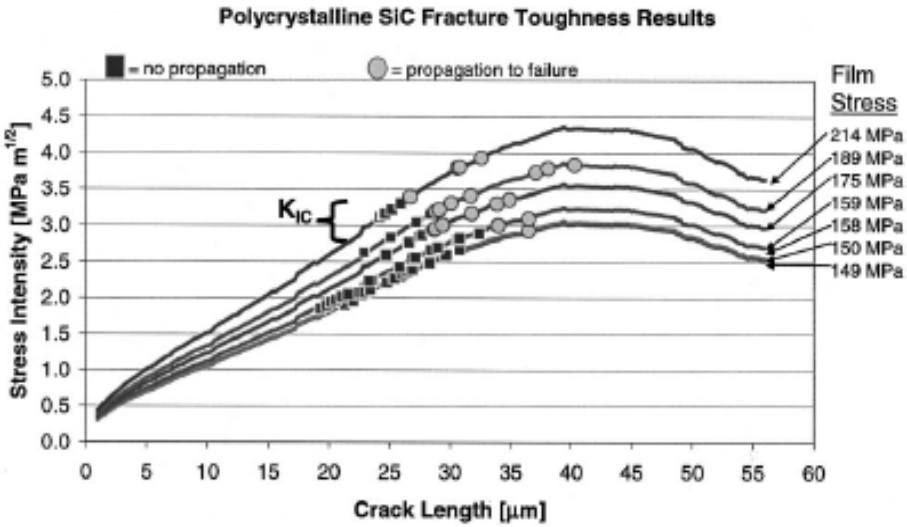

Bellante, Kahn, Ballarini, Zorman, Mehregany, and Heuer, *Appl Phys Lett,* 2005

In this work, the beam was doubly clamped to the substrate. During fabrication, residual stress is built up in the SiC layer. Prior to release, an indent is used to "precrack" the beam. After release, the residual tensile stress "tests" the beam. From these tests, the fracture toughness was determined to be in the range of 2.8-3.5 MPa√m. These specimens show no signs of static stress-corrosion cracking.

Outline

1. Introduction
2. MEMS fabrication technologies
3. Examples of passive devices for nanomechanics
4. Passive device technology
   1. Advantages of Passive Devices
   2. External and Passive Actuators
   3. Displacement and Strain Sensors
   4. Force and Stress Sensors
5. Examples of active devices for nanomechanics
6. Active device technology

4.1 Advantages of Passive Structures

1. External sensors can be readily calibrated against known standards.

2. Structures do not require on-chip actuators or sensors so they take up less real estate.

3. Structures can be easily used as process and lifetime health monitors, since the evolution or degradation does not affect the off-chip sensors.

4. Structures are relatively simple leading to greater chance of first-fab success.

5. External sensors and actuators are not limited by the fabrication process.

4.2 External and Passive Actuators

1. Electrodynamic (motorized screw) stages

-Based on Lorenz force generated with a current-carrying conductor in a magnetic field
-Rotational motion converted to linear motion often using gears and a screw
-Resolution depends on motor rotational accuracy, gearing, and screw pitch.
-Resolution also typically limited by the bearing configuration and possible ingestion of particulates in the gear/drive train.
-Travel can range from <1 μm to >1m.
-Best resolution achieved when coupled with a feedback-controlled displacement sensor (i.e. glass-scale encoder, LVDT, capacitive plate, etc.)
-Can be geared for high force output (20,000 lb Instron!)
-Low cost and extensive availability.
-See www.newport.com for examples of lab-grade stages

2. Piezoelectric actuator

-Based on voltage differential applied across a piezoelectric ceramic.
-Due to non-repeatable hysterisis, high-resolution applications require feedback control from an appropriate displacement sensor.
-High-voltage feedback-controlled drive systems can be somewhat expensive.
-See /www.physikinstrumente.com for examples of lab-grade piezo actuators.

4.2 External and Passive Actuators

3. Electromagnetic actuator

-Relies on electromagnetic force
-Can be high resolution (sub-μm): basis for Bose Electroforce system and MTS Nanoindenter XP actuation
-see www.bose-electroforce.com for examples of electromagnetic actuators (in the high-force rage). See mts nanoinstruments for examples of nano-scale electromagnetic actuators.

4. Hydraulic / Pneumatic actuators

-Traditional actuation method for servohydraulic loadframes
-Reliance on seals makes high-resolution applications challenging.
-Typically used for mini-to-macro scale testing.
-see www.mts.com for examples of conventional hydraulic actuators for mechanical testing.

5. Optical Tweezers

-uses a focused laser beam to provide an attractive or repulsive force, depending on the index mismatch (typically on the order of piconewtons) to physically hold and move microscopic dielectric objects
-1997 Nobel prize in physics for Steven Chu
-Force limited

4.3 Displacement and Strain Sensors

1. Thin Film Strain Gage

-Operates by resistance increase with elongation and Poisson contraction of an electrical trace.
-Requires direct attachment to deforming substrate, typically using epoxy adhesives with limited ductility (<15%)
-Reqiures >1 mm^2 (typical) , averages strain over the "active gage region"
-Appropriate for high-speed strain measurement (>100 kHz)
-Temperature range limited to the epoxy adhesive and thermal expansion compensation.
-Cheap and relatively easy to use.
-"Gage Factor" calibrations available with purchase
-Requires an amplification circuit and a wheatstone bridge.
-see www.vishay.com/strain-gages for examples of strain-gages

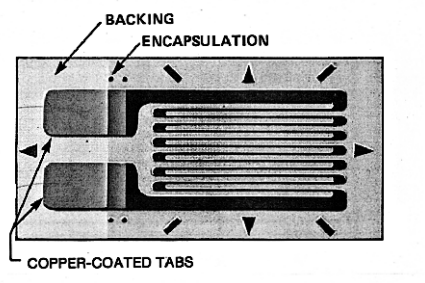

2. Extensometer

-Large, strain-gage based point-to-point displacement measurement over a gage length.
-Typically not used for small-scale testing
-see www.mts.com for examples of extensometers

3. Interferometer

- Measures the interference pattern observed between incident and reflected waves, with displacement resolution much better than the wavelength of the light.
-Requires a reflective surface (i.e. non-transparent)
-Resolution of ~nm is typical with a white-light interferometer
-optical axis is paralllel to the displacement vector therefore in MEMS it is typically used to measure "out-of-plane displacement", and is challenging to employ for in-plane displacement.
-see www.zygo.com for examples of interferometers.

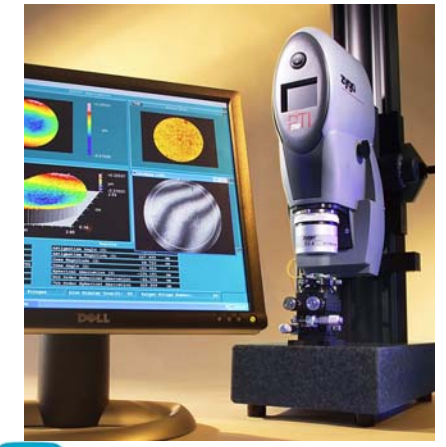

4.3 Displacement and Strain Sensors

4. Direct visual measurement

-Typically uses optical or electron microscopes.
-Resolution typically limited by the wavelength of the imaging medium
-Techniques such as digital image correlation can be used to obtain sub-pixel deformation resolution.
-Requires a line-of-sight and manual or automated image analysis.

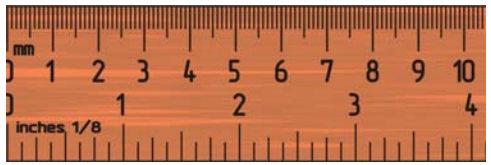

5. Capacitance

-Resolution dictated to first order by the size of the capacitor, distance between plates, and the dielectric constant of the medium between the plates.
-Can be used for high-resolution applications: the basis for Hysitron sensing.

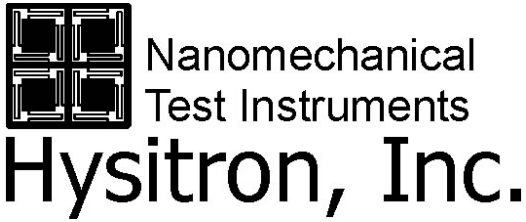

6. Linear Variable Digital Transformer (LVDT)

-Based on a permanent magnet displacing within an electromagent
-Typical resolution no better than 1 μm.
-Could conceivably be microfabricated
-see LVDTs at www.macrosensors.com or www.sensotec.com

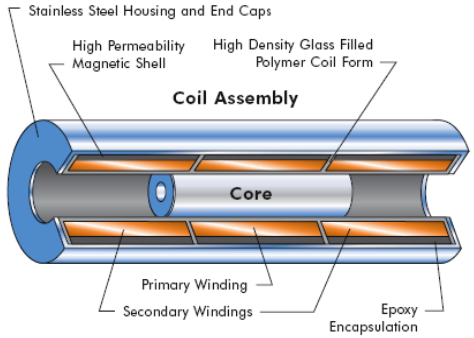

7. Laser Doppler Velocimeter

-Based on doppler effect of reflected laser light
-Velocity is integrated to determine displacement
-Good for dynamic measurements, such as resonant modes

4.4 Force and Stress Sensors

1. Strain Gage Load Cell

-Smallest off-the-shelf load cell is 10 g with a resolution of ~10 μN
-Cheap, common, and easy to use. Designed for linearity over the operating range and overload protection.
-see www.interfaceforce.com for examples of load cells

2. Quartz Load Washer

-Uses piezoelectric effect
-Good for transient load measurement
-Typically not used for small-scale testing
-see www.kistler.com for exampels of quartz load washers

3. Diffraction (x-ray and neutron)

-measures the crystallographic lattice constant
-directly related crystallographic elastic strain
-can be converted to stress via "x-ray" elastic constants (i.e. the particular elastic constant associated with the

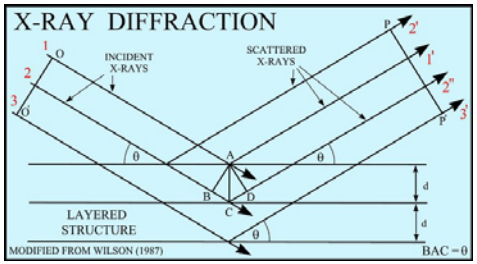

4. Proving Ring or "Optical Load Cell"

-Optical measurement of deflection of an elastic member with known stiffness such as a ring or cantilever beam.
-Resolution limited by the displacement-measuring resolution and the compliance of the elastic member.

Any displacement sensor can be used as a force sensor when it is coupled with an elastic member of known stiffness. Interferometery, capacitors, etc can all be used as force sensors.

Outline

1. Introduction
2. MEMS fabrication technologies
3. Examples of passive devices
4. Passive device technology
5. Examples of active devices for nanomechanics
   1. Electrostatically actuated devices
   2. Thermally actuated devices
6. Active device technology

5.1 Electrostatically actuated devices

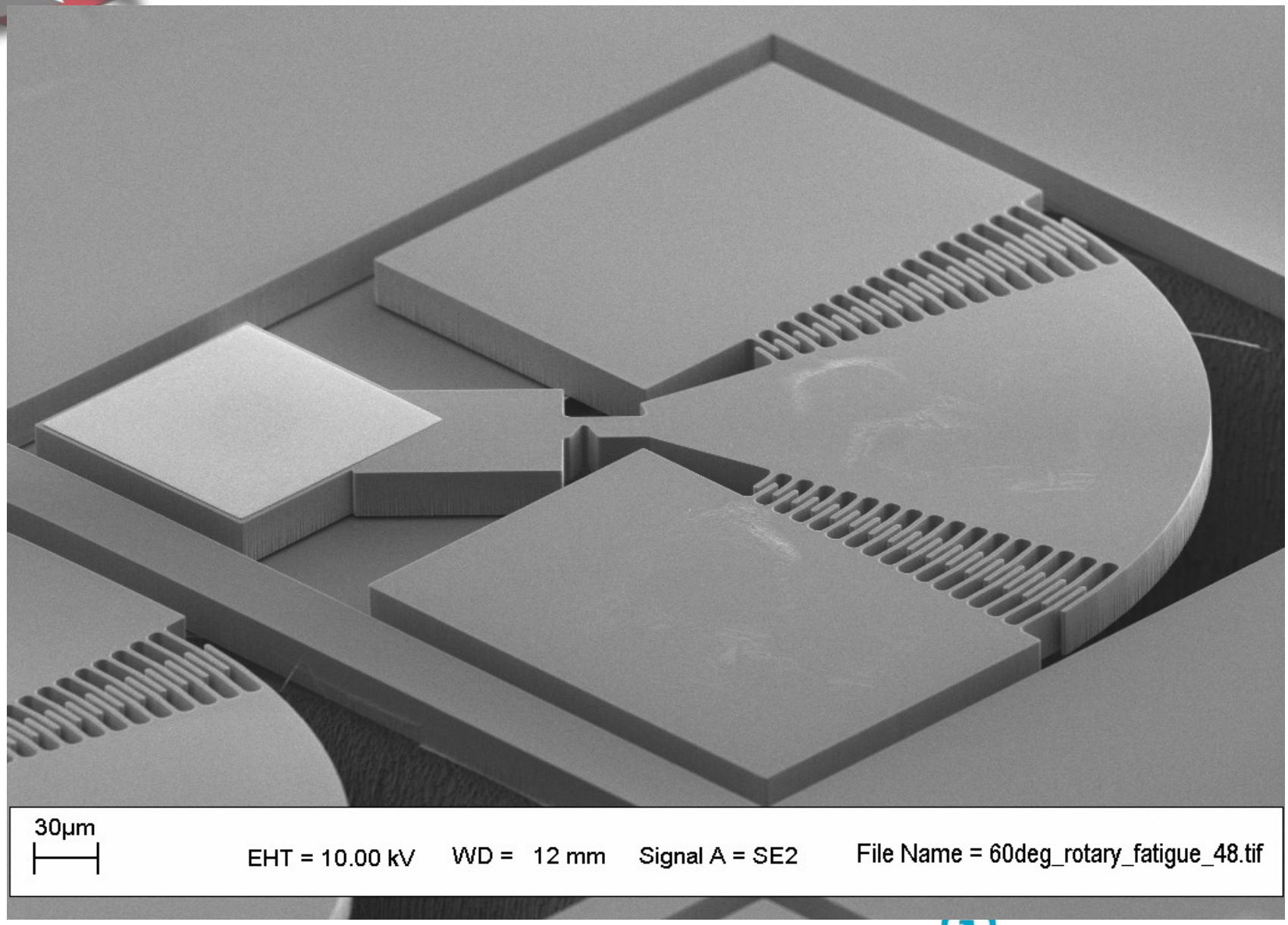

Active Cantilever Adhesion Structures

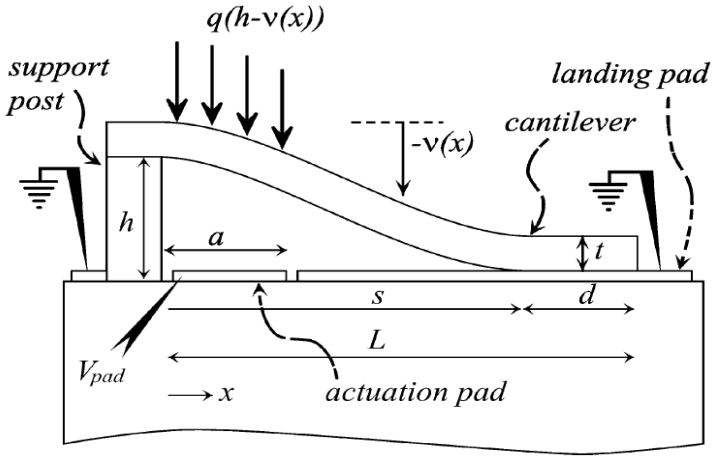

$$G_q = G_o + \frac{a^6 q^2 (4s-3a)^2}{288 s^4 D} - \frac{q a^3 h}{2 s^4}(4s-3a).$$

$$q < q_{\max} = \frac{72hD}{a^3(4s-3a)}.$$

$$F_e(x) = \left[\frac{\varepsilon_0 w}{2}\left(\frac{V_{\text{pad}}}{y(x)}\right)^2\right] \times \left[1 + 0.65\left(\frac{y(x)}{w}\right)\right]$$

The electrostatic cantilever allows the determination of work of adhesion as a function of force per unit area, *q*. The force *F* is a function of the applied voltage V_{pad} and the distance between the beam and pad *y(x)*.

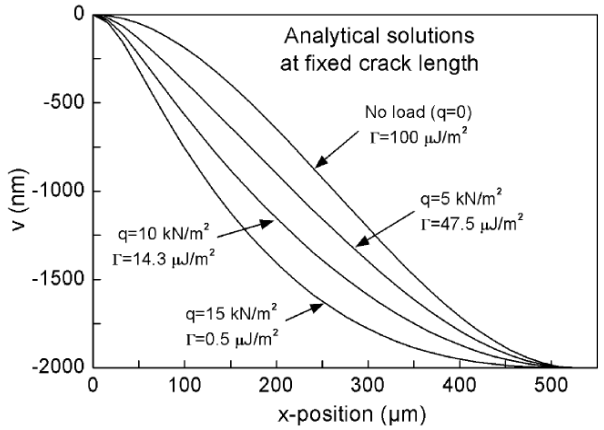

Fig. 2. Analytical solutions to the beam deflections for a crack length of 526.4 μm ($q_{\max} = 16079.6$).

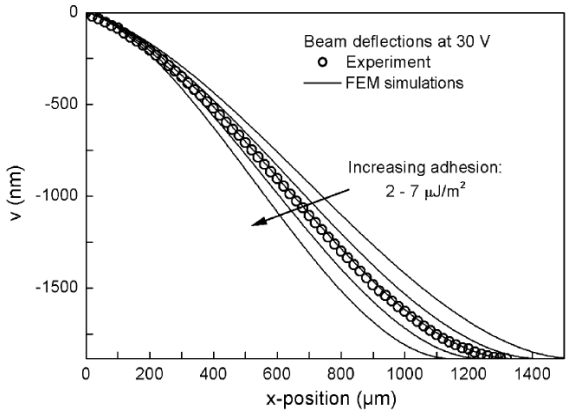

Fig. 8. Experimental and calculated beam deflections for an actuation voltage = 30 V. The adhesion values shown are 2, 2.8, 3.6, 5, and 7 μJ/m^2.

Knapp and de Boer, *J MEMS,* 2002

Active Cantilever Adhesion Structures

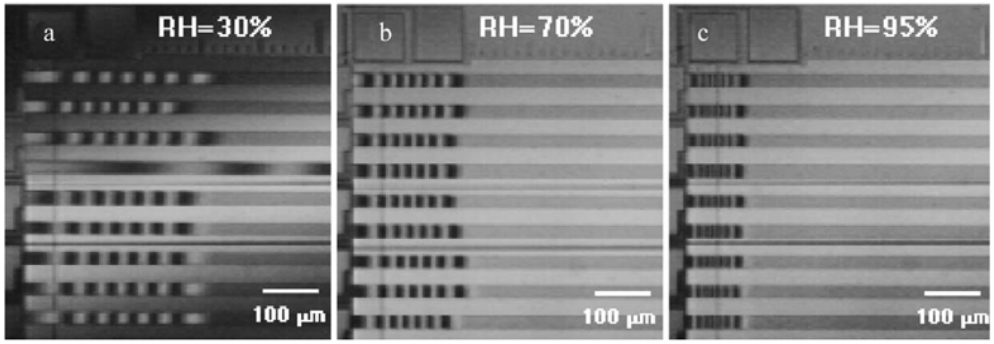

Fig. 2 Interferograms of crack length s vs. RH (p/p_s) after 40 h exposure

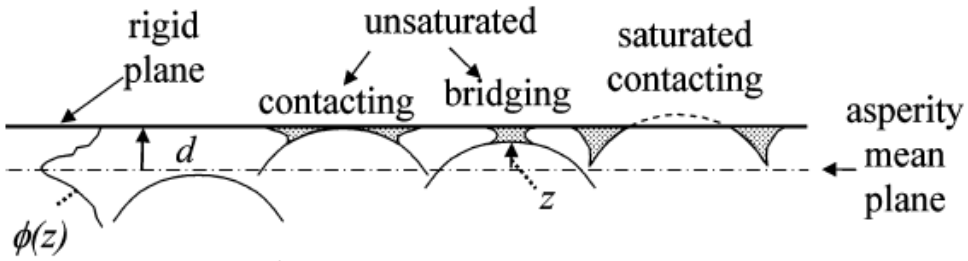

AFM Scan of Si

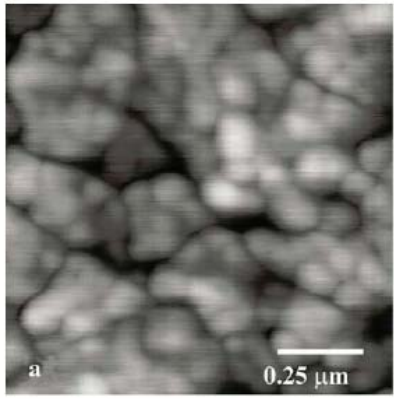

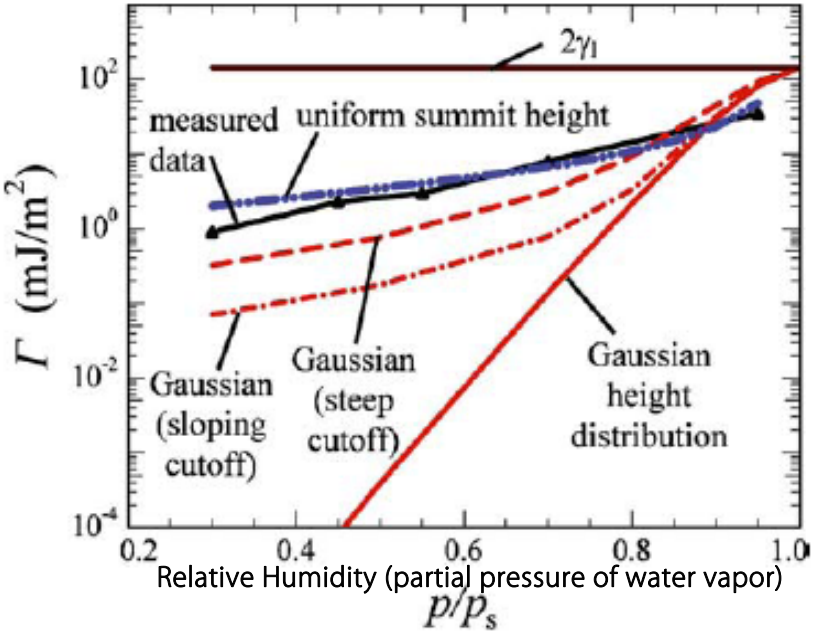

Fig. 10 Adhesion versus p/p_s trend for measured data and the model with Gaussian and Gaussian-cutoff distributions. Also equation (11), the uniform summit height model with free parameter n_{asp} is plotted (similar results are obtained with a steep Gaussian cutoff at d/σ_s=1.7). The results can be rationalized if there is a topographic correlation between the upper and lower surfaces (see text)

The capillary effect on work of adhesion depends on the uniformity of the asperities and the relative humidity.

de Boer, *Exp Mechanics,* 2007

MIT Fatigue Resonator

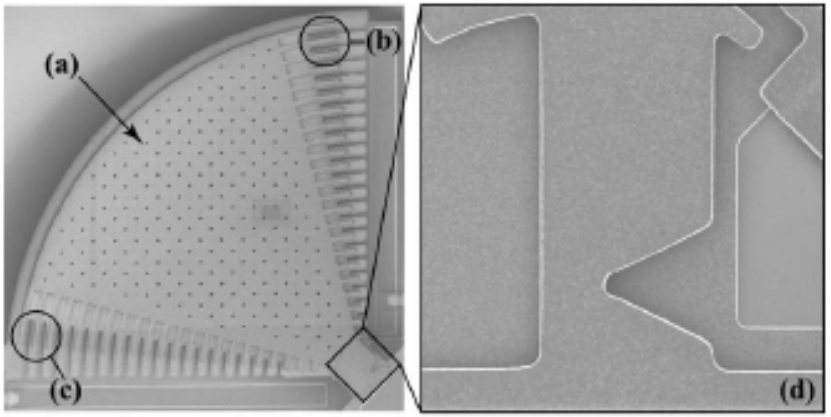

Muhlstein, Stach, and Ritchie, *Acta Materialia,* 2002

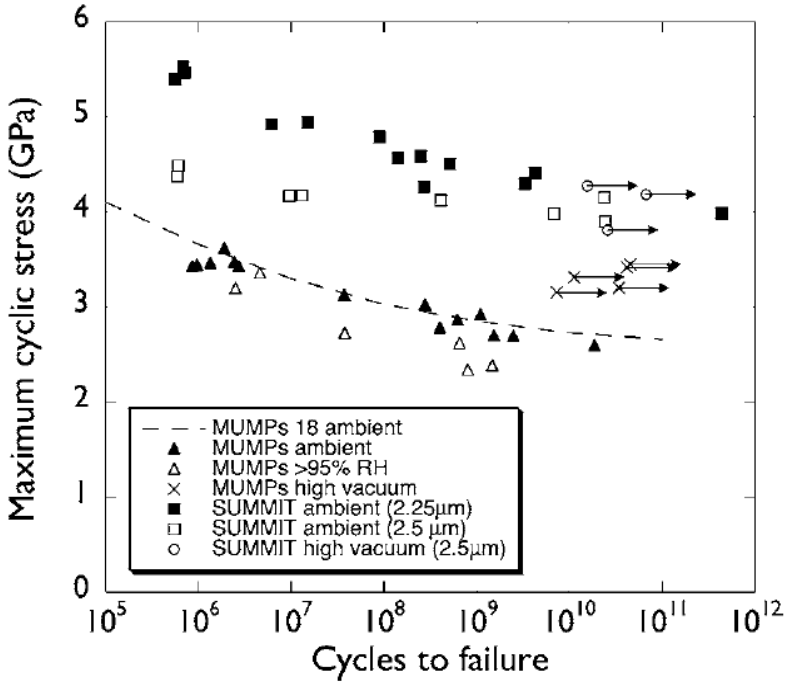

Alsem, Timmerman, Boyce, Stach, DeHosson, and Ritchie, *Acta Materialia,* 2002

The MIT fatigue "resonator" uses one bank of combs for electrostatic actuation and the other bank of combs for capacitive displacement sensing. The device is operated at resonant frequency to induce sufficient stresses at the notch tip to cause fatigue failure.

Kahn-Ballarini-Heuer "City-of-Comb Drives"

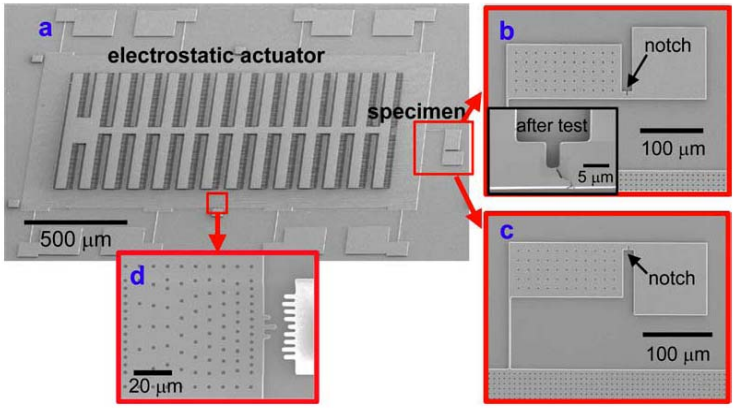

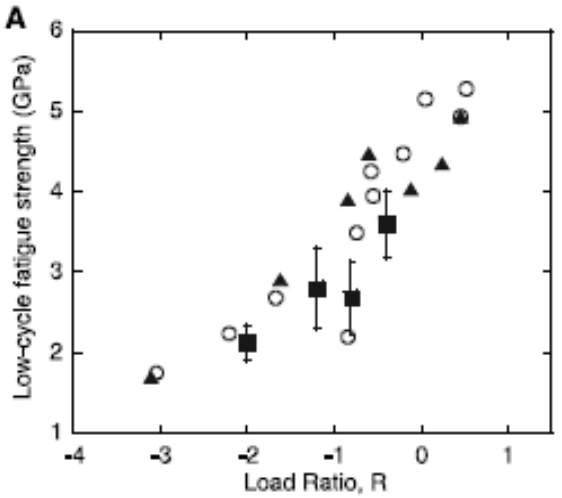

Kahn, Ballarini, Bellante, and Heuer, *Science,* 2002

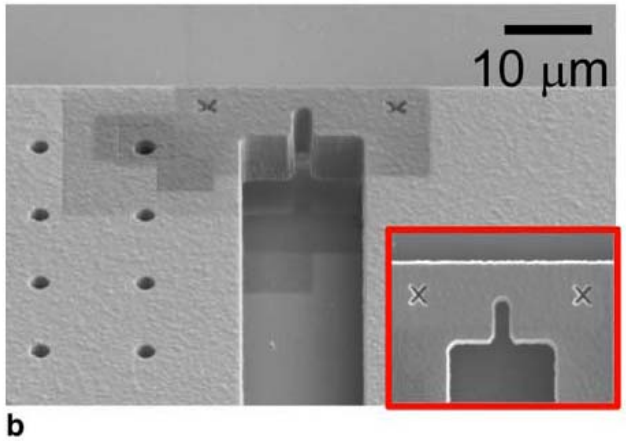

Kahn, Chen, Ballarini, and Heuer, *Acta Materialia,* 2006

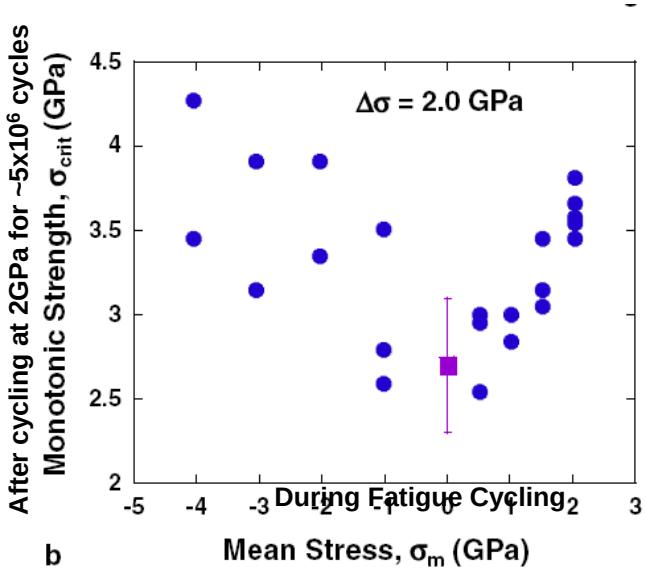

Sidewall MEMS Tribometer

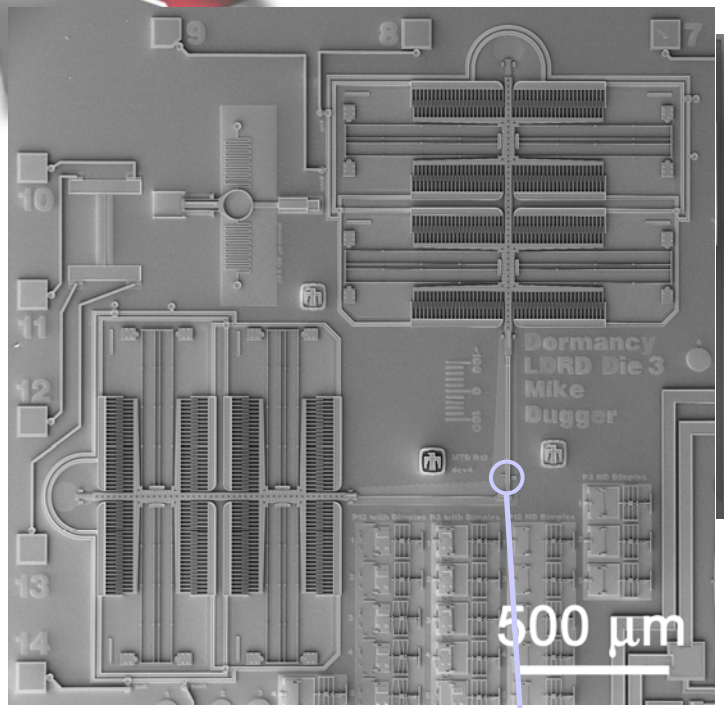

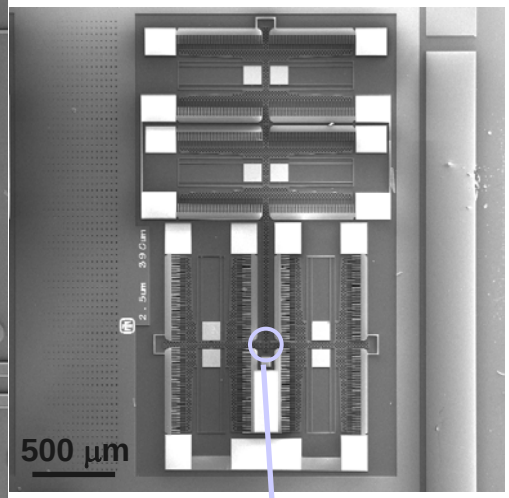

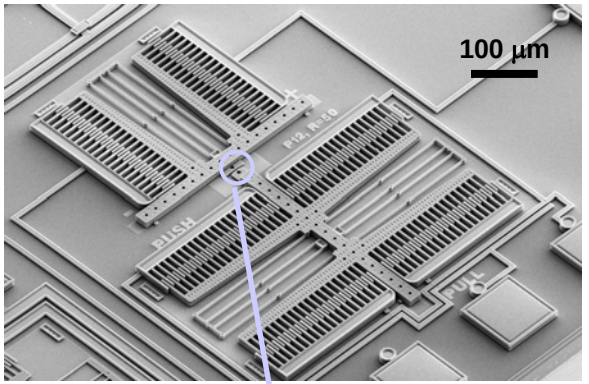

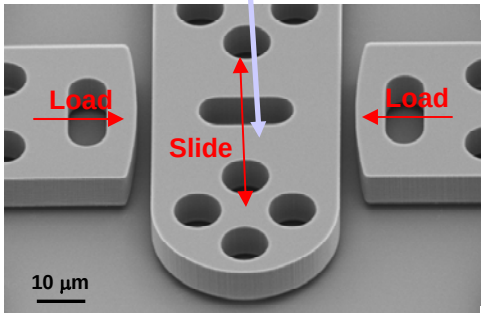

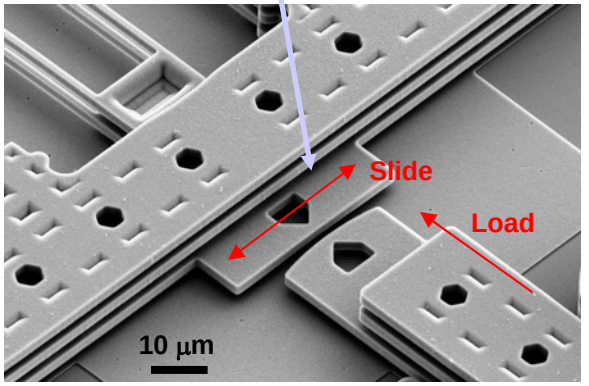

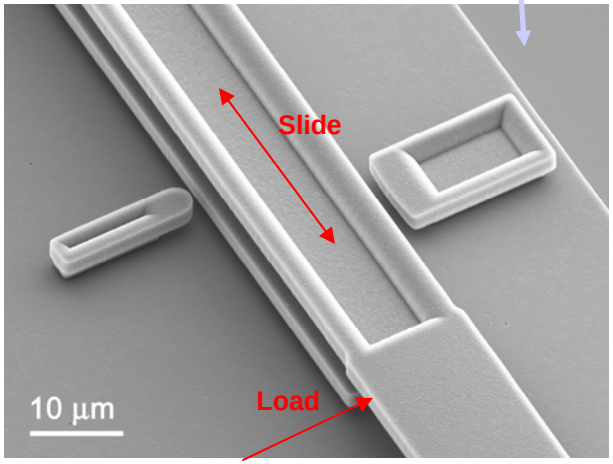

Three variants of the MEMS sidewall tribometer are shown here. In all cases, 2 or 3 independent comb drive actuators apply normal and tangential forces. Direct optical observation of displacements and force-voltage relationship leads to quantiative measurements of adhesion, static friction, and dynamic friction.

Images Courtesy of Michael Dugger, Sandia National Labs

Sidewall MEMS Tribometer

- Process image data to calculate forces
  - adhesion
  - static friction
  - dynamic friction

$$F_{ad} = F_{unload} - F_{load} + F_r = a(V_c^2 - V_p^2) + kx$$

$$F_{fr} = F_{push} - F_{pull} - F_r = a(V_{slip}^2)$$

$$F_d = k\Delta x$$

Timed Image Capture
Displacement vs Input (V)

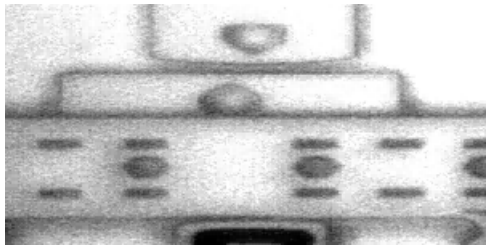

MEMS Environmental Test Chamber

Role of FOTAS SAM Coating on Friction Coefficient

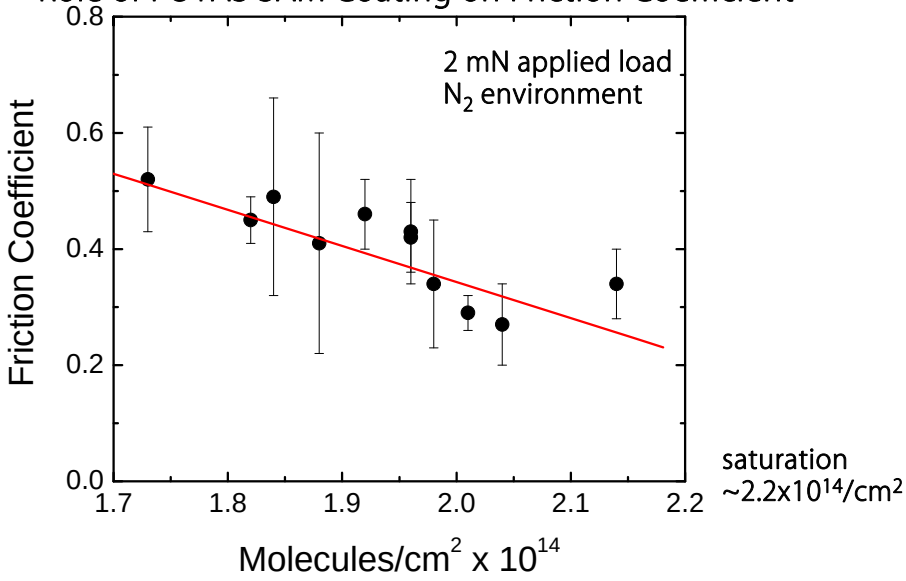

Partial Pressures of Pentanol provide "Vapor Phase Lubrication"

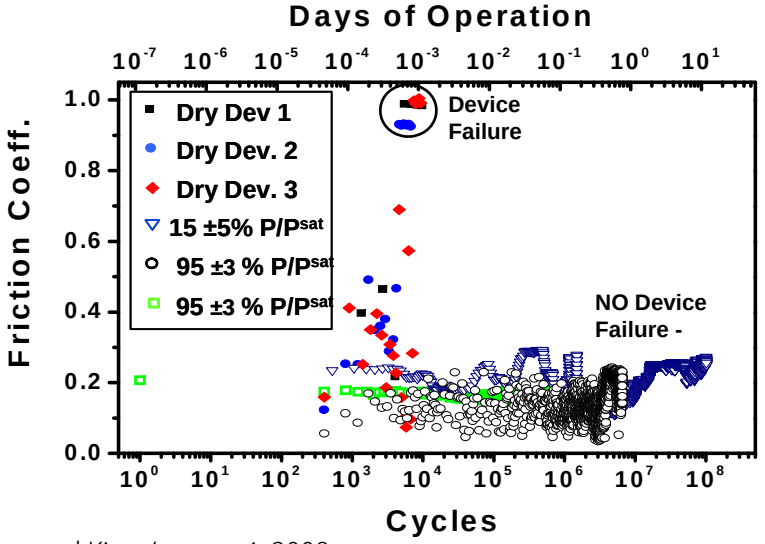

Asay, Dugger, Ohlhausen, and Kim, *Langmuir*, 2008
Asay, Dugger, and Kim, *Tribology Letters*, 2008

Nanotractor Inchworm Actuator

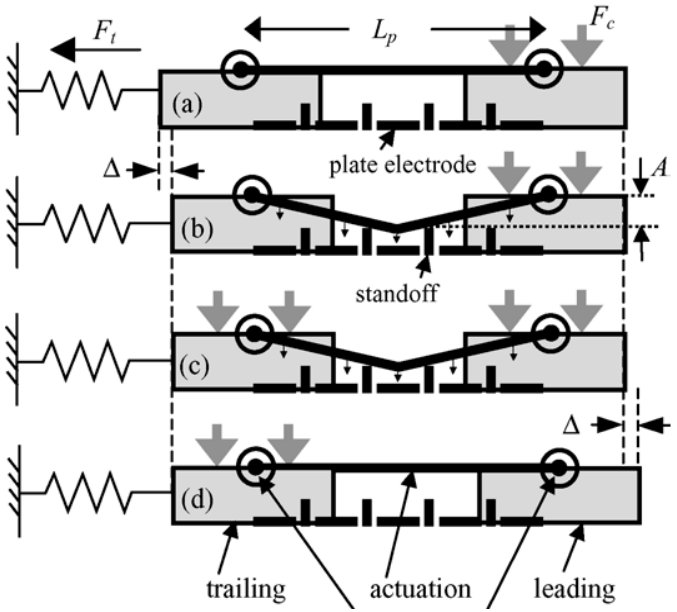

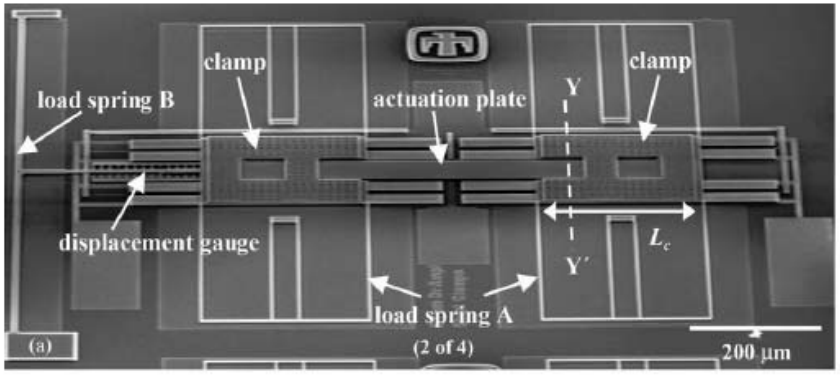

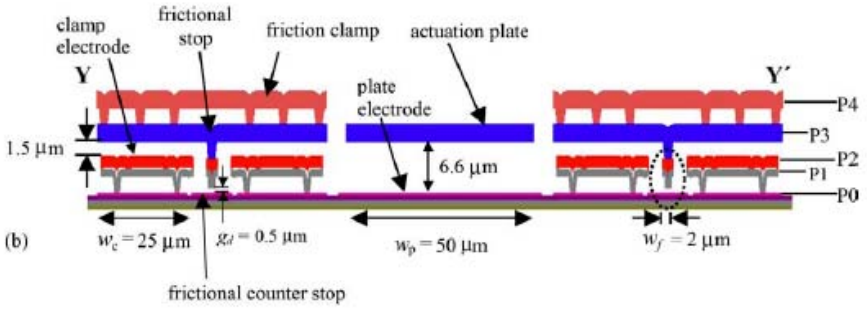

$$F_c(V_c) = 2\varepsilon_0 w_c L_c \left(\frac{V_c}{g_c}\right)^2$$

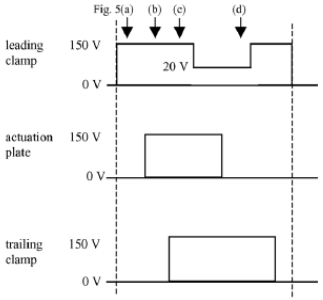

Flater, Corwin, de Boer, and Carpick, *Wear,* 2006

The nanotractor moves 100 µm in 50 nm steps. The nanotractor permits tribological studies of flat-on-flat contact when the top-surface of p0 contacts the bottom-surface of the p12 dimple cut. Normal contact force is controlled by the clamp voltage.

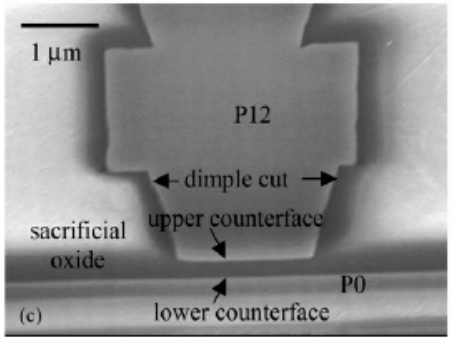

Nanotractor Inchworm Actuator

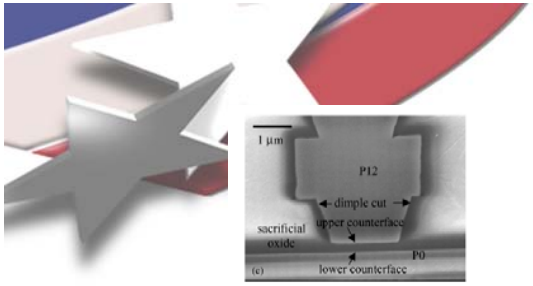

SEM of wear track

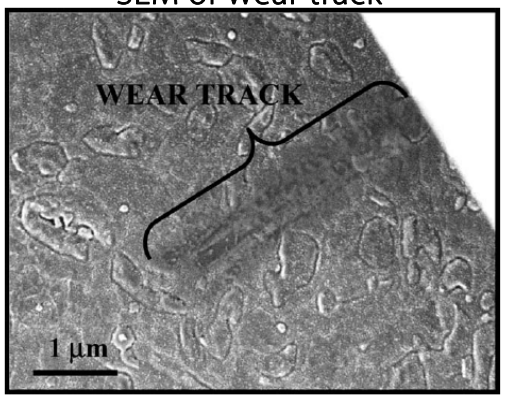

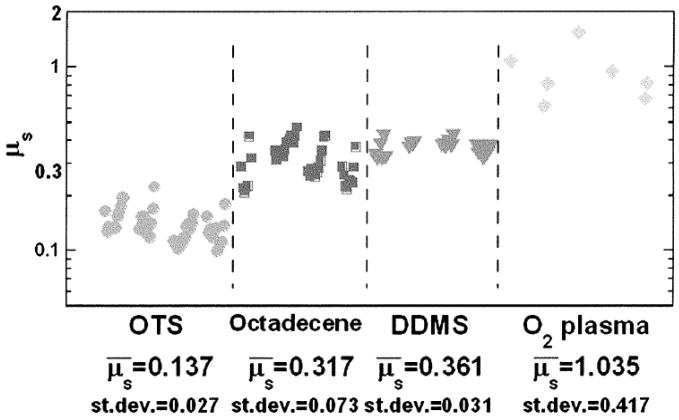

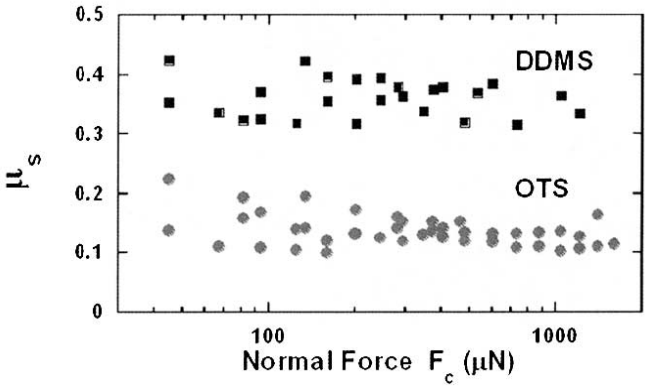

de Boer, Luck, Ashurst, Maboudian, Corwin, Walraven, and Redmond, *J MEMS,* 2004

AFM of wear track

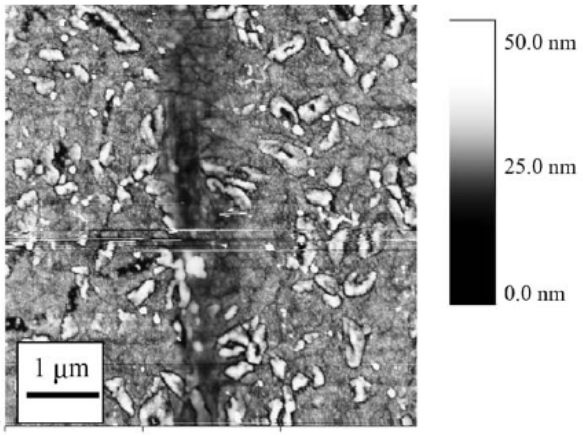

Chemomechanically Polished (CMP) Surface

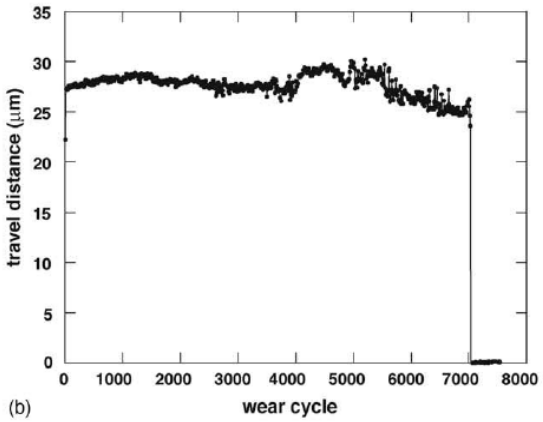

Oxidized Surface

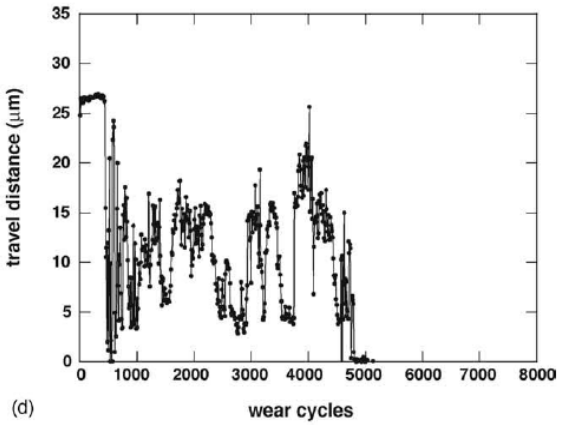

Flater, Corwin, de Boer, and Carpick, *Wear,* 2006

Electrostatically Actuated Loadframe For "1D" Nanostructures

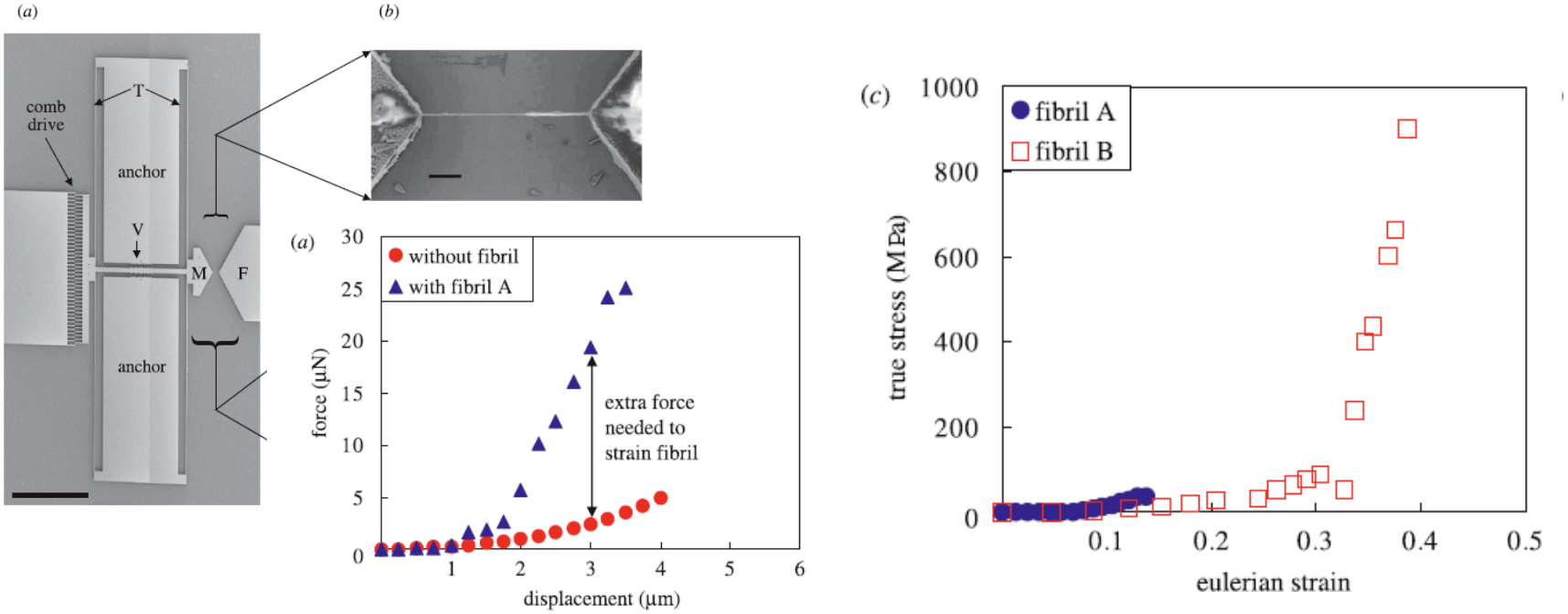

Type I collagen fibrils were manipulated using a pulled-glass micropipette tip with a micromanipulator. They were affixed to the MEMS test structure with epoxy. The resulting stress-strain curve of fibril B exhibited the expected non-linear response with a "toe" region. This behavior may also be attributed to the taking-up of slack in the system (?)

Eppell, Smith, Kahn, and Ballarini, *Proc Royal Soc Interface,* 2006

5.2 Thermally Actuated Devices

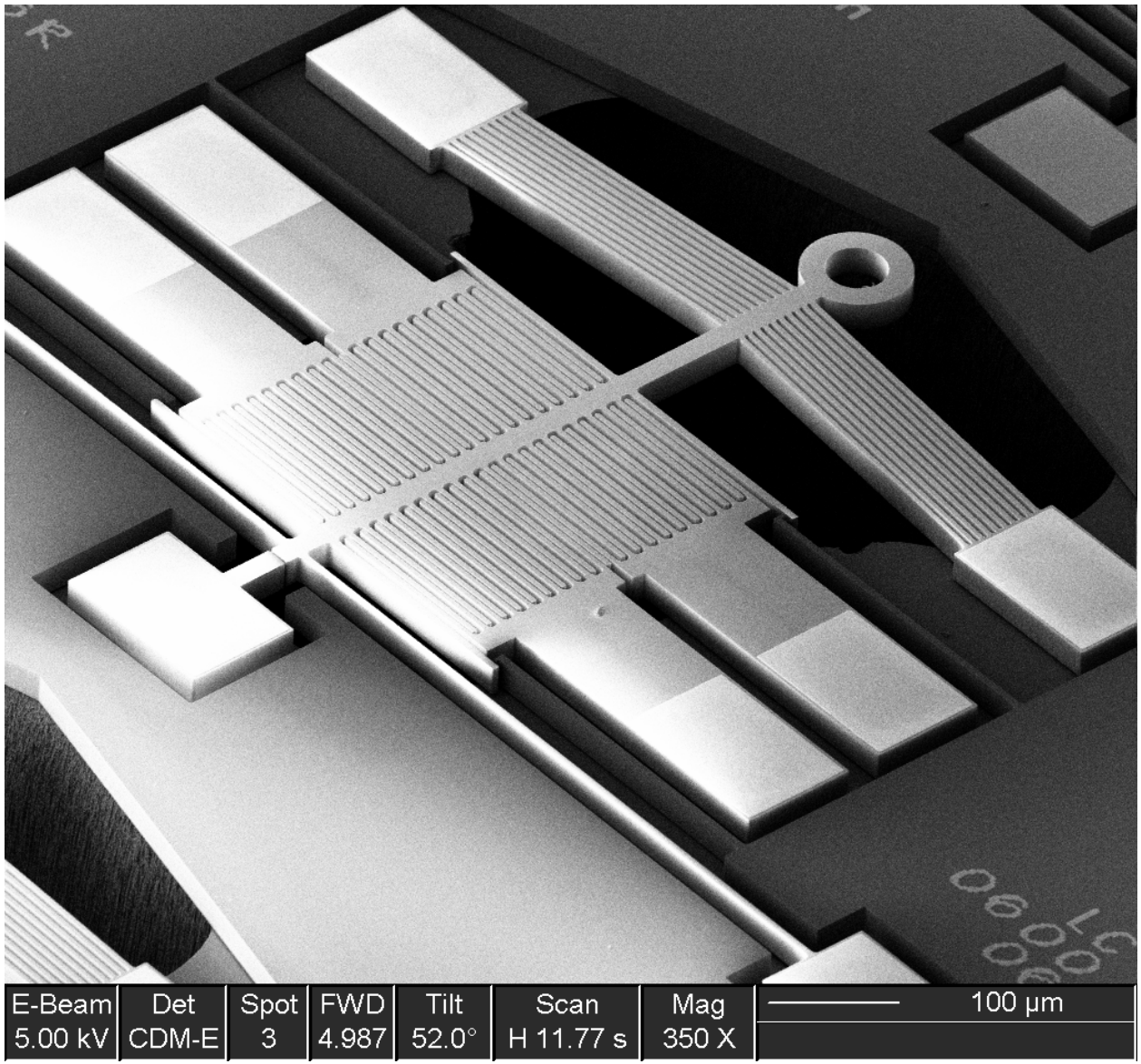

Laser Thermal Actuator

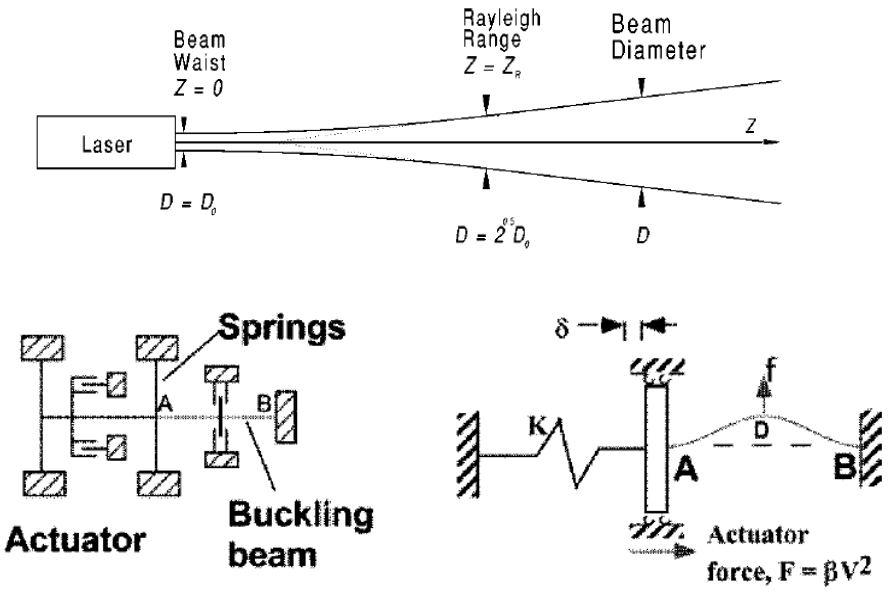

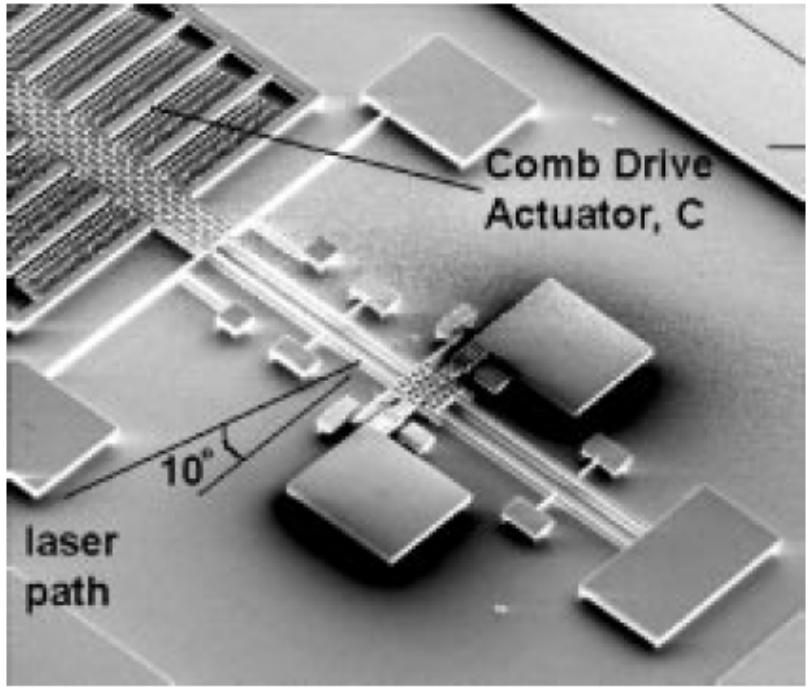

Fig. 4. SEM image of the bistable MEMS device.

Sulfridge, Saif, Miller, and O'Hara, *J MEMS,* 2002

Thermally Actuated Loadframe for "1D" Nanostructures

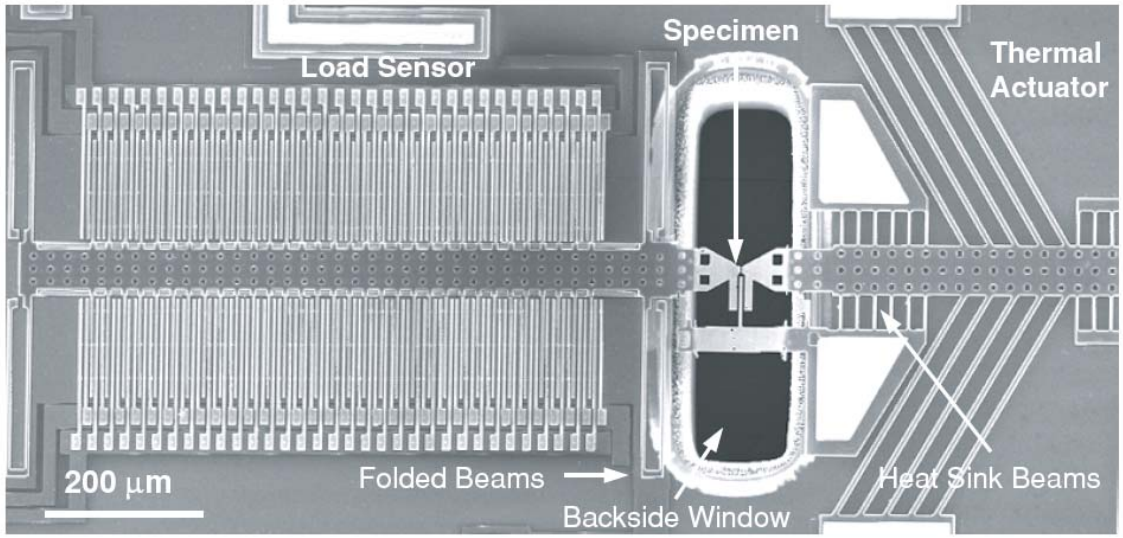

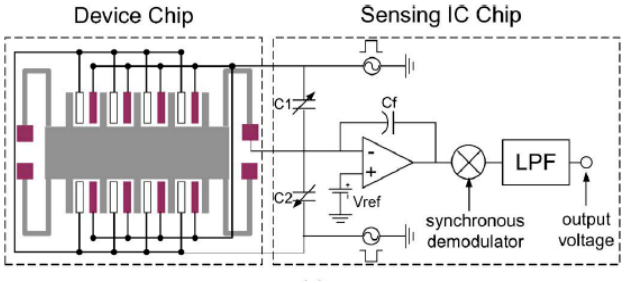

Operation

- displacement range ~ 500 nm
- applied force range ~ 6 μN
- K_{LC}=11.8 N/m

MWCNT Fractured in Zhu,Moldovan,Espinosa MEMS Tester

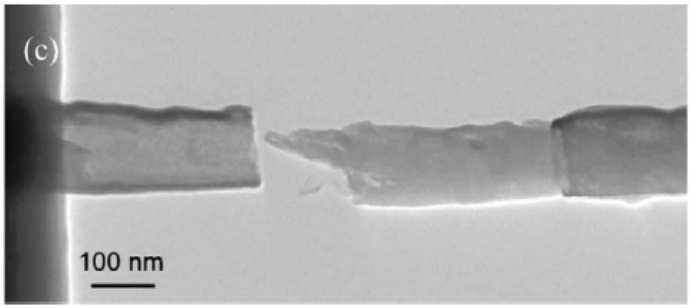

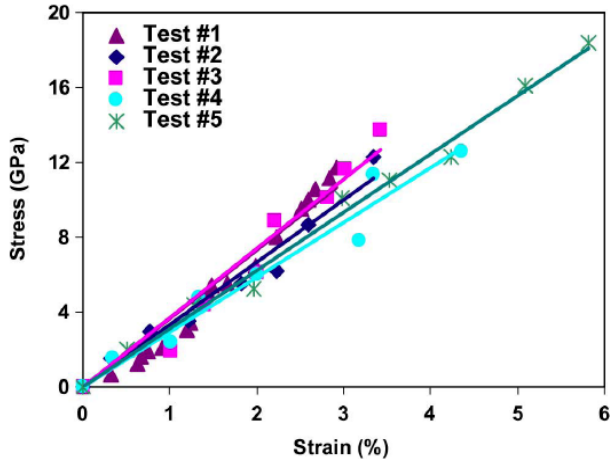

Fig. 14. Stress–strain curves for the tested MWCNTs. See text for definition of cross-sectional area.

The on-chip test platform for 1D nanostructures consists of a thermal actuator and differential capacitance load sensor. The tool can be used in an SEM, and conceivably in a TEM.

Espinosa, Zhu, and Moldovan, *J MEMS,* 2007

Zhu, Moldovan, and Espinosa, *Appl Phys Lett,* 2007

"Pick-And-Place" Techniques for Nanowire Loading

Pick & place sequence for Au wire (300 nm ∅, 4 μm space)

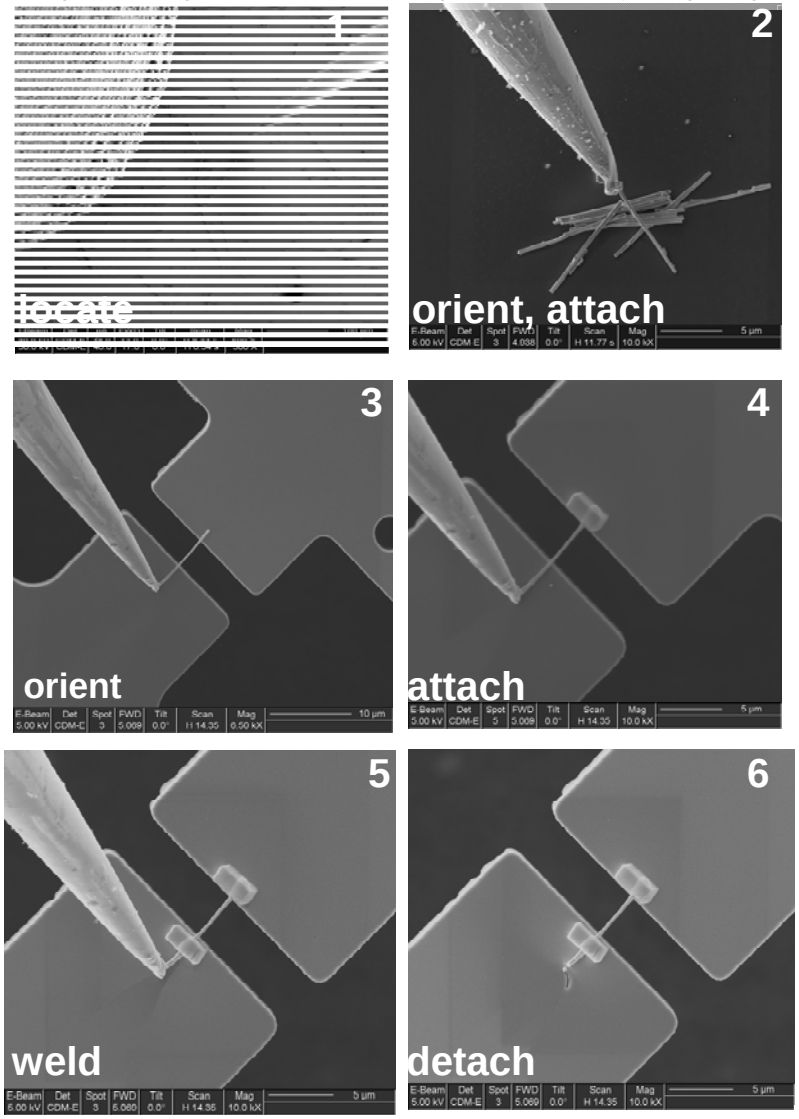

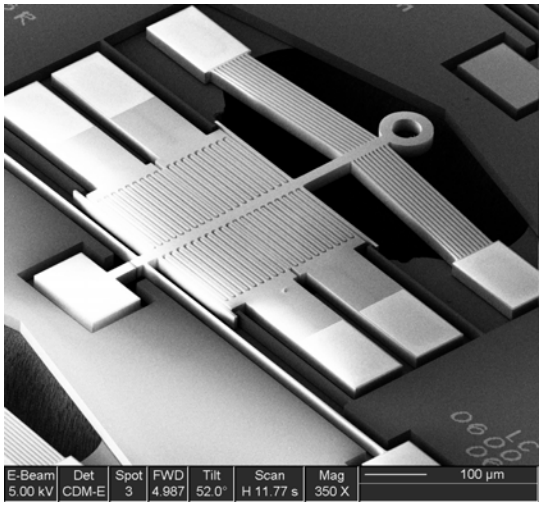

Miller and Boyce, *unpublished*

"Perfect" Si without etch defects?

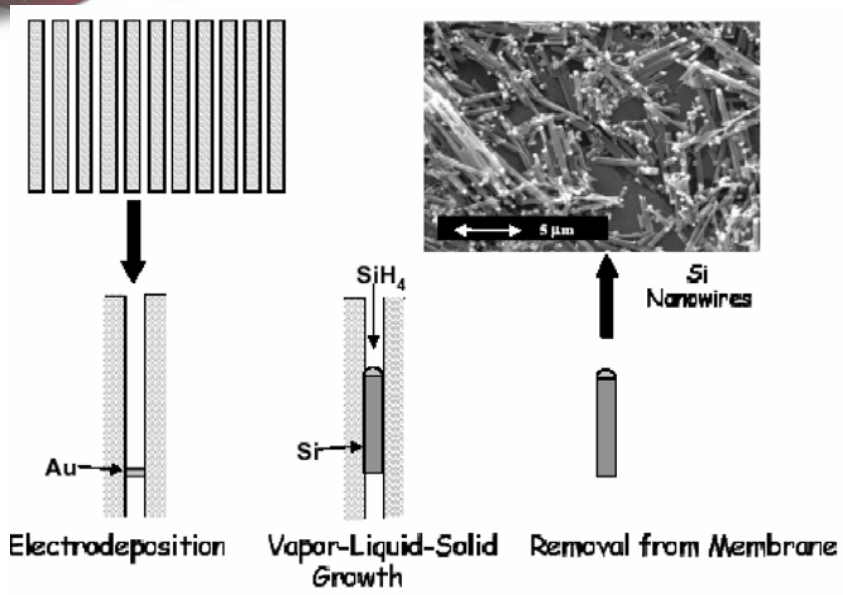

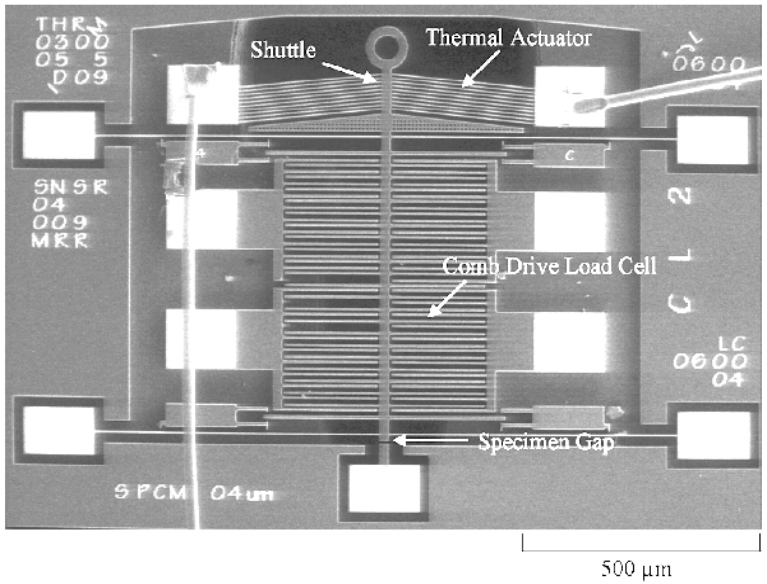

43. Redwing, J.M., Lew, K.K., Bogart, T.E, Pang, L., Dickey, E.C., Carim, A.H., Wang, Y., Cabassi, M.A., Mayer, T.S. *Synthesis and properties of Si and Si/Ge/Si nanowires*. in *Quantum Dots, Nanoparticles, and Nanoclusters*. 2004. Bellingham, WA: SPIE.

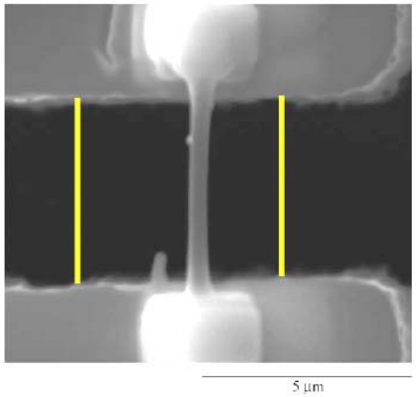

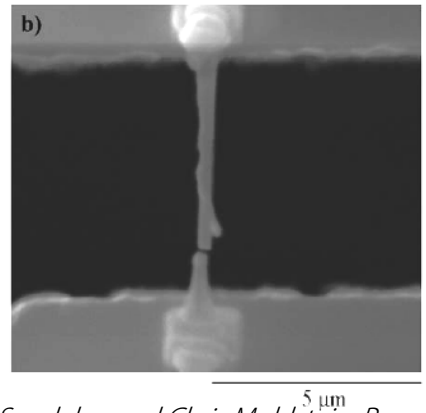

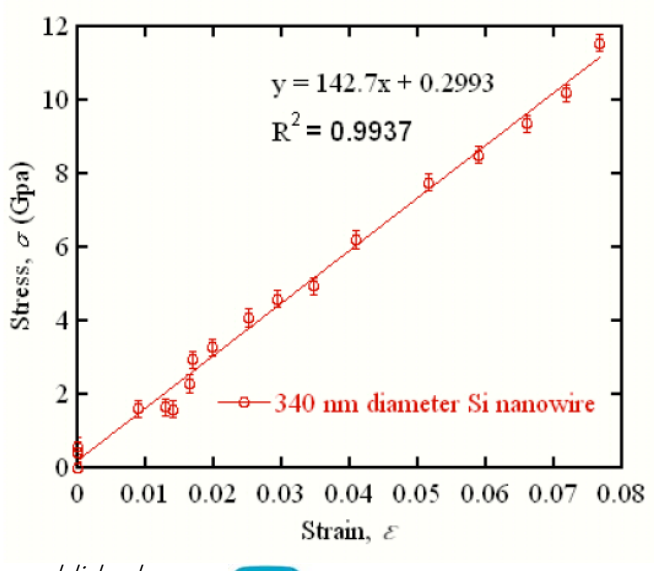

Lauren Snedeker and Chris Muhlstein, Penn State Univ., unpublished

Outline

1. Introduction
2. MEMS fabrication technologies
3. Examples of passive devices
4. Passive device technology
5. Examples of active devices for nanomechanics
6. **Active device technology**
   1. Advantages of on-chip testing
   2. On-chip actuators
   3. On-chip displacement and strain sensors
   4. On-chip force and stress sensors

6.1 Advantages of on-chip testing

1. No need for costly lab equipment for evaluating the behavior of the on-chip structures.

2. Microscale sensors and actuators are amenable to *in situ* techniques such as in a TEM.

3. Microfabricated sensors and actuators can benefit from the close design tolerances.

4. Sensors and actuators are inherently mated and aligned to the test structure.

5. Tests can be executed electronically and are readily automated.

6.2 On-chip actuators

1. Electrostatic Actuator

-Typically operates with a large voltage gradient between interdigitated combs (150 V is not uncommon).
-Low force output (<<1 mN typically) or large real estate
-Sensitive to contaminants and debris
-Force of comb-drive actuators proportional to voltage squared.

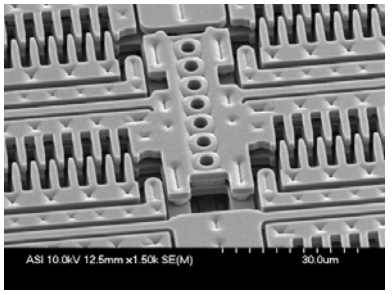

www.memx.com

2. Thermal Actuator

-Relies on thermal expansion caused by Joule heating
-Results in local heating of the structure
-Displacement and force can be optimized by adjusting the number of legs, leg angle, temperature, etc.
-Temperatures should be kept low enough to avoid any permanent damage in the actuator (i.e. creep)

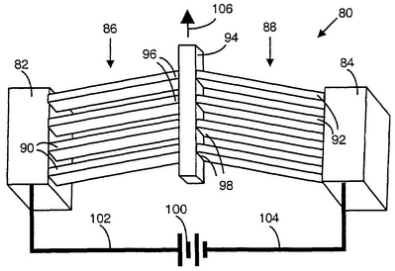

United States Patent 7007471

3. Residual Stress Actuator

-Relies on residual stresses induced during fabrication, such as by differential thermal mismatch between silicon and silica.
-Typically high force output.
-Displacements limited by the strain in the component multiplied by the length of the stressed element.
-This is really a passive structure, since it can not be re-actuated after fabrication.

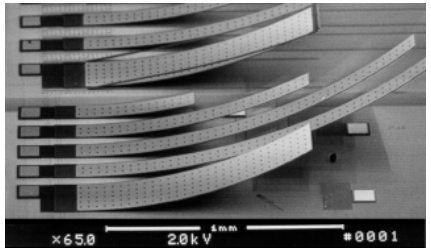

www.swri.edu

4. Piezoelectric Actuator

-Requires fabrication from a material that exhibits piezoelectric behavior.
-High force output, limited displacement output.

6.3 On-chip displacement and strain sensors

1. Features for visual measurement

-Requires line-of-sight to the objects of interest
-Can use optical (low resolution), electron microscopy, or even AFM (see Chasiotis and co-workers with digital image correlation).
-Relatively easy to employ but difficult to automate

2. Capacitive Sensor

-Relies on the change in spacing between two conductors separated by a dielectric.
- Very small (<pF) capacitance changes typically associated with displacement requires high-sensitivity techniques for capacitance observations.

6.4 On-chip force and stress sensors

Force is not a directly measurable quantity. It is measured indirectly, typically through observations of deflection of a structure of known stiffness. Therefore, displacement and strain sensors are also used as force sensors in conjunction with an elastic member.

Summary….

Microfabrication is a pathway to study the nanomechanical behavior of all things small. The dimensional tolerances associated with microfabrication are the key to their improved performance over conventional mechanical behavior techniques. The pallate of available MEMS techniques is already broad, and growing every year.

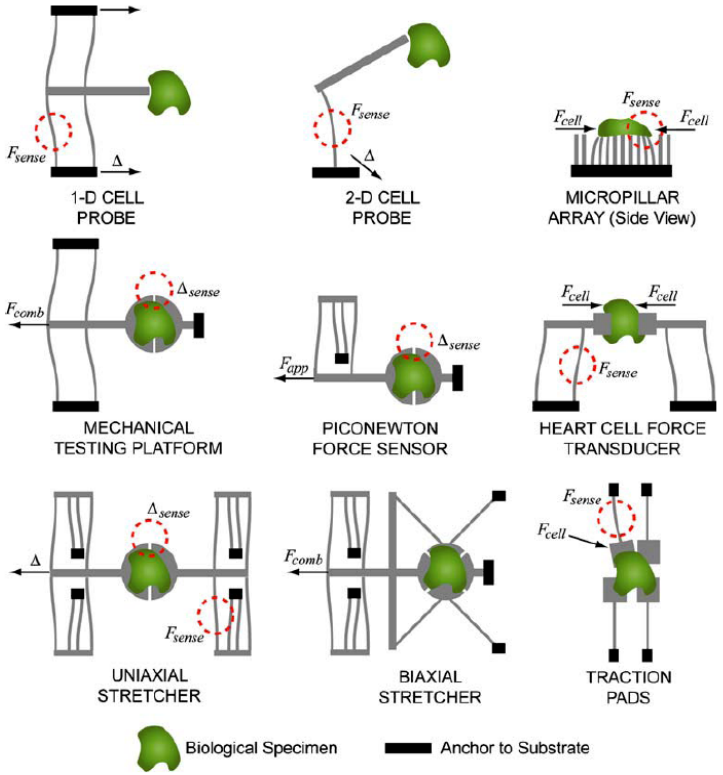

Fig. 4 Schematic depiction of MEMS for cell mechanics emphasizing the use of compliant beams. The actuation in each device is depicted by an arrow. Δ denotes a displacement imposed by an external actuator. F_{comb}, F_{cell}, F_{app}, refer to forces imposed by an electrostatic comb-drive actuator, the cell, or other actuator respectively. F_{sense} denotes load measurement by optical imaging of beam deflection (note that they are not necessarily imaged at this location). Δ_{sense} denotes the measurement of displacement by optical microscope. See Table 2 for references for each device

Loh, Vaziri, and Espinosa, *Exp Mech,* 2007

Acknowledgments

- Amit Misra (Los Alamos): tutorial organizer
- Lawrence Friedman (Penn State): tutorial organizer
- Michelle Dickinson (Hysitron): tutorial sponsorship
- Nate Natale (TMS): TMS tutorial coordinator
- Moses Noh (Drexel): Lectures on Microfabrication
- David Miller (CU Boulder): Assorted SEM images and devices
- Michael Dugger (Sandia): MEMS Tribometer
- Oden Warren (Hysitron): Hysitron indenter MEMS device
- John Sullivan (CINT/Sandia): CINT Nanomechanics Discovery Platform

.

Additional References

1. MEMS Handbook, CRC Press, Mohamed Gad-el-Hak, editor, 2002.
2. M.J. Madou, Fundamentals of Microfabrication, 2nd edition, CRC Press, 2002.
3. Y. Zhu, C-H. Ke and H.D. Espinosa. "Experimental Techniques for the Mechanical Characterization of Thin Films and One-Dimensional Nanostructures" Experimental Mechanics, Vol. 47, No. 1, p. 7-24, 2007.